

Optimal Integration of Battery Energy Storage Systems in Smart Grids

A Dissertation by

Shahab Khormali

*Submitted in Partial Fulfilment of the Requirements for the Degree of
Doctorate of Philosophy
in*

Electrical Engineering

Supervisors:

Prof. Guido Carpinelli

Prof. Angela Russo

Coordinator:

Prof. Claudio Serpico

*Department of Electrical Engineering and Information Technology
University of Naples Federico II
March – 2015*

Optimal Integration of Battery Energy Storage Systems in Smart Grids

A Dissertation by

Shahab Khormali

*Submitted in Partial Fulfilment of the Requirements for the Degree of
Doctorate of Philosophy
in*

Electrical Engineering

Supervisors:

Prof. Guido Carpinelli

Prof. Angela Russo

Coordinator:

Prof. Claudio Serpico

*Department of Electrical Engineering and Information Technology
University of Naples Federico II
March – 2015*

Contents

<i>List of figures</i>	IV
<i>List of tables</i>	VI
<i>List of abbreviations</i>	VII
<i>List of symbols</i>	VIII
<i>Acknowledgement</i>	XI
<i>Introduction</i>	XII
Chapter 1: Battery Energy Storage Systems and Smart Grids	1
1.1. Battery energy storage system	1
1.1.1. History	2
1.1.2. Technologies	3
1.1.3. Characteristics	6
1.1.4. Costs	8
1.2. Smart grid	10
1.2.1. Structure	10
1.2.2. Components	11
1.2.3. Challenges	12
1.2.4. Advantages	15
1.3. Applications of battery energy storage system in smart grid	17
1.3.1. Generation unit services	17
1.3.2. Transmission unit services	19
1.3.3. Distribution unit services	20
1.3.4. End-use customer unit services	21
1.4. References	24
Chapter 2: Optimal Operation Strategies of Battery Energy Storage Systems	29
2.1. An advanced optimal operation strategy for load leveling	30
2.1.1. State of the art	30
2.1.2. Proposed strategy	30
2.1.3. Problem formulation and solving procedure	32
2.1.4. Numerical application	36
2.2. An advanced optimal operation strategy for demand response under real time pricing	40
2.2.1. State of the art	41
2.2.2. Proposed strategy	41
2.2.3. Problem formulation and solving procedure	41
2.2.4. Numerical application	44
2.3. An advanced optimal operation strategy for demand response under energy demand charge	49
2.3.1. State of the art	50
2.3.2. Proposed strategy	50
2.3.3. Problem formulation and solving procedure	51
2.3.4. Numerical application	57
2.4. An advanced optimal operation strategy for microgrid scheduling	63
2.4.1. State of the art	63
2.4.2. Proposed strategy	64
2.4.3. Problem formulation and solving procedure	65
2.4.4. Numerical application	68
2.5. References	73

Chapter 3: Optimal Sizing of Battery Energy Storage Systems	78
3.1. <i>Deterministic optimal sizing of battery energy storage system based on TOU tariff</i>	78
3.1.1. <i>State of the art</i>	79
3.1.2. <i>Problem formulation and solving procedure</i>	80
i. <i>Economic analysis</i>	80
ii. <i>BESS sizing procedure under TOU pricing</i>	82
3.1.3. <i>Numerical application</i>	85
3.2. <i>Probabilistic optimal sizing of battery energy storage system based on decision theory</i>	90
3.2.1. <i>State of the art</i>	91
3.2.2. <i>Problem formulation and solving procedure</i>	92
i. <i>Formulation of the optimization problem</i>	93
ii. <i>Decision Theory</i>	95
3.2.3. <i>Numerical application</i>	98
3.3. <i>References</i>	105
Conclusions	109

List of figures

Figure 1.1:	Development of the secondary batteries over the time	3
Figure 1.2:	Depth of discharge for lead-acid battery	7
Figure 1.3:	Smart grid structure	12
Figure 1.4:	Load demand with and without regulation	18
Figure 1.5:	Real-time pricing	23
Figure 1.6:	Time of use pricing (summer tariff)	23
Figure 2.1:	Grid architecture	31
Figure 2.2:	Flowchart of the two-step procedure	32
Figure 2.3:	Load leveling schematic view	33
Figure 2.4:	Day-ahead forecasting (feeder power)	36
Figure 2.5:	Day-ahead scheduling (feeder and substation powers)	37
Figure 2.6:	Day-ahead scheduling (BESS power)	37
Figure 2.7:	Day-ahead scheduling (BESS energy)	38
Figure 2.8:	Very short term predictive control (substation power)	38
Figure 2.9:	Very short term predictive control (BESS power)	39
Figure 2.10:	Very short term predictive control (BESS energy)	39
Figure 2.11:	Very short term predictive control (substation power)	39
Figure 2.12:	Time steps during 24 hours	42
Figure 2.13:	Industrial facility	45
Figure 2.14:	Energy price profile	45
Figure 2.15:	Battery power profile (<i>case a</i>)	46
Figure 2.16:	Battery energy profile (<i>case a</i>)	46
Figure 2.17:	Load and grid powers (<i>case a</i>)	47
Figure 2.18:	Energy price and total power of the batteries (<i>case a</i>)	47
Figure 2.19:	Battery power profile (<i>case b</i>)	48
Figure 2.20:	Battery energy profile (<i>case b</i>)	48
Figure 2.21:	Load and grid powers (<i>case b</i>)	48
Figure 2.22:	Energy price and total power of the batteries (<i>case b</i>)	49
Figure 2.23:	Time intervals during the day (indices refer to the day ahead)	52
Figure 2.24:	Flowchart of the scheduling procedure	53
Figure 2.25:	Day-ahead forecasted values and actual values of load	58
Figure 2.26:	Energy charge	58
Figure 2.27:	Day-ahead power profile of the facility with and without the BESS	59
Figure 2.28:	Day-ahead profile of the BESS's power	59
Figure 2.29:	Day-ahead profile of the BESS's energy	60
Figure 2.30:	BESS's reference power signal	60
Figure 2.31:	Actual energy stored in the BESS	61
Figure 2.32:	Actual power profile of the facility with and without a BESS	61
Figure 2.33:	Actual power profile of the facility with and without very short time predictive control	62
Figure 2.34:	MV test system	68
Figure 2.35:	Load demand at bus#6 (a). DG power production at bus#15 and DC privileged load demand at bus#7 (b). Energy price (c)	70
Figure 2.36:	Active power imported from the HV grid (a). Active power of the aggregator at bus #13 (b). Active power of a battery of DC bus #7 (c)	71
Figure 3.1:	Residential load profile (a), Industrial load profile (b)	85
Figure 3.2:	Total customer cost with $\alpha=5\%$, $\beta=5\%$, $\eta_{ch}=95\%$, $\eta_{dch}=98\%$, for 5% annual load variations and for different installation costs (residential load)	87
Figure 3.3:	Total customer cost with $\alpha=5\%$, $\beta=5\%$, $\eta_{ch}=95\%$, $\eta_{dch}=98\%$, BESS installation cost = 600 \$/kWh, for different values of annual load variation (residential load)	87
Figure 3.4:	Total customer cost with an annual load variation of 5%, $\eta_{ch}=95\%$, $\eta_{dch}=98\%$, installation cost = 600 \$/kWh, for different values of α and β (residential load)	88

Figure 3.5:	Total customer cost with $\alpha=5\%$, $\beta=5\%$, 5% annual load variation and different values of BESS efficiency (residential load)	88
Figure 3.6:	Total customer cost with $\alpha=5\%$, $\beta=5\%$, $\eta_{ch}=95\%$, $\eta_{dch}=98\%$, for 5% annual load variations (industrial load)	89
Figure 3.7:	Total customer cost with $\alpha=5\%$, $\beta=5\%$, $\eta_{ch}=95\%$, $\eta_{dch}=98\%$, BESS installation cost = 600 \$/kWh, for different values of annual load variation (industrial load)	89
Figure 3.8:	Total customer cost with a annual load variation of 5%, $\eta_{ch}=95\%$, $\eta_{dch}=98\%$, BESS installation cost = 600 \$/kWh, and for different values of α and β (industrial load)	90
Figure 3.9:	Total customer cost with $\alpha=5\%$, $\beta=5\%$, 5% annual load variation, BESS installation cost = 600 \$/kWh, and different values of BESS efficiency (industrial load)	90
Figure 3.10:	Flowchart of the proposed procedure	93
Figure 3.11:	Hourly energy price	99
Figure 3.12:	Load demand daily profile	99
Figure 3.13:	Stability areas - (a) approach (a); (b) approach (b); and (c) approach (c)	102

List of tables

Table 1.1:	Characteristics of different battery technologies	6
Table 1.2:	Capital cost components for different BESS technologies	9
Table 1.3:	BESS services in the different levels of the grid	17
Table 1.4:	Time of use tariff periods	24
Table 1.5:	Time of use tariff prices	24
Table 2.1:	Peak value and load factor of the substation power with and without BESS	40
Table 2.2:	Objective function reduction	49
Table 2.3:	Performance of the very short time procedure	62
Table 2.4:	Test system data	69
Table 2.5:	Load base values ($P_{BASE}=10\text{ MVA}$)	69
Table 2.6:	Energy requests by the aggregators	69
Table 2.7:	Objective function values for different strategies	72
Table 3.1:	Time of use tariff periods	86
Table 3.2:	Time of use tariff prices	86
Table 3.3:	Decision matrix: total cost ($k\$$) for each size (kWh) - Case 1	100
Table 3.4:	Decision matrix of weighted regrets ($\$$) for each size (kWh) - Case 1	101
Table 3.5:	Expected value of the costs ($k\$$) and maximum weighted regret ($\$$) of each size (kWh) - Case 1	101
Table 3.6:	Decision matrix: total cost ($k\$$) for each size (kWh) - Case 2	104
Table 3.7:	Decision matrix of weighted regrets ($\$$) for each size (kWh) - Case 2	104
Table 3.8:	Expected value of the costs ($k\$$) and maximum weighted regret ($\$$) of each size (kWh) - Case 2.	105

List of abbreviations

BESS	Battery Energy Storage System
CCHP	Combined Cycle Heat and Power
CCS	Centralized Control System
CPP	Critical Peak Pricing
DC	Direct Current
DCs	Data Centers
DG	Distributed Generation
DOD	Depth of Discharge
DP	Dynamic Programming
DR	Demand Response
DM	Decision Maker
DSM	Demand Side Management
EC	Energy Charge
EDC	Energy Demand Charge
EV	Electric Vehicle
EES	Electrical Energy Storage
FFNN	Feed Forward Neural Network
GA	Genetic Algorithm
HV	High Voltage
ICT	Information and Communication Technology
kW	Kilo Watt
LOA	Linear Optimization Algorithm
LMP	Locational Marginal Pricing
MAPE	Mean Absolute Percentage Error
MP	Market Price
MU	Monetary Unit
MV	Medium Voltage
MW	Mega Watt
NaS	Sodium Sulphur Battery
Ni-Cd	Nickel-Cadmium Battery
Ni-MH	Nickel-Metal Hydride Battery
NSRS	NATO Submarine Rescue System
PEV	Plug-in Electric Vehicle
PHEV	Plug-in Hybrid Electric Vehicle
PLC	Power Line Carrier
PV	Photovoltaic
PWM	Pulse width Modulation
RES	Renewable Energy Source
RTP	Real Time Price
RTTR	Real Time Thermal Rating
SCADA	Supervisory Control and Data Acquisition
SG	Smart Grid
TOU	Time of Use
T&D	Transmission and Distribution
UPS	Uninterruptable Power Supply
ZEBRA	Sodium Nickel Chloride Battery
μ G	Microgrid

List of symbols

A_{opt}	Solution of the optimization problem
$B_{i,k}$	System's susceptance matrix for (i,k) -term
C_0	Capital cost of the BESS
C_{batt}	Cost of the battery
C_{ch}	Electricity cost sustained for charging the battery
C_{conv}	Cost of the converter
C_{dch}	Electricity cost for discharging the battery saved by customer
C_{disp}	Disposal cost of the BESS
$C_{in,j}^{dis}$	State of charge of the j^{th} battery at the beginning of the discharge
C_{en}	Energy cost of the BESS
C_i	BESS state of the charge at the beginning of the i^{th} time interval
C_{ik}	Cost incurred in the k^{th} future F_k by the i^{th} alternative
$C_{j,i+1}$	State of charge of the j^{th} battery at the begin of the $i^{th}+1$ time interval
$C_k(n)$	Cost (energy, maintenance or replacement cost) related to year n
$C_k(n)_{npv}$	Net present value of the cost
C_{LCC}	Life cycle cost or total customer cost
C_{load}	Total electricity cost required to supply the loads without considering the BESS
C_{max}	Capacity of the Battery
$C_{max,j}$	Capacity of the j^{th} battery
C_{min}	Admissible minimum value of the BESS state of charge
$C_{min,j}$	Admissible minimum value of the BESS state of charge of the j^{th} battery
C_{mt}	Maintenance cost of the BESS
C_k^{min}	Minimum cost for the k^{th} future
C_{rep}	Replacement cost of the BESS
C_{in}^{sp}	Specified value of the BESS state of charge at the beginning of the day
C_{fin}^{sp}	Specified value of the BESS state of the charge when the charge ends
$C_{j,i}^{sp}$	Specified value of the j^{th} battery state of charge at the end of the 24 hours ($i^{th}+n_i$ time interval)
$E[\cdot]$	Expected value
$E_{ch,i,n}$	Daily energy absorbed by the battery in the same time intervals
$E_{dch,i,n}$	Daily energy supplied by the battery in the same time intervals
$E_{i,DOD}$	Minimum stored energy according to the allowable depth of discharge
$E_{t,ch}^{in}$	Initial stored energy at the beginning of the charging
$E_{t,dch}^{in}$	Initial stored energy at the beginning of the discharging
E_i^{max}	Maximum value of the energy to be stored in the battery
E_i^{min}	Minimum value of the energy to be stored in the battery
E_{size}	Size of the battery
$E_{t,j}^{sp}$	Specified value of energy which the grid has to supply to the PEV fleet aggregators
D_h	h^{th} individual
$G_{i,k}$	System's conductance matrix for (i,k) -term
$I_{l,t}$	Current through the l^{th} line at time t
I_l^r	Rated current through the l^{th} line
N_{cycles}	Number of charging/discharging cycles declared by the battery
N_i	Number of days of the i^{th} season
$P_{b,i,n}(t)$	Absolute value of the power of the battery at time t of the i^{th} season of the n^{th} year
$P_{b,max}$	Maximum power that can be supplied by the battery
$P_{b,i}^{da}$	Day-ahead forecasted BESS power at time interval i

$P_{l,i}^{da}$	Day-ahead forecasted feeder power at time interval i
$P_{grid,i}^{da}$	Day a-ahead forecasted power requested by the facility to the grid at time interval i
$P_{grid,max}^{da}$	Maximum value of day a-ahead forecasted power requested by the facility to the grid
P_{lev}	Leveling power
$P_{l,i,n}(t)$	Power requested by the loads at time t of a typical day of the i^{th} season of the n^{th} year
$P_{loss,t}$	Power losses at time slot t
$P_{l,t}$	Active power imported from the upstream grid
$P_{l,\mu}$	Mean value of active power absorbed from the upstream grid during the day
$P_{i,t}$	Net active power injected in the bus i at time t
P_k	Probability of the k^{th} future
P_{max}	Maximum charge/discharge power of BESS
$P_{i,ch}^{max}$	Maximum power that can be absorbed by the battery
$P_{i,dch}^{max}$	Maximum power that can be supplied by the battery
$P_{max,j}$	Maximum charge/discharge power of the j^{th} battery
$P_{b,j}^{vst}$	Very short time forecast of the BESS power at time interval j
$P_{l,j}^{vst}$	Very short time forecast of the feeder power at time interval j
$P_{grid,j}^{vst}$	Very short time forecast of the power requested by the facility from the grid
$P_{sub,j}^{vst}$	Very short time forecast of the substation power at time interval j
$Pr_{ch,i}$	Energy price during the off-peak hours, that is the time intervals included in $\Omega_{ch,i}$
$Pr_{dch,i}$	Energy price during the on-peak hours, that is in the time intervals included in $\Omega_{dch,i}$
Pr_{En}	Energy price
$Pr_{En,i,n}(t)$	Energy price at time t of the i^{th} season of the n^{th} year
Pr_{peak}	Demand charge
$Q_{i,t}$	Net reactive power injected in the bus i at time t
RG_{ik}	Regret felt for having chosen a certain alternative A_i when the k^{th} future occurred
S_i^{max}	Maximum apparent power of converters
T_{day}	Duration of the day
$V_{i,t}$	Voltage in busbar i at time slot t
V^{max}	Maximum admissible magnitudes of the bus voltage
V^{min}	Minimum admissible magnitudes of the bus voltage
W_{st}	Total energy stored
W_{ut}	Usable released energy
WRG_{ik}	Weighted regret felt for having chosen a certain alternative A_i when the k^{th} future occurred
X	Vector of the optimization variables
f_{GEDC}	Generalized energy demand charge tariff
f_{obj}	Objective function
g_k	Equality constraints
h_j	Inequality constraints
n	Number of year(s)
n_b	Number of the battery banks
n_{ec}	Number of equality constraints
n_{in}^{dis}	Initial time interval of discharging
n_{fin}^{dis}	Final time interval of discharging
n_{ic}	Number of inequality constraints
n_t	Number of time intervals
α	Effective rate of change assumed for cost of the BESS
β	Assumed discount rate for cost of the BESS
$\gamma_{i,t}$	Efficiency of the battery in both charging and discharging modes

η	BESS efficiency
η_{ch}	BESS efficiency during the charge mode
η_{dch}	BESS efficiency during the discharge mode
$\eta_{ch,j}$	Charging efficiency of the j^{th} battery
$\eta_{dch,j}$	Discharge efficiency of the j^{th} battery
η_{inv}	Inverter efficiency
η_{rec}	Rectifier efficiency
$\eta_{selfdch}$	Self-discharge efficiency
η_{st}	Storage efficiency
τ	Discharge time
v	Number of daily charging/discharging cycles
Δt	Length of time intervals
δ	Percentage value of the maximum depth of discharge of the battery
$\delta_{i,t}$	Argument of the voltage
Ω_l	Set of all the lines of the grid
Ω_{CONV}	Set of buses equipped by converters
Ω_{CH}	Set of time slots in which the UPS storage system is allowed to charge
Ω_{DC}	Set of buses where data centers are installed
Ω_{DCH}	Set of time slots in which the UPS storage system is allowed to discharge
Ω_{PEV}	Set of buses where PEV fleet aggregators are installed
$\Omega_{ch,i,n}$	Set of all the time intervals of the day, in which the battery is allowed to charge
$\Omega_{dch,i,n}$	Set of all the time intervals of the day, in which the battery is allowed to discharge
Ω_{grid}	Set of all buses

Acknowledgement

This journey would not have been interesting without the people I met along the way. I would like to express my very great appreciation to my supervisors, **Prof. Guido Carpinelli and Prof. Angela Russo**, for the opportunity to carry out this research work. Thanks a lot for the trust, support and the freedom to create that **Prof. Guido Carpinelli** has provided throughout my PhD course. I am particularly grateful for the assistance given by **Dr. Daniela Proto** in completing the PhD Thesis. A special thank you goes out to **Dr. Fabio Mottola** for the many supports and guides which he gave to me. I am most grateful for the encouragement and support he gave me during these years to complete my PhD course successfully.

This work is funded in the framework of the GREAT Project supported by GETRA Distribution Group (Italy). I would like to thank all of participated people in this project who gave me the chance to have an experimental work based on their real and valuable data.

Thank you to all of my kind colleagues and friends in the Department of Electrical Engineering and Information Technology who I worked during this period and it was a real pleasure for me.

Finally, I would like to express my deep gratitude to my wonderful family. Thanks a lot to **my parents** for their continuous helps in different steps of my life and very great appreciation to my kind wife, **Alieh**, for her kindly and friendly supports during these years. I never forget your helps and supports.

Introduction

Power systems have been undergoing radical changes in recent years, and their planning and operation will be surely undertaken according to the Smart Grid (SG) vision in the near future. The SG initiatives aim at introducing new technologies and services in power systems, to make the electrical networks more reliable, efficient, secure and environmentally-friendly. In particular, it is expected that communication technologies, computational intelligence and distributed energy sources will be widely used for the whole power system in an integrated fashion. In particular, nowadays, unprecedented challenges like as stringent regulations, environmental concerns, growing demand for high quality, reliable electricity and rising customer expectations are forcing utilities to rethink about electricity generation and delivery from the bottom up. Moreover, the availability of low cost computing and telecommunications technologies, new generation options, and scalable, modular automation systems push utilities to be dynamic, innovative and ambitious enough to take advantage of them. Driven by the dynamics of the new energy environment, leading utilities, technology vendors and government organizations have created a vision of the next generation of energy delivery systems: the Smart Grid.

Operational changes of the grid, caused by restructuring of the electric utility industry and electricity storage technology advancements, have created an opportunity for storage systems to provide unique services to the evolving grid. Especially Battery Energy Storage Systems (BESSs), thanks to the large number and variety of services they can provide, are powerful tools for the solution of some challenges that future grids will face. This consideration makes BESSs critical components of the future grids. The BESS can be applied for different services into the different levels of power system chain to satisfy technical challenges and provide financial benefits.

In the context of the application of BESSs in SGs, there are two main problems that need to be addressed in a way that exploits the BESS potential, that are linked to their operation and sizing. This thesis focuses on both these aspects, proposing new strategies that allow optimizing the BESS adoption. When dealing with BESSs, sizing and operation are strictly linked. The correct sizing of a BESS, in fact, needs to take into account its operation which in turn will be effected with the aim of optimizing the whole system where it is included.

In the first part of this research study, advanced optimal operating strategies were proposed for BESSs by considering both the distribution system operator perspective and the end user. Thus, the proposed operating strategies were performed with the aim of *(i)* leveling the active power requested by the loads connected to a distribution system (distribution system operator service), *(ii)* reducing the electricity costs sustained by an end-use customer that provides demand response (DR) (end user service) and *(iii)* scheduling a microgrid (μ G) with DR resources such as Plug-in Electric Vehicles (PEVs) and Data Centers (DCs) (both the two section service). The proposed strategies also satisfied technical constraints of BESSs and other components of the μ G.

The second part of the thesis presented the optimal sizing of BESSs aimed at maximizing the benefits related to their use. In the thesis, the sizing, which is performed by considering the end user point of view with reference to both the industrial and residential customers, is effected by adopting both deterministic and probabilistic approaches. With reference to the deterministic approach, a simple and quick closed form procedure for the sizing of BESSs in

residential and industrial applications was proposed. In case of probabilistic approach, the case of a BESS installed in an industrial facility was considered and the sizing was performed based on the decision theory.

Technical improvements and economic benefits of optimal operation and optimal sizing of BESSs in SG are demonstrated by the obtained results which are reported in the numerical applications. More specifically, it was clearly determined that BESSs can offer technical supports into the distribution operator section of the grid in terms of load management and security challenges. Moreover optimal integration of BESSs into the grid was also appealing for end users thanks to valuable amounts of electricity bill cost reduction.

Regarding the original contribution of the thesis, the following considerations can be done.

With reference to the load leveling service, an innovative two-step procedure (day-ahead scheduling and very short time predictive control) was proposed which optimally controls a BESS connected to a distribution substation in order to perform load leveling.

In case of DR, a proper control of the BESS was proposed in order to perform DR under different price schemes, such as Real Time Pricing (RTP) and Time of Use (TOU) without modifying the daily work cycle of the industrial loads. The control procedure allows achieving contemporaneously two important goals that are the reduction of the bill costs and the prolonging the battery's lifetime so further reducing the costs sustained by the customer.

With reference to the scheduling of microgrids, the original contribution of the thesis is focused on the proposal of optimization strategies aimed at managing and coordinating, simultaneously, batteries on board of vehicles or equipping data centers' Uninterruptable Power Supply (UPS) and Distributed Generation (DG) units. Also comparisons among different single-objective based strategies are made in order to highlight the most convenient.

With reference to the sizing based on deterministic approach, unlike the other relating literature, the innovative contribution is that the closed form procedure takes into account both the technical constraints of the battery and contractual agreements between the customer and the utility. Moreover, in the economical analysis performed for the sizing, which is applied with reference to both residential and small industrial customers and is based on actual TOU tariffs, a wide sensitivity analysis to consider different perspectives in terms of life span and future costs was performed.

Some aspects that affect the profitability of the battery, such as technological limitations (e.g. the battery and converter efficiency), economic barriers (e.g. capital cost and the rate of change of the cost) and variation of the load profile along the years were deeply analyzed.

In case of sizing based on probabilistic approach, the original contributions of the thesis are mainly referred to the proposal of a new method that uses a decision theory-based process to obtain the best sizing alternative considering the various uncertainties affecting the sizing procedure.

The thesis is organized in three chapters which are dealing with integration of BESSs in SGs. The first chapter reports basic concepts and characteristics of BESSs, fundamental components and features of SGs and different services that BESSs can provide. The optimal operation strategies of BESS are considered in second chapter which includes their problem formulation, solving procedures and results. The third chapter deals with the optimal sizing problem of BESSs for which the problem formulation, solving procedures and results are reported. Finally, the conclusions are presented in the last part of thesis.

Chapter 1: Battery Energy Storage Systems and Smart Grids

This chapter presents basic concepts and characteristics of Battery Energy Storage Systems (BESSs), Smart Grids (SGs) and applications of BESSs in SGs including an overview on features of dynamic pricing schemes for electrical energy. It is organized in four sections as follows:

- Battery energy storage system
- Smart grid
- Applications of battery energy storage system in smart grid
- References

1.1. Battery energy storage system

The initial idea of using electrical energy storage (EES) dates back to the turn of the 20th century, when power generating stations were often shut down overnight, with lead-acid accumulators supplying the residual loads on the direct current (DC) networks. Then progresses of the ESS were developed at large central generating stations, transmission and distribution networks [1-3]. In the recent years, electrical power systems are forced to move away from major and traditional energy sources to renewable energy sources (RESs) which are more environmentally friendly and sustainable [2]. This is due to several factors such as increasing demand for electric power, the need to reduce greenhouse gas emission, take care about climate changes, lacking the resources to build the power plants and distribution networks.

RESs like solar, wind and tidal wave with considerable potential to generate electrical power will play an important role in the future power generation systems. These are only available when there is adequate sun, wind and tide. Then, integration of RESs into the grid due to their variable and intermittent nature will be problematic. This is where EES becomes an enabling technology and a proper solution to integrate RESs into the grid and make the non-dispatchable resources into a dispatchable energy source by introducing new applications of EES [2, 4].

EES refers to a process of converting electrical energy from a power network into a form that can be stored for converting back to electrical energy when needed. Then, this type of process in EES can offer an opportunity for electricity to be stored at times of either low demand, low generation cost or from intermittent energy sources and to be used at times of high demand, high generation cost or when no other generation means is available [1, 2].

There are different technologies for EES; the most common form is battery. Battery is modular, quiet and non-polluting. It can be located almost anywhere and can be installed relatively quickly. Battery in the larger size is called Battery Energy Storage System (BESS) [4]. BESS is a potential solution for some challenges that face today's power grid due to the large number and variety of services that they can furnish like as manufacturing industrial services, renewables energy facilities, portable electronic devices and electric vehicles. This consideration makes a BESS as a critical component of future SGs [2, 4, 5]. As such, deep and proper research works are needed to study progress of BESSs in different aspects in more

details. Historical, technological, characteristically and economic aspects of BESSs are considered in the following sections.

1.1.1. History

The expression ‘battery’ was originally used for assemblies of cannons in artillery units, but Benjamin Franklin used this expression to describe the connection of Leyden jar capacitors around 1750 [6]. Fifty years later in 1800, Alessandro Volta invented the first true battery, which came to be known as the voltaic pile. The voltaic pile consisted of pairs of copper and zinc discs piled on top of each other and separated by a layer of cloth or cardboard soaked in brine (i.e., the electrolyte). Comparing by Leyden jar, the voltaic pile generated a continuous and stable current, but it lost little charge over time when not in use. There were some technical faults in Volta's original pile models, like as the electrolyte leaking and causing short-circuits due to the weight of the discs compressing the brine-soaked cloth [7]. Later in 1808, an Englishman named William Cruickshank solved this problem by laying the elements in a box instead of piling them in a stack. Then, it evolved into the Daniel cell in 1836 which included two electrolytes [8]. Golding Bird invented the first single-cell version of the Daniel cell in 1837 by using a plaster of Paris barrier to keep the solutions separate and also the porous pot version of the Daniel cell was found by John Dancer in 1838 [9,5]. Later during the 1860s, Callaud invented a variant of the Daniel cell called the gravity cell. All of these are called as primary cells, which are single-use galvanic cells that store electricity for convenient usage, usually showing a good shelf life; however, they are not usually rechargeable. According to the mentioned history, the expression ‘battery’ should be used only for an assembly of cells in series or parallel arrangements; but, the word battery became a technical and commercial common practice to use even for single cells [6]. Unlike primary battery, a secondary battery is rechargeable and it can be reused many times; therefore, it was called a storage or rechargeable battery. The rechargeable or secondary battery was born in 1803 when a German physicist, Johann Wilhelm Ritter, combined layered disks of copper and cardboard soaked in a brine of table salt. The ‘Ritter pile’ could be charged by a current and delivered energy when discharged but the secondary current was very transitory. That’s why it was only known charging equipment at that time. Later in 1859, Gaston Plante invented the first practical rechargeable battery which was based on lead-acid chemistry. Use of lead-acid batteries in automobiles for starting, lighting, and ignition purposes was and is one of the most common applications of lead-acid battery [10].

Over the time, other types of rechargeable batteries were introduced into the market. In 1899 Ernst Waldemar Jungner developed the nickel-cadmium accumulator. Also nickel-metal hydride (Ni-MH) batteries, different from sealed nickel-cadmium batteries in that hydrogen is used as the active mass instead of cadmium, were introduced in 1985[10].

Another type of rechargeable battery which was known as alkaline battery was realized for the first time by the French chemists, Felix de Lalande and Georges Chaperon, in 1882 and it evolved to the rechargeable alkaline manganese battery by Karl Kordesch (Austria) in 1992.

In continuous of the pioneer work of Lewis (1912) and Wright (1975), the first rechargeable lithium batteries born earlier than 1980, then Sony Corporation in Japan was able to commercialize lithium secondary cells in 1990. In 1999, the commercialization of lithium-ion polymer batteries was accomplished [6]. Figure 1.1 illustrates the development of some of the main secondary batteries over the time [10].

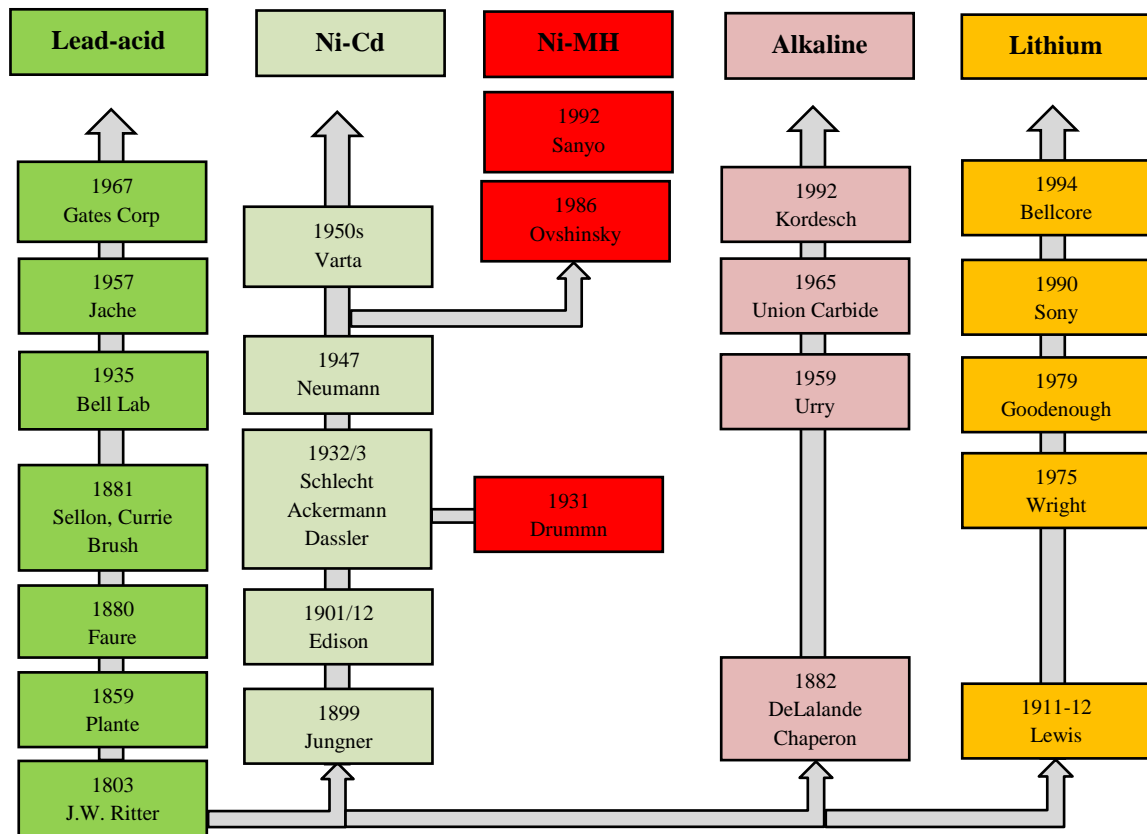


Figure 1.1: Development of the secondary batteries over the time [10].

1.1.2. Technologies

Based on use of different chemicals to produce electrical energy, different kinds of batteries have been developed. A battery comprised of one or more electrochemical cells and each cell consist of a liquid, paste, or solid electrolyte together with a positive electrode (anode) and a negative electrode (cathode) [1, 11]. Today, there is a wide range of battery technologies in the market where each one has its advantages and disadvantages. Among the various battery technologies, some of them seem to be more suitable for power system applications due to approved technical and economic benefits [11]. They are discussed below in more detail.

Lead-acid batteries

The oldest known type of rechargeable battery is the lead-acid battery which was invented in 1859 by the French physicist Gaston Plante [11]. It has been commercially deployed around 1890. It is used in both mobile and stationary applications. Some of popular applications of lead-acid battery are; emergency power supply systems, stand-alone systems with photovoltaic (PV), battery systems for mitigation of output fluctuations from wind power and as starter batteries in vehicles [12]. In the charged state, this type of battery consists of electrodes of lead metal and lead oxide in an electrolyte of 37% sulphuric acid whereas in the discharging state both electrodes turn into lead sulphate and the electrolyte loses its dissolved sulphuric acid and becomes primarily water [1]. Lead-acid battery has a typical service life from 5 to 15 years with high reliability and efficiency (70-90%) [1, 12]. Several types of lead acid batteries are available. Lead-acid batteries are popular storage choice for power quality,

uninterruptable power supply (UPS) and some spinning reserve applications but in case of energy management applications they are very limited due to their short cycle life (500-1000 cycles) and low energy density (30-50 Wh/kg) [1].

Lithium-ion batteries

Lithium is the lightest metal with the highest potential due to its very reactive behavior which, in theory, makes it very fitting as a compound for batteries. The first lithium-ion battery is proposed in the 1960s and then, the first commercial lithium-ion batteries came into the market by Sony in 1990. Later in 2000, Lithium ion batteries have become the most important storage technology in the areas of portable and mobile applications like laptop, cell phone, electric bicycle and electric car. These progresses are still increasing according to the improvements of used materials in this type of batteries and of characteristics of battery like energy density, life cycle and the battery efficiency. For example, the energy density increased from 75 to 200 Wh/kg and life cycle increased to as high as 10,000 cycles [1, 12].

In this kind of battery the cathode is a lithiated metal oxide and the anode is made of graphitic carbon with a layering structure. The construction looks somehow similar to a capacitor, when it uses three different layers curled up in order to minimize space. The first layer acts as the anode and is made of a lithium compound; the second layer is the cathode and it is usually made of graphite. The third layer which is located between anode and cathode is the separator that separates them while allowing lithium-ions to pass through. The separator can be made of various compounds allowing different characteristics and, accordingly, different benefits and flaws. In addition, the three layers are submerged in an organic solvent. Electrolyte is allowing the ions to move between the anode and the cathode. In the charging process, the lithium ions pass through the micro porous separator into spaces between the graphite (though not compounded), receiving an electron from the external power source.

Li-ion batteries are used in more than 50% of the small portable devices and since 2000 have successfully begun to enter industrial markets. But there are some important challenges to provide large scale Li-ion batteries. Also the cost of this type of batteries due to using special packing and internal overcharge protection circuit are still high (more than 600 $$/kWh$) [1].

The implementation of Li-ion batteries in the stationary field has significantly increased since 2010 and has benefited from the extensive experience gained in the development of batteries for electric and hybrid vehicles. About 100 MW of stationary Li-ion batteries are operating worldwide in grid connected installations. Systems in association with distributed renewable generators from a few kW to several MW , as well as for grid support with voltages up to 6000V have been designed and successfully tested [13].

Nickel-cadmium batteries

Along with lead-acid batteries, a Nickel-cadmium battery (Ni-Cd) is also ranked in terms of maturity and popularity. Ni-Cd batteries include a nickel hydroxide positive electrode plate, a cadmium hydroxide negative electrode plate, a separator, and an alkaline electrolyte. Ni-Cd batteries usually have a metal case with a sealing plate equipped with a self-sealing safety valve. The positive and negative electrode plates, isolated from each other by the separator, are rolled in a spiral shape inside the case.

In case of battery energy density, Ni-Cd batteries have a high energy density (50-75 Wh/kg) and they can provide robust reliability with very low maintenance requirements. Their

relatively cycle life is in the range of 2000 to 2500. These mentioned advantages of Ni-Cd make them favored over lead acid batteries for power tools, portable devices, emergency lighting, UPS, telecoms and generator starting. However, portable devices such as mobile telephones and laptops have effectively been displaced from these markets by other electro chemistries over the past decade.

An important disadvantage of Ni-Cd batteries is their relatively high cost (800-1500 $\$/kWh$) due to the expensive manufacturing process. Cadmium is a toxic heavy metal hence posing issues associated with the disposal of Ni-Cd batteries. Ni-Cd batteries also suffer from “memory effect”, where the batteries will only take full charge after a series of full discharges. Proper battery management procedures can help to mitigate this effect [1].

They serve special markets where energy must be stored in extreme climate or cycling or fast charging conditions.

Sodium sulphur batteries

A sodium sulphur (NaS) battery consists of liquid (molten) sulphur at the positive electrode and liquid (molten) sodium at the negative electrode as active materials separated by a solid beta alumina ceramic electrolyte [1, 14]. NaS batteries have a typical cycle life of 2500 cycles. Also, typical energy and power density of them are in the range of 150-240 Wh/kg and 150-230 W/kg , respectively. Efficiency of NaS battery cells is in the range of 75% to 90% and they have a pulse power capability over six times their continuous rating (for 30s). This attribute enables NaS batteries to be economically used in combined power quality and peak shaving applications. The first demonstration of the NaS system in America is launched by American Electric Powers in Ohio with a capacity up to 1.2 MW. The major disadvantage is that a heat source is required which uses own stored energy of the battery, partially reducing the battery performance, as the NaS battery needs to operate at a high temperature (300-350°C). Another disadvantage is initial capital cost (300-500 $\$/kWh$), but it is expected to fall as the manufacturing capacity is expanding [1].

Sodium nickel chloride

Sodium nickel chloride battery is better known as the ZEBRA battery [1, 15, 16]. This type of batteries are high temperature (300°C) systems which use nickel chloride as positive electrode and have the ability to operate across a broad temperature range from -40 to +70°C without cooling. ZEBRA batteries can withstand limited overcharge and discharge and have potentially better safety characteristics and a high cell voltage in comparing with NaS batteries (2.58V).

The drawbacks with respect to NaS batteries are their low energy density (100-120 Wh/kg) and power density (150-200 W/kg), although the former still represents a considerable improvement over the lead acid battery technology. Another disadvantage is that only one company, the Beta R&D (UK), in the world produces this kind of battery and the technology was acquired by MES (Swiss) in 1999. At present Beta R&D is developing a high power version of the ZEBRA battery for hybrid electric vehicles, a high energy version for storing renewable energy and a load-levelling battery for industrial applications [15, 16]. The application of the ZEBRA batteries in the new NATO Submarine Rescue System (NSRS) has also been announced recently. Table 1.1 compares the characteristics of above mentioned technologies of batteries [1].

Technology	Power rating (MW)	Self-discharge (% per day)	Energy density (Wh/kg)	Power density (W/kg)	Life time (year)	Cycle life (cycle)	Capital cost (\$/kWh)
Lead-acid	0 - 20	0.1 - 0.3	30 - 50	75 - 300	5 - 15	500 - 1000	200 - 400
Li-ion	0 - 0.1	0.1 - 0.3	75 - 200	150 - 315	5 - 15	1000 - 10000	600 - 2500
Ni-Cd	0 - 40	0.2 - 0.6	50 - 75	150 - 300	10 - 20	2000 - 2500	800 - 1500
NaS	0.05 - 80	20	150 - 240	150 - 230	10 - 15	2500	300 - 500
ZEBRA	0 - 0.3	15	100 - 200	150 - 200	10 - 14	2500	100 - 200

Table 1.1: Characteristics of different battery technologies.

1.1.3. Characteristics

Various types of BESSs with different technical and economical characteristics relied on their manufacturing technology are available in the market. To select the best technology of BESSs for the specific application, it is necessary to analyze the following fundamental characteristics of BESSs [2, 17, 18].

Storage capacity

Storage capacity is the available energy in the BESS after charging. Discharge is often incomplete. It is defined on the basis of total energy stored, W_{st} (Wh), which is superior to that actually retrieved (operational), W_{ut} (Wh). The usable energy which is limited by the DOD represents the limit of discharge depth (minimum-charge state). In conditions of quick charge or discharge, the efficiency deteriorates and the retrievable energy can be much lower than storage capacity. On the other hand, self-discharge is the attenuating factor under very slow regime [2, 17, 18].

Depth of discharge

Energy storage is a slow process that subsequently must quickly release energy on demand. The power output, or discharge, can be a limiting factor called the power transmission rate. This delivery rate determines the time needed to extract the stored energy [17- 18]. In many types of batteries, the full energy stored in the battery cannot be fully discharged without causing serious and often irreparable damage to the battery. The Depth of Discharge (DOD) of a battery determines the fraction of power that can be withdrawn from the battery. For example, if the DOD of a battery is given by the manufacturer as 25%, then only 25% of the battery capacity can be used by the load.

Almost all batteries, particularly for renewable energy applications, are rated in terms of their capacity. However, the actual energy that can be extracted from the battery is often

significantly less than the rated capacity. This occurs since, extracting the full battery capacity from the battery dramatically reduced battery lifetime. For example, a lead-acid battery operated with a DOD of 20% has a lifetime of 2800 charging/discharging cycles, while with a DOD of 80% the lifetime is about 500 cycles (figure 1.2) [19,20].

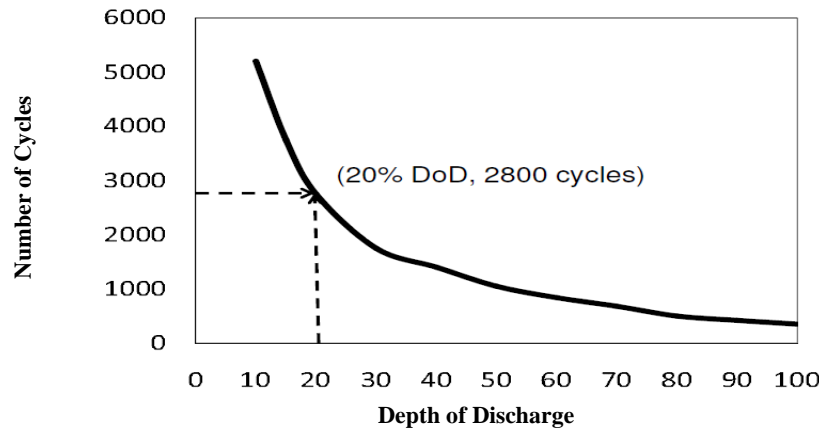


Figure 1.2: Depth of discharge for lead-acid battery [20].

Discharge time

It is the maximum power discharge duration of battery, $\tau = W_{st} / P_{max}$, which depends on the DOD and operational conditions of the system, constant power or not. It is a characteristic of system adequacy for certain applications [17]. The discharge time is usually referred as *C-rate* or *E-rate*. A *C-rate* is a measure of the rate at which a battery is discharged relative to its maximum capacity. A *1C* rate means that the discharge current will discharge the entire battery in 1 hour. For a battery with a capacity of 100 Ah, this equates to a discharge current of 100 A. A *5C* rate for this battery would be 500 A, and a *C/2* rate would be 50 A. Similarly, *E-rate* describes the discharge power. A *1E* rate is the discharge power to discharge the entire battery in 1 hour [21].

Efficiency

All energy transfer and conversion processes have losses. Storage system round-trip efficiency (efficiency) reflects the amount of energy that comes out of storage relative to the amount put into the storage [22]. The efficiency for BESS is the ratio between released energy (W_{ut}) and stored energy (W_{st}), $\eta = W_{ut} / W_{st}$. This definition is often oversimplified because it is based on a single operation point [23]. Yet, systems have charging, no-load, and self-discharge losses. The definition of efficiency must therefore be based on one or more realistic cycles for a specific application. Instantaneous power is a defining factor of efficiency. In more details, the efficiency can be discussed with the reference of rectifier efficiency (η_{rec}), inverter efficiency (η_{inv}), storage efficiency (η_{st}) and storage self-discharge ($\eta_{selfdch}$). For example, η_{st} for lead-acid battery is 85% while it is 95% for Li-ion and 75% for Ni-Cd. With reference to other efficiencies, rectifier, inverter and self-discharge efficiency for the best case of lead acid battery are 95%, 98% and 0%, respectively [24]. Self-discharge efficiency can be neglected for the technology scenarios due to short time periods between charge and discharge cycles.

Mass and volume densities of energy

These represent the maximum amounts of energy accumulated per unit of mass or volume of the storage unit, and demonstrate the importance of mass and volume for certain applications (especially for mass density of energy in portable applications, but less so for permanent applications).

Reliability

Reliability of BESS is always an important factor because it is a guarantee of on demand service [17].

Operational constraints

This characteristic of BESS is specially related to the safety or other operational conditions like temperature, pressure, etc. They can influence the choice of a BESS's technology as a function of energy needs [17].

Environmental aspects

While this parameter is not a criterion of storage system capacity, the environmental aspect of the product (recyclable materials) is a strong sales pitch. For example, in Nordic countries (Sweden, Norway), a definite margin of the population prefers to pay more for energy than to continue polluting the country [25]. This is a dimension that must not, therefore, be overlooked.

Other characteristics

The ease of maintenance, simple design, operational flexibility (this is an important characteristic for the utility) and fast response time for the release of stored energy are other considerable characteristics of BESS. Finally, it is important to note that these characteristics apply to the overall storage system: storage units and power converters.

1.1.4. Costs

Economic analysis of BESSs considers all the costs related to the inclusion of the BESS into the grid. To evaluate the total costs related to the BESS adoption, capital, maintenance, replacement, disposal and energy costs have to be taken into account [26]:

$$C_{LCC} = C_0 + C_{mt} + C_{rep} + C_{disp} + C_{en} \quad (1.1)$$

Where C_{LCC} is the life cycle cost (or total customer cost), C_0 is the capital cost of the BESS, C_{mt} is the BESS maintenance costs, C_{rep} is the cost related to the replacement of the batteries, C_{disp} is the BESS disposal cost and C_{en} is the energy cost. The maintenance, replacement and energy costs refer to their sum over the specified time period in which the economic analysis is performed. The net present value of the maintenance, replacement and energy costs have to be calculated as:

$$C_k(n)_{npv} = C_k(n) \frac{(1+\alpha)^{n-1}}{(1+\beta)^{n-1}} \quad (1.2)$$

where $C_k(n)$ is the cost (energy, maintenance and replacement cost) related to year n , $C_k(n)_{npv}$ is its net present value, β is the assumed discount rate and α is the effective rate of change assumed for the cost in the years.

Capital cost

It includes equipment purchase cost and installation cost. Both the cost of the battery system C_{batt} and the converter C_{conv} are considered:

$$C_0 = C_{batt} + C_{conv} \quad (1.3)$$

C_0 is calculated by adding the cost of the storage unit (C_{batt}) and the power conditioning system (C_{conv}). These subsystems are treated separately because they provide different functions and are priced by different ratings. Power components are priced in $$/kW$ and energy storage units are priced in $$/kWh$. For this reason, the individual subsystem costs are needed, although they are often difficult to separate from vendor system prices. Table 1.2 compares these costs for different BESS technologies [27]. The actual costs of any storage system depend on many factors and the assumptions and the means of calculating some of the values used are subjective and continue to be debated, even among experts in the field. The cost of the power conversion equipment is proportional to the power rating of the system.

Technology	Efficiency (%)	Power subsystem cost ($$/kW$)	Energy storage cost ($$/kWh$)
Lead-acid	80	400	300
Li-ion	85	400	600
NaS	75	350	350

Table 1.2: Capital cost components for different BESS technologies [27].

Maintenance cost

BESS maintenance cost includes corrective maintenance and preventive maintenance costs [28]. They can also be included as percentage of capital costs [29]. For example, the annual maintenance cost as percentage of the initial investment for the lead acid battery is 2% [24].

Replacement cost

Replacement costs have to be sustained for purchasing a new battery if the battery lifetime is lower than the time period considered in the economic analysis. The life time of the battery, expressed in years, depends on the number of charging/discharging stages per day:

$$\text{Battery lifetime} = \frac{N_{cycles}}{365 * v} \quad (1.4)$$

where N_{cycles} is the total number of charging/discharging cycles declared by the battery manufacturer and v is the number of daily charging/discharging cycles.

Disposal cost

With reference to the BESS disposal cost, it is assumed that they can take into account also the benefit derived from the recycling of the battery. This cost/benefit may vary depending on the country where the disposal is performed. Based on the expected development of recycling technology, disposal activity could also be assumed to represent a benefit rather than a cost [30].

Energy cost

The energy cost (C_{en}) can be evaluated as follows:

$$C_{en} = C_{ch} - C_{dch} \quad (1.5)$$

where C_{ch} is the electricity cost sustained for charging the battery and C_{dch} is that avoided by the customer as loads are supplied by the BESS. Both C_{ch} and C_{dch} depend on the energy tariff applied to the customer and on the battery operation strategy, as it will be shown in the next Chapter. Utilities usually propose different tariffs depending on the periods (season) of the year [31]. In the evaluation of the energy costs in (1.5) the variations of the price of energy due to the inflation can be taken into account by imposing a percentage variation per year. Eventually, by substituting (1.5) in (1.1) the total customer cost will be:

$$C_{LCC} = C_0 + C_{mt} + C_{rep} + C_{disp} + C_{ch} - C_{dch} \quad (1.6)$$

1.2. Smart grid

Power systems have been undergoing radical changes in recent years, and their planning and operation will be surely undertaken according to the SG vision in the near future. The SG initiatives aim at introducing new technologies and services in power systems, to make the electrical networks more reliable, efficient, secure and environmentally-friendly. In particular, it is expected that communication technologies, computational intelligence and distributed energy sources will be widely used for the whole power system in an integrated fashion [32]. In particular, nowadays, unprecedented challenges like as stringent regulations, environmental concerns, growing demand for high quality, reliable electricity and rising customer expectations are forcing utilities to rethink about electricity generation and delivery from the bottom up [33]. Moreover, the availability of low cost computing and telecommunications technologies, new generation options, and scalable, modular automation systems push utilities to be dynamic, innovative and ambitious enough to take advantage of them. Driven by the dynamics of the new energy environment, leading utilities, technology vendors and government organizations have created a vision of the next generation of energy delivery systems: the Smart Grid.

1.2.1. Structure

In the 21st century's energy equation, environmental and economic sustainability are essential variables. But existing infrastructure and systems lack the flexibility to evolve to meet higher demands for efficiency and reliability. Then, SGs will return balance to this "cost-benefit" paradigm by introducing intelligent response into the interaction between supply availability and demand [33].

Similar to the internet (a dynamic network), the SG will be interactive for both power generation sources and power consumption sinks (loads). Utilities will enable end-users to produce their own electricity and participate in demand-side management (DSM) programs. The gateway for access to the grid of the future is supported by a high-speed, two-way communication infrastructure, intelligent metering and electronic control technologies. In this context, utilities are investing an enormous amount of money in smart meters and advanced metering infrastructure in the first step towards implementing the SG. At the utility level, Information and Communication Technology (ICT) and business process integration will be valuable tools in the real-time management of the value chain across suppliers, active networks, meters, customers and corporate systems. In case of transmission and distribution infrastructure, the SG will be a web-like network of interconnected nodes with no “beginning” or “end”. Consumers and generators of all sizes will be tied together with new grid components, such as energy storage units and intermittent renewable supplies. Like a living organism, the grid will control energy flow to dynamically balance changes in supply and demand. IT and automation systems will act as the central nervous system by collecting and processing the massive amounts of sensory data coming in from the extremities and control system elements. Refer to figure 1.3 for a visual representation of the smart grid structure [32, 33].

1.2.2. Components

At the physical level, SG is comprised of the following five fundamental components [32].

New grid components

Distributed energy components, such as residential-scale Combined Cycle Heat and Power (CCHP) units, Plug-in Hybrid Electric Vehicles (PHEV), micro-turbines, solar photovoltaic cells, wind turbines and grid energy storage units enable increased bi-directional power flow between power distributors and end-users.

Sensing and control devices

Sensing and control devices evaluate congestion and grid stability, monitor equipment health, prevent energy theft and support control strategies. Technologies include: advanced microprocessor meters (smart meter) and meter reading equipment, wide-area monitoring systems, dynamic line rating systems, electromagnetic signature measurement/analysis, time-of-use and real time pricing tools, advanced switches and cables, backscatter radio technology and digital protective relays.

In particular, a SG replaces analog mechanical meters with digital meters used in real time. Smart meters are similar to advanced metering infrastructure meters and provide a communication path extended from generation plants to electrical outlets (smart socket) and other SG enabled devices. By customer option, such devices can shut down during times of peak demand.

Communications infrastructure

Transferring massive amounts of data in the SG by communication networks are based on fiber-optics, microwave, infrared, power line carrier (PLC), and/or wireless radio networks. Some communications are up to date, but are not uniform because they have been developed in an incremental fashion and not fully integrated.

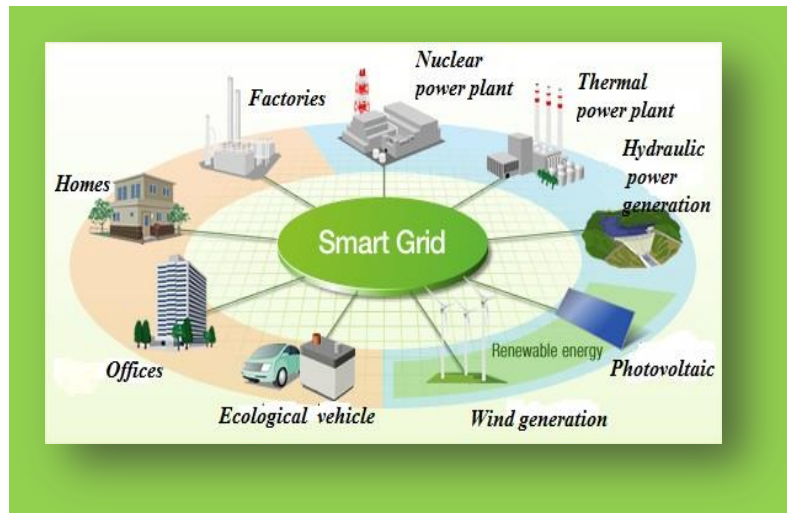


Figure 1.3: Smart grid structure [33].

In most cases, data is being collected via modem rather than direct network connection. In order to improve this part of grid, there are different areas for improvement which are substation automation, demand response, distribution automation, supervisory control and data acquisition (SCADA), energy management systems, wireless mesh networks and other technologies, power-line carrier communications, and fiber-optics. Integrated communications will allow for real-time control, information and data exchange to optimize system reliability, asset utilization, and security.

Automation and IT backend technologies

In case of specific grid disruptions or outages, automation can provide rapid diagnosis of precise solutions. These technologies rely on and contribute to each of the other four key areas. Three technology categories for advanced control methods are as follows:

- Distributed intelligent agents (control systems)
- Analytical tools (software algorithms and high-speed computers)
- Operational applications (SCADA, substation automation, DR, etc.)

Technologies for advanced analysis

Grid operators, project managers and business executives can analyze and extract useful information from the grid based on the advanced applications with increased functionality and versatility. When information systems reduce complexity then operators and managers have tools to effectively and efficiently operate a grid with an increasing number of variables. Technologies include visualization techniques that reduce large quantities of data into easily understood visual formats, software systems that provide multiple options when systems operator actions are required, and simulators for operational training and “what-if” analysis.

1.2.3. Challenges

Based on adding new components to the grid, the new operating strategies challenge the security, reliability and quality of the electric power supply. For example, implementation of intermittent energy resources, such as wind, will greatly stress transmission grid operations. The distribution grid will be stressed by solar generation as well as plug-in electric vehicles

(PEVs). PEVs could significantly increase the circuit loading. These intermittent renewable resources pose many challenges for the grid and grid operators and pushes for the adoption of ESSs. Also, there are challenges with the implementation of a SG information technology system where most utility companies have limited interoperability across the different systems for operations and business management. But, economics aspects of these resources are fast improving, reaching a close parity with fossil generation. Some of these challenges are presented as follows [32, 33].

Challenges in transmission system

One of the important challenges for DG sources is the distance from transmission lines because good sites for wind or large-scale solar plants (greater than 100 MW) may be located in areas distant from any existing transmission lines or areas with limited available transmission capacity. These capacity limits are also the most fundamental constraint facing wind power project developers, since it can take many years to plan and build new transmission infrastructure. Planning for transmission expansion to support increasing levels of wind generation in dispersed areas is essential to the growth of the wind sector.

Planning and system stability studies also are needed to determine seasonal requirements for up regulation, down regulation (seconds) and ramping (minutes) capacities. It is significant that higher levels of regulation and ramping capacity might not be readily available in regions with a thermal and nuclear generation base. Long-term resource adequacy issues also need to be addressed.

Challenges in distribution system

Residential and municipal solar generation as well as PEVs can impose challenges for the existing distribution infrastructure and the system operator. New flow patterns may require changes to the protection and control strategies, enhanced distribution automation and micro-grid capabilities, voltage and var management, and overall enforcement of distribution grid infrastructure.

End-use customer challenges

By moving from traditional load managements to the new load management strategies, such as peak shaving and peak shifting in the framework of SG, then end use consumers will face some challenges. For example, in addition to the traditional load management, advanced metering infrastructures to develop the dynamic pricing programs and using end use devices such as intelligent applications and smart chargers are needed. Challenges are involved also from the application of BESSs that can have a significant role for an end-use, because they provide the possibility of absorbing energy from the grid in the charging condition (i.e., load mode) and of supplying the loads in discharging operating conditions (i.e., generator mode) and have the ability to change their operating condition very quickly. In addition, BESSs are ideal candidates for performing peak shaving, which is an important service for some high-consumption customers (e.g., industrial customers).

Operational challenges

The grid will face the operational challenges in the transmission, distribution and end-use levels due to the presence of renewable resources and new components, when intermittent nature of the wind and solar generation can cause certain operational challenges in

transmission grid, including additional ramping and regulation requirements and impacts on system stability. Also, the distribution grid will be stressed with the introduction and rapid adaptation of solar generation as well as PEVs. For example, PEVs can increase the distribution network load if charging and discharging time and schedules are not properly managed and controlled. In case of wind generation resources, due to the steepness of the wind turbine power curve, a wind farm creates significant ramping needs as wind speed changes, with the wind farm typically operating at either low output or high output at any given time. At high wind speeds, the turbine controls cut-off the power generation to prevent damage to the blades and the turbine-generator assembly due to over speed and possible tensional oscillation. This power cut-off poses additional operational challenges due to a very steep reduction in generation levels. These new operating strategies when combined with the available transmission and distribution infrastructure challenge the security, reliability and quality of the electric power supply.

Forecasting and scheduling challenges

The grid operators need forecasting and scheduling to supply the additional ancillary services when there are limited dispatch ability and intermittent nature of wind and solar generation. For example, according to the California Independent System Operator, an additional 350 MW of regulation and 800 MW of ramping capacity will be needed to support the planned 9,000 MW of new wind generation capacity. The large penetration of renewable generation sources may also lead to over generation conditions.

Accurate day-ahead, hourly and sub hourly wind and solar generation forecasting is needed to allow for other unit commitment and ancillary service provision as well as the scheduling and dispatch of the required hourly ramping and load following.

Regional scheduling practices for intermittent resources need to be further enhanced to address banking and shaping in addition to energy balancing needs. Energy storage, DR, distributed resource management, and the dispatch of wind and solar resources could partially alleviate some of these challenges.

Interconnection standards challenges

To mitigate any transient stability issues the interconnection standards may have to be further unified and broadened to address greater levels of power factor control and low-voltage ride through needed.

Other challenges associated with smart grid projects

- *No clearly defined end state.* Function of many external factors like as economy, oil prices, political and regulatory mandates are the driving forces for the SG. Then, the requirements and the timing of the end state are not established well enough to allow the development of detailed technical and business specifications.
- *The incremental and evolving nature of the applications.* Many of the changing requirements are incremental with respect to the existing capabilities.
- *The many legacy business functions and systems they touch.* SG functions touch many existing operational systems and business processes. As such, an implementation plan endorsed by all stakeholders will be required.

- *A rollout with minimum impact on existing operations.* The reliable supply of electric power cannot be disrupted, and incremental additions should not have any negative impact on the existing and unaffected operations.
- *The required data interfaces with external and third party systems.* Cybersecurity and integration issues need to be addressed where the SG requires interfaces with external users and systems, including smart devices, customers, service providers, and energy markets.
- *The high cost of implementation.* The business cases for SG initiatives should be made based on operational and societal benefits. The regulatory framework for rate based SG projects needs to be further strengthened.

1.2.4. Advantages

Based on all improvements by adding new components and control features to the grid the following characteristics and advantages can be considerable for the grid [32, 33].

Grid integration

One of the greatest engineering projects of this century will be the national integration of all levels of the transmission and distribution networks. Once geographically dislocated, electric power grids are now being expanded and transformed into millions of interconnected nodes. Grid integration enables utilities to deliver a highly secure and efficient electricity supply with reduced environmental impact by allowing for interregional power transactions, added capacity, and network redundancy.

Self-healing and adaptive

The SG will perform continuous self-assessments to monitor and analyze its operational status. For problems that are too large and too fast for human intervention, it will automatically restore grid components or network sections after abnormal events via “self-healing” mechanisms. The SG will also be capable of predicting potential failures and future outages by mining data from past events.

Interaction with consumers

SG concept is based on the high technology communication lines and smart components, then based on this concept SG will motivate end-users to actively manage their energy consumption. For example, price signals and DR programs will encourage consumers to modify consumption based the electric system’s capacity to meet their demands. Some factors like as new cost saving and energy efficiency products will plug consumers back into the network and make them active participants in the grid.

Enhanced cyber security

Nowadays, enhanced security is an important characteristic of the SG when society is increasingly aware of the criticality of energy delivery infrastructure and the need for defense against malicious attack and disruption. The SG’s integrated security systems will reduce physical and cyber vulnerabilities and improve the speed of recovery from disruptions and security breaches. SG security protocols will contain elements of deterrence, prevention, detection, response and mitigation, and a mature SG will be capable of thwarting multiple,

coordinated attacks over a span of time. Enhanced security will reduce the impact of abnormal events on grid stability and integrity, ensuring the safety of society and the economy.

Improved quality of power

Designed and constructed over a half a century ago, existing grid infrastructure cannot meet the demands of today's digital economy for reliable, high quality electric power. As part of the SG, new power quality standards will enable utilities to balance load sensitivity with power quality, and consumers will have the option of purchasing varying grades of power quality at different prices. Additionally, power quality events that originate at the transmission and distribution level of the grid will be minimized, and irregularities caused by certain consumer loads will be buffered to prevent propagation.

Integration of a wide variety of generation options

Wide variety of generation options will be available in the SG at all voltage levels. Residential and commercial users will increasingly adopt distributed energy resources such as roof-top solar panels and advanced batteries as economically viable options for meeting on-site energy needs, and reducing their carbon footprint as good stewards of the environment. Improved grid-tie standards will enable interconnection at all voltage levels. And improved communications protocols and grid intelligence will allow distributed generation resources to seamlessly integrate with the grid in a "plug-and-play" fashion, where users can sell excess power back to the grid at peak-hours based on real-time market pricing. At the same time, large central power plants, including environmentally-friendly sources such as wind farms and advanced nuclear plants will continue to play a major role in the grid of the future.

Interaction with energy markets

The SG will enable energy markets to flourish, exposing and mitigating resource allocation inefficiencies. For instance, parameters such as total energy, capacity, congestion, and environmental impact may be most efficiently managed through the supply and demand interactions of markets. Market participation will be encouraged through increased transmission paths, aggregated DR initiatives and the rise of distributed energy resources as discussed above. Moreover, by reducing congestion, the SG also expands markets by bringing more buyers and sellers together. Real-time pricing will allow consumers to respond dynamically to price increases, spurring lower-cost solutions and technology development. For consumers wishing to reduce their carbon footprint, they will have the option to purchase new, clean energy products from a mix of renewable sources.

Increased grid visibility

The SG's ubiquitous sensing infrastructure and backbone communications network will enable network operators to have greater grid observability into the grid's operational status, particularly with respect to the historically "blind" spots of the distribution networks. Aided by advanced visualization tools, operators will be able to quickly and accurately identify critical information, allowing them to provide essential human oversight to automated processes.

Optimized asset and resource management

Increased asset life and optimized operations are a major objective for the SG. Advanced information technologies will provide a vast amount of data and information to be integrated

with existing enterprise-wide systems, giving utilities the power to significantly enhance their operations and maintenance processes. This same information will allow engineers to improve equipment design, and give network planners the data they need to improve their processes.

1.3. Applications of battery energy storage system in smart grid

Operational changes of the grid, caused by restructuring of the electric utility industry and electricity storage technology advancements, have created an opportunity for storage systems to provide unique services to the evolving grid. Especially BESSs, due to the large number and variety of services they can provide, are powerful tools for the solution of some challenges that future grids will face. This consideration makes a BESS as a critical component of the future grids. The BESS can be applied for different services into the different level of power system chain to satisfy technical challenges and provide financial benefits. Some of these services are listed in the table 1.3 and discussed in the following sections [22, 34].

Generation unit services	Bulk energy services
	Electric energy time shift (Arbitrage)
	Ancillary services
	Regulation
	Spinning, non-spinning and supplemental reserves
	Frequency response
Transmission unit services	Transmission upgrade deferral
	Transmission congestion relief
Distribution unit services	Load levelling
	Distribution upgrade deferral
	Voltage support
Customer unit services	Power quality
	Power reliability
	Peak shaving
	Demand response

Table1.3: BESS services in the different levels of the grid [22].

1.3.1. Generation unit services

Services which are applicable to the generation level of the grid are considered as bulk energy and ancillary services.

Electric energy time-shift (Arbitrage)

One of bulk energy services is electric energy time-shift which involves purchasing inexpensive electric energy, available during periods when prices or system marginal costs are low, to charge the BESS so that the stored energy can be used or sold at a later time when the price or costs are high. Alternatively, in the generation level from renewable sources such as wind or PV, storage can provide similar time-shift duty by storing excess energy production.

In this service, both BESS variable operating cost (non-energy-related) and BESS efficiency are especially important. Electric energy time-shift involves many possible transactions with economic merit based on the difference between the cost to purchase, store, and discharge energy (discharge cost) and the benefit derived when the energy is discharged.

Regulation

Regulation is one of the ancillary services of BESS that involves managing interchange flows with other control areas to match closely the scheduled interchange flows and momentary variations in demand within the control area. Regulation is used to reconcile momentary differences caused by fluctuations in generation and loads. It is used for damping that difference. Figure 1.4 shows an example that compares a load demand profile with and without regulation. The load demand is faced many variations without regulation (yellow line) while these variations are controlled by regulation service (gray line) [22].

Regulation service is applicable for generating units which are online and ready to increase or decrease power as needed and their output is increased when there is a momentary shortfall of generation to provide up regulation. Conversely, regulation resources' output is reduced to provide down regulation when there is a momentary excess of generation.

An important consideration in this case is that large thermal base-load generation units in regulation incur significant wear and tear when they provide variable power needed for regulation duty.

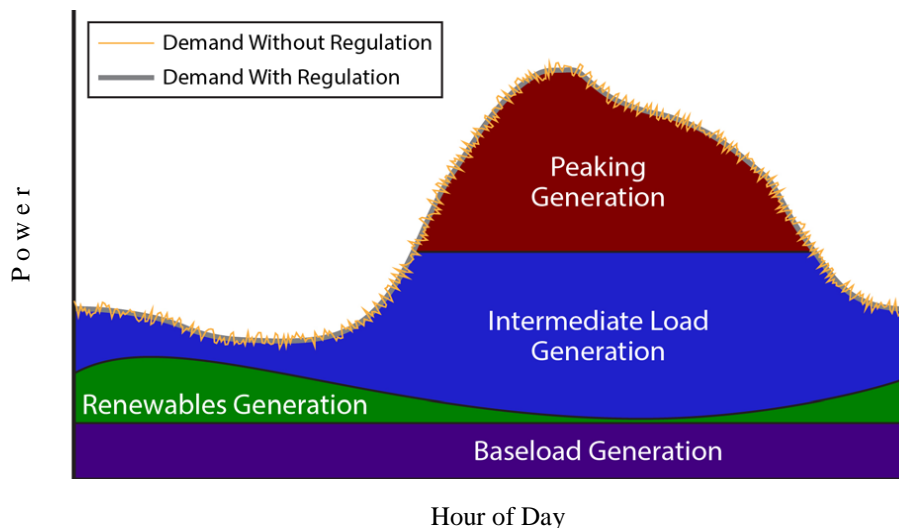


Figure 1.4: Load demand with and without regulation [22].

Spinning, non-spinning and supplemental reserves

When some portions of the normal electric supply resources become unavailable unexpectedly, then a reserve capacity is requested to provide continuous operation in the electric grid. Generally, reserves are at least as large as the single largest resource (e.g., the single largest generation unit) serving the system and reserve capacity is equivalent to 15% to 20% of the normal electric supply capacity [22].

- *Spinning reserve (Synchronized)*: generation capacity that is online but unloaded and that can respond within about 10 minutes to compensate for generation or transmission outages.
- *Non-spinning reserve (Non-synchronized)*: generation capacity that may be offline or that comprises a block of curtailable and/or interruptible loads and that can be available within about 10 minutes.

- *Supplemental reserve*: generation that can pick up load within one hour. Its role is, essentially, a backup for spinning and non-spinning reserves. Backup supply may also be used as backup for commercial energy sales. Unlike spinning reserve capacity, supplemental reserve capacity is not synchronized with grid frequency. Supplemental reserves are used after all spinning reserves are online. Importantly for storage, generation resources used as reserve capacity must be online and operational (i.e., at part load). Unlike generation, in almost all circumstances, storage used for reserve capacity does not discharge at all; it just has to be ready and available to discharge when needed.

Frequency response

Another applicable service of BESS is frequency response that is very similar to regulation, described above, except it reacts to more general system needs in even shorter time periods of seconds to less than a minute when there is a sudden loss of a generation unit or a transmission line. The size of storage systems to be used in frequency response mode is proportional to the grid or balancing area in which they are needed. Generally, storage systems up to 20 MW and greater size can provide effective frequency response due to their fast action. However, location of the storage system within the grid with respect to other generation, transmission corridors and loads plays a crucial role in the effectiveness as a frequency response resource.

1.3.2. Transmission unit services

In case of transmission unit services, transmission upgrade deferral and transmission congestion relief are popular services which are explained in the following lines:

Transmission upgrade deferral

This service involves delaying, in some cases avoiding entirely, utility investments in transmission system upgrades by using relatively small amounts of storage. Let us consider a transmission system with peak electric loading that is approaching the system's load-carrying capacity (design rating). In some cases, installing a small amount of energy storage downstream from the nearly overloaded transmission node could defer the need for the upgrade for a few years [22].

The key consideration is that a small amount of storage can be used to provide enough incremental capacity to defer the need for a large lump investment in transmission equipment. Doing so reduces overall cost to ratepayers, improves utility asset utilization, allows use of the capital for other projects, and reduces the financial risk associated with lump investments. Notably, for most nodes within a transmission system, the highest loads occur on just a few days per year, for just a few hours per year. Often, the highest annual load occurs on one specific day with a peak somewhat higher than any other day. One important implication is that storage used for this application can provide significant benefits with limited or no need to discharge. Given that most modular storage has a high variable operating cost, this may be especially attractive in such instances.

Although the emphasis for this application is on transmission upgrade deferral, a similar rationale applies to transmission equipment life extension. That is, if storage use reduces loading on existing equipment that is nearing its expected life, the result could be to extend

the life of the existing equipment. This may be especially compelling for transmission equipment that includes aging transformers and underground power cables.

Transmission congestion relief

Transmission congestion occurs when available, least-cost energy cannot be delivered to all or some loads because transmission facilities are not adequate to deliver that energy. When transmission capacity additions do not keep pace with the growth in peak electric demand, the transmission systems become congested. Thus during periods of peak demand, the need and cost for more transmission capacity increases along with transmission access charges. Transmission congestion may also lead to increased congestion costs or locational marginal pricing (LMP) for wholesale electricity at certain transmission nodes.

Electricity storage can be used to avoid congestion-related costs and charges, especially if the costs become onerous due to significant transmission system congestion. In this service, storage systems would be installed at locations that are electrically downstream from the congested portion of the transmission system. Energy would be stored when there is no transmission congestion, and it would be discharged (during peak demand periods) to reduce peak transmission capacity requirements.

1.3.3. Distribution unit services

Among several services of BESS for different parts of the power system, load leveling, voltage support and distribution upgrade deferral are applied into the distribution level of the grid. These services and their technical and economic benefits are presented in the following.

Load leveling

Load leveling is a service addressed to the distribution utility for reducing the fluctuations of the load demand along the day. Load leveling can be achieved by using ‘demand side’ measures which reduce the peak demand or by using storage systems able to store energy during light load hours and discharge it during peak load hours. In this case, the installation of a BESS at the secondary side of the transformer of a distribution substation allows for a minimization of the difference between the mean and peak power requests. One of the main advantages for the distribution system operator based on using BESS is related to avoid new investments in transmission and distribution facilities [35].

Distribution upgrade deferral and voltage support

Distribution upgrade deferral involves using storage to delay or avoid investments that would otherwise be necessary to maintain adequate distribution capacity to serve all load requirements. The upgrade deferral could be a replacement of an aging or over-stressed existing distribution transformer at a substation or reconductoring distribution lines with heavier wire. A storage system allows not only deferring the upgrade decision point, but also allows time to evaluate the certainty that planned load growth will materialize, which could be a two-year to three-year window. Notably, for most nodes within a distribution system, the highest loads occur on just a few days per year, for just a few hours per day. Often, the highest annual load occurs on one specific day with a peak somewhat higher than any other day. One important implication is that storage used for this application can provide significant benefits with limited or no need to discharge.

A storage system that is used for upgrade deferral could simultaneously provide voltage support on the distribution lines. Utilities regulate voltage within specified limits by tap changing regulators at the distribution substation and by switching capacitors to follow load changes. This is especially important on long, radial lines where a large load such as an arc welder or a residential PV system may be causing unacceptable voltage excursions on neighboring customers. These voltage fluctuations can be effectively damped with minimal draw of real power from the storage system [22].

1.3.4. End-use customer unit services

With reference to the end-use costumers, various services of BESS, including power quality, power reliability, peak shaving and cost management, can provide advantages in terms of power quality and reliability improvement as well as reduction of electricity bill costs for the end-use costumers. Some of these services and their advantages are reported as follows [22, 36].

Power quality

The electric power quality service involves using storage to protect customer on-site loads downstream (from storage) against short-duration events that affect the quality of power delivered to the customer's loads. The use of BESSs can enhance solutions also to compensate harmonic disturbances.

Power reliability

A storage system can effectively support customer loads when there is a total loss of power from the source utility. This support requires the storage system and customer loads to island during the utility outage and resynchronize with the utility when power is restored. The storage system can be owned by the customer and is under customer control at all times. An alternate ownership scenario could be that the storage system is owned by the utility and is treated as a demand-side, dispatchable resource that serves the customer needs as well as being available to the utility as a demand reduction resource.

Peak shaving

End-user peak shaving as an application of BESS refers to industrial customers that can install a BESS to discharge power during peak power periods and charge during low demand periods [36-38]. In particular, BESS can provide advantages in terms of reduction of electricity bill costs. In fact, it has to be evidenced that power companies charge some high-consumption customers (e.g. industrial customers) not just for the amount of energy used, that is the Time of Use (TOU) energy charge expressed in monetary units (*m.u.*) per *kWh*, but also for the maximum amount requested overtime (typically the billing period is one month), that is the peak demand charge expressed in *m.u.* per *kW*. This last term can assume significant values as its per-unit cost may be on the order of 100 times the per-unit cost for total usage (e.g. in USA, companies quote rates of about 6.40 *\$cents/kWh* as “energy charge” and 6.50 *\$/kW* as “demand charge” [39, 40]). Recently, efforts have been made for providing pricing schemes that should optimize the economic benefits of both consumers and producers [31, 41]. The more general problem of the reduction of bill cost due to the BESS presence will be analyzed in more details in the next subsection when we dealt with the DR.

Demand response

The resulting mismatches in supply and demand have impacts on both the grid's operators and the end-use customers. Two important consequences are the risk of a threat to the integrity of the grid over very large areas and the increase of energy prices in electricity markets during peak demand periods [42, 43]. Demand response (DR) is an interesting solution that has been used to face these challenges. In fact, the grid's operators can benefit from DR in order to guarantee the integrity of the grid, while end consumers are interested in applying DR in order to reduce their costs for electricity.

With reference to the grid's operators, benefits are related to the capability of DR to lower the likelihood and consequences of forced outages. This is mainly related to the great flexibility that can be obtained by applying DR, which has the capability of providing additional capacity more quickly and efficiently than a new supply could [39]. Regarding end consumers, financial benefits can be achieved through cost savings and incentive payments earned by adjusting their electricity demand in response to time-varying electricity rates or incentive-based programs. Price-based demand response refers to changes in usage by customers in response to changes in the electricity prices [31, 42]. Time varying energy prices can be classified in two broad categories: static and dynamic time-varying prices [44].

Dynamic pricing is interesting for regulators and utilities when it has the good potential for lowering energy costs for the society [45, 46]. The most natural or the most extreme approach to price-responsive demand is Real-Time Pricing of electricity (RTP) which charges different retail electricity prices for different hours of the day and for different days. While RTP has not been widely accepted or implemented, TOU pricing has been used extensively. Under TOU, the retail price varies in a preset way within certain blocks of time. A recent innovation in time-varying pricing is Critical Peak Pricing (CPP), which has some attributes of RTP and some of interruptible programs. CPP programs usually start with a TOU rate structure, but then they add one more rate that applies to "critical" peak hours, which the utility can call on short notice. Another pricing approach is Energy/Demand Charge (EDC) tariffs which involves a structure directly linked to both the consumed energy and the peak load [31, 47]. Eventually, dynamic pricing tariff that reflect the day-ahead power market pricing can be also considered. This type of tariff varies on the hourly base and is usually referred to Market Price (MP) [48]. All of above mentioned approaches for dynamic pricing and their comparisons are explained in more details in the following sections.

Real time pricing: defines a system that charges different retail electricity prices for different hours of the day and for different days. RTP introduces economic incentives by allowing the retail price to change at fixed time intervals, usually hourly. The RTP for each hour can be announced at the beginning of (or minutes before) the hour or it can be announced in advance [31]. An example of RTP is provided in figure 1.5 [49].

RTP programs currently in effect typically announce the prices for all hours of a day on the previous day. Obviously, a longer lag time between the price announcement and the price implementation will result in prices that less accurately reflect the actual real time supply/demand situation in the market. Additionally, the longer lag time means that the prices will be less volatile than, for instance, the real time wholesale electricity price.

Time of use pricing: under TOU, the retail price varies in a preset way within certain blocks of time (figure 1.6). As an example, Table 1.4 reports the certain blocks of time for a typical TOU pricing scheme where the blocks of time are different for the summer and winter. For the summer three certain blocks of time are introduced which are on peak, part peak and off peak-

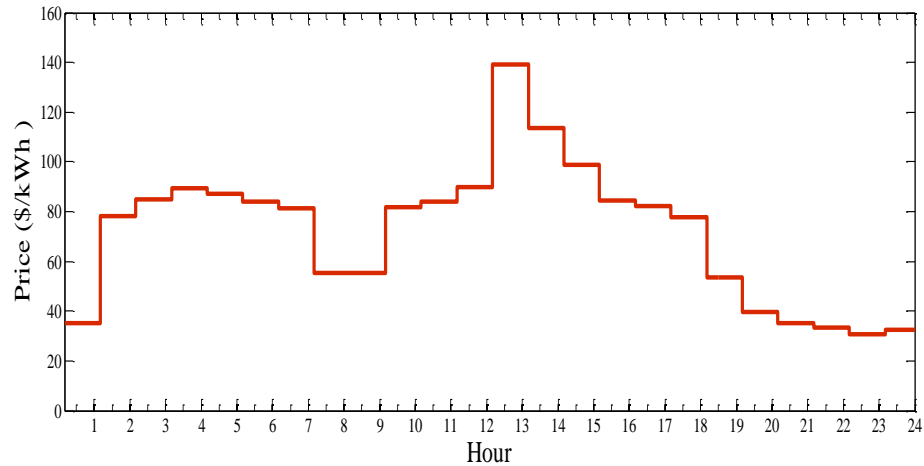


Figure 1.5: Real-time pricing.

while the number of blocks are decreased to two blocks, part peak and off peak, for the winter. Tariffs for different time periods in the different seasons are presented in the table 1.5 [26]. For example in the summer tariff, the price for on peak time which starts from 12.00 noon to 6.00 p.m. is 542.04 (\$/MWh) where in the winter the maximum price rate is 161.96 (\$/MWh). The rates for each time block are adjusted infrequently, typically only two or three times per year. Yet, RTP with a long lag time between price and implementation is approximately time-of-use pricing. TOU programs set prices months in advance and therefore logically cannot capture any of the shorter-term variation in supply/demand balance.

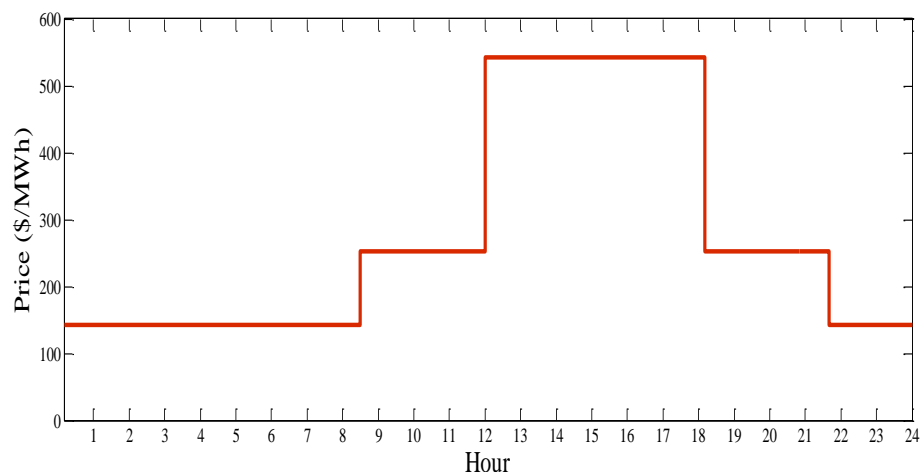


Figure 1.6: Time of use pricing (summer tariff).

Critical peak pricing: one of popular variant of dynamic pricing is critical peak pricing (CPP), in which prices during the top 40-150 hours of the year rise to previously specified levels designed to recover the full capacity and energy cost of power plants that run primarily during those hours. Prices are lower than existing rates during the other hours of the year [46]. CPP has some attributes of RTP and some of interruptible programs. CPP programs usually start

with a TOU rate structure, but then they add one more rate that applies to “critical” peak hours, which the utility can call on short notice. CPP is a clear improvement on TOU with demand charges, because the additional charges are based on consumption when the system is actually constrained, rather than when the particular customer’s demand peaks. The demand charge can be assumed equal to 100 times greater than the energy charge (i.e. 100 *m.u.*) [39].

Summer tariff	
On peak	12:00 noon to 6:00 p.m.
Part peak	8:30 a.m. to 12:00 noon and 6:00 p.m. to 9:30 p.m.
Off peak	9:30 p.m. to 8:30 a.m.
Winter tariff	
Part Peak	8:30 a.m. to 9:30 p.m.
Off Peak	9:30 p.m. to 8:30 a.m.

Table 1.4: Time of use tariff periods.

TOU periods	Summer tariff (\$/MWh)	Winter tariff (\$/MWh)
On peak	542.04	161.96
Part peak	252.90	
Off peak	142.54	132.54

Table 1.5: Time of use tariff prices.

Energy demand charge: Because TOU rates don’t capture the price variation within a price block, TOU pricing is often combined with a separate charge for peak usage. These “demand charges” are a price per kilowatt for the customer’s highest usage during the billing period (usually a month). Demand charges are based on the customer’s maximum usage (during a 15 minute interval) regardless of whether that usage occurs at a time when the system as a whole has a tight supply/demand balance or not. In addition, along with all of mentioned price schemes, another possible scheme is energy/demand charge (EDC) tariff. EDC tariff has a structure which is directly linked to both the consumed energy and the peak load [47]. This tariff can involve also energy prices varying hourly taking into account the peak value of the power [50].

1.4. References

- [1] H. Chen, T. N. Cong, W. Yang, C. Tan, Y. Li, and Y. Ding, "Progress in electrical energy storage system: a critical review," *Progress in Natural Science Journal*, vol. 19(3), pp. 291-312, March 2009.

- [2] H. Ibrahim, and A. Ilinca, "Techno economic analysis of different energy storage technologies," *Energy Storage Technologies and Applications*, Rijeka, Croatia, Intech, 2013.
- [3] J. N. Baker, and A. Collinson, "Electrical energy storage at the turn of the millennium," *Power Engineering Journal*, vol. 13(3), pp. 107-112, June 1999.
- [4] S. C. Smith, P. K. Sen, and B. Kroposki, "Advancement of energy storage devices and applications in electrical power system," in *Proc. IEEE Power and Energy Society General Meeting*, Pittsburgh, PA, USA, 20-24 July, 2008.
- [5] G. Bird, "*Report of the seventh meeting of the British society for the advancement of science*," London, UK, Forgotten Books, 1837.
- [6] K. Kordesch, and W. Taucher-Mautner, "*Primary batteries*," Graz, Austria, Elsevier, 2009.
- [7] DTI, (2004). Status of electrical energy storage systems. [Online]. Available: <http://webarchive.nationalarchives.gov.uk/20100919181607/http://www.ensg.gov.uk/assets/dgdti00050.pdf>
- [8] R. Walawalkar, J. Apt, and R. Mancini, "Economics of electric energy storage for energy arbitrage and regulation," *Energy Policy Journal*, vol. 35(4), pp. 2558-2568, April 2007.
- [9] A. Watt, and A. Philip, "*Electroplating and electrorefining of metals*," California, USA, Wexford College Press, 2005.
- [10] P. Kurzweil, "*Secondary batteries*," Amberg, Germany, Elsevier, 2009.
- [11] A. Oberhofer, and P. Meisen, (2012). Energy storage technologies & their role in renewable integration. Global Energy Network Institute. [Online]. Available: <http://www.geni.org/globalenergy/research/energy-storage-technologies/Energy-Storage-Technologies.pdf>
- [12] IEC, (2011). White paper on electrical energy storage. [Online]. Available: <http://www.iec.ch/whitepaper/pdf/iecWP-energystorage-LR-en.pdf>
- [13] EUROBATT, (2013). Battery energy storage for smart grid applications. [Online]. Available: http://www.eurobat.org/sites/default/files/eurobat_smartgrid_publication_may_2013_0.pdf
- [14] A. Brown, "Developments in energy storage," in *Proc. 8th Annual UT Texas Energy Law Symposium*, Austin, TX, USA, 17-18 January, 2013.
- [15] OSPE Energy Task Force, (2013). Electrical energy storage options. [Online]. Available: http://c.ymcdn.com/sites/www.ospe.on.ca/resource/resmgr/doc_advocacy/2013_doc_energystoragelimit.pdf
- [16] G. Carpinelli, P. Caramia, F. Mottola, and D. Proto, "Exponential weighted method and a compromise programming method for multi-objective operation of plug-in vehicle aggregators in microgrids," *International Journal of Electrical Power and Energy Systems*, vol. 56, pp. 374-384, March 2014.
- [17] H. Ibrahim, A. Ilinca, and J. Perron, "Energy storage systems - characteristics and comparisons," *Renewable and Sustainable Energy Reviews*, vol. 12(5), 1221-1250, June 2008.

- [18] H. Ibrahim, A. Ilinca, and J. Perron, "Comparison and analysis of different energy storage techniques based on their performance," in *Proc. IEEE Electrical Power Conference*, Montreal, Que. Canada, 25-26 October, 2007.
- [19] Photovoltaic Education Network, (2014). Battery charging and discharging. [Online]. Available:
<http://pvcdrom.pveducation.org/BATTERY/charge.htm>.
- [20] S. Govindan, A. Sivasubramaniam, and B. Urgaonkar, "Benefits and limitations of tapping into stored energy for datacenters," in *Proc. 2011 International Symposium on Computer architecture, ISCA'11*, San Jose, CA, USA, 4-8 June, 2011.
- [21] MIT Electric Vehicle Team, (2008). A guide to understanding battery specifications. [Online]. Available:
http://web.mit.edu/evt/summary_battery_specifications.pdf
- [22] J. Eyer, and G. Corey, (2010). Energy storage for the electricity grid: benefits and market potential assessment guide. Sandia National Laboratories. [Online]. Available:
<http://www.sandia.gov/ess/publications/SAND2010-0815.pdf>
- [23] B. Multon, and J. Ruer, (2003). Stockage de l'énergie. Oui, c'est indispensable, et c'est possible pourquoi, oul, comment. ECRIN. [Online]. Available:
<http://www.ecrin.asso.fr/energies>
- [24] K. H. Ahlert, and C. V. Dinther, "Sensitivity analysis of the economic benefits from electricity storage at the end consumer level," in *Proc. 2009 IEEE Power Tech Conference*, Bucharest, BU, Romania, 28 June-2 July 2009.
- [25] Institute National Polytechnique de Grenoble, (2003). Suspension magnetique pour volant d'inertie. [Online]. Available:
https://tel.archivesouvertes.fr/file/index/docid/383510/filename/These_Faure_2003.pdf
- [26] G. Carpinelli, S. Khormali, F. Mottola, and D. Proto, "Battery energy storage sizing when time of use pricing is applied," *The Scientific World Journal*, vol. 2014, pp. 1-8, September 2014.
- [27] S. Schoenung, (2011). Energy storage system cost update. Sandia National Laboratories. [Online]. Available:
<http://prod.sandia.gov/techlib/access-control.cgi/2011/112730.pdf>
- [28] Norsok Standard, (1996). Life cycle cost for production facility. [Online]. Available:
<http://www.standard.no/pagefiles/1137/o-cr-002r1.pdf>
- [29] A. A. Akhil, G. Huff, A. B. Currier, B. C. Kaun, D. M. Rastler, S. B. Chen, A. L. Cotter, D. T. Bradshaw, and W. D. Gauntlett, (2013). Electricity storage handbook. Sandia National Laboratories. [Online]. Available:
<http://www.sandia.gov/ess/publications/SAND2013-5131.pdf>
- [30] Y. Zheng, Z. Y. Dong, Y. Xu, K. Meng, J. H. Zhao, and J. Qiu, "Electric vehicle battery charging/swap stations in distribution systems: comparison study and optimal planning," *IEEE Trans. on Power Systems*, vol. 29(1), pp. 221-229, January 2014.
- [31] S. Borenstein, M. Jaske, and A. Rosenfeld, (2002). Dynamic pricing, advanced metering and demand response in electricity markets. Center for the Study of Energy Markets. Berkeley, CA. [Online]. Available:
<http://www.escholarship.org/uc/item/11w8d6m4>

- [32] C. Wei, "A conceptual framework for smart grid," in *Proc. IEEE Asia Pacific Power and Energy Engineering Conference*, Chengdu, SC, China, 28-31 March, 2010.
- [33] A. Ipakchi, and F. Albuyeh, "Grid of the future," *IEEE Power&Energy Magazine*, vol. 7(2), pp. 52-62, Mar. /Apr. 2009.
- [34] Z. M. Fadlullah, Y. Nozaki, A. Takeuchi, and N. Kato, "A survey of game theoretic approaches in smart grid," in *Proc. IEEE International Conf. on Wireless Communications and Signal Processing*, Nanjing, JS, China, 9-11 November, 2011.
- [35] G. Carpinelli, S. Khormali, F. Mottola, and D. Proto, "Load leveling with electrical storage systems: a two-step optimization procedure," *International review of electrical engineering*, vol. 8(2), pp. 729-736, March/April 2013.
- [36] A. Oudalov, D. Chartouni, C. Ohler, and G. Linhofer, "Value analysis of battery energy storage applications in power systems," in *Proc. 2006 IEEE Power Systems Conference and Exposition, PSCE '06*, Atlanta, GA, USA, 29 October-1 November, 2006.
- [37] S. Yoda, and K. Ishihara, "The advent of battery-based societies and the global environment in the 21st century," *Journal of Power Sources*, vol. 81-82, pp. 162-169, September 1999.
- [38] A. Even, J. Neyens, and A. Demousselle, "Peak shaving with batteries," in *Proc. 12th International Conference on Electricity Distribution*, Birmingham, WM, UK, 17-21 May, 1993.
- [39] G. Carpinelli, S. Khormali, F. Mottola, and D. Proto, "Optimal operation of electrical energy storage systems for industrial applications," in *Proc. IEEE Power and Energy Society General Meeting*, Vancouver, BC, Canada, 21-25 July, 2013.
- [40] M. P. Johnson, A. Bar-Noy, O. Liu, and Y. Feng, "Energy peak shaving with local storage," *Sustainable Computing: Informatics and Systems*, vol. 1(3), pp. 177-188, September 2011.
- [41] M. Roozbehani, M. A. Dahleh, and S. K. Mitter, "Volatility of power grids under real-time pricing," *IEEE Trans. on Power Systems*, vol. 27(4), pp. 1926-1940, November 2012.
- [42] G. Carpinelli, S. Khormali, F. Mottola, and D. Proto, "Demand response and energy storage systems: an industrial application for reducing electricity costs. part I: theoretical aspects," in *Proc. International Symposium on Power Electronics, Electrical Drives, Automation and Motion, SPEEDAM 2014*, Ischia, CA, Italy, 18-20 June, 2014.
- [43] U.S. Department of Energy, (2006). Benefits of demand response in electricity markets and recommendations for achieving them. [Online]. Available: http://energy.gov/sites/prod/files/oeprod/DocumentsandMedia/DOE_Benefits_of_Demand_Response_in_Electricity_Markets_and_Recommendations_for_Achieving_Them_Report_to_Congress.pdf
- [44] G. Carpinelli, S. Khormali, F. Mottola, and D. Proto, "Multi-battery management under real-time pricing for industrial facility applications," in *Proc. 12th International Conference on Environment and Electrical Engineering, EEEIC 2013*, Wroclaw, LS, Poland, 5-8 May, 2013.
- [45] A. Faruqui, S. Sergici, and L. Akaba, "Dynamic pricing of electricity for residential customers: the evidence from Michigan," *Energy Efficiency*, vol. 6(3), pp. 571-584, February 2013.

- [46] A. Faruqi, "The ethics of dynamic pricing," *Smart Grid: Integrating Renewable, Distributed & Efficient Energy*, Waltham, MA, USA, Elsevier, 2012.
- [47] G. Carpinelli, S. Khormali, F. Mottola, and D. Proto, "Demand response and energy storage systems an industrial application for reducing electricity costs," *IEEE Trans. on Industry Applications*, submitted to.
- [48] S. X. Chen, H. B. Gooi, and M. Q. Wang, "Sizing of energy storage for microgrids," *IEEE Trans. on Smart Grid*, vol. 3(1), pp. 142- 151, March 2012.
- [49] G. Carpinelli, S. Khormali, F. Mottola, and D. Proto, "Demand response and energy storage systems: an industrial application for reducing electricity costs. part II: numerical application," in *Proc. International Symposium on Power Electronics, Electrical Drives, Automation and Motion , SPEEDAM 2014*, Ischia, CA, Italy, 18-20 June, 2014.
- [50] A. Mishra, D. Irwin, P. Shenoy, and T. Zhu, "Scaling distributed energy storage for grid peak reduction," in *Proc. Fourth International Conference on Future Energy Systems*, New York, NY, USA, 2013.

Chapter 2: Optimal Operation Strategies of Battery Energy Storage Systems

As it is discussed in the first chapter, BESSs can provide several benefits based on different services that can be furnished in different levels of the SG. Generation systems, transmission systems, distribution systems and end-use customers are all involved in the entire value chain of the power system where the BESSs benefits can be identified.

In this chapter, optimal operation strategies of BESS with the aim of furnishing different services to the distribution systems and end-use customers are proposed.

Among different services of BESS, a load leveling service in order to avoid new investments in transmission and distribution facilities is firstly considered. Then, DR service with the aim of savings on the electricity bill cost under the two different dynamic pricing approaches is practically performed. Finally, in a general case study, an optimal scheduling of a μ G is presented.

Different advanced optimal operation strategies of BESS to furnish the above mentioned services are formulated, solved and applied by relying on specific objective functions and technical constraints in the frame single objective optimization model. In particular, on the basis of single objective optimization model, advanced optimal operation strategies for load leveling, demand response and microgrid scheduling are investigated.

Generally, a single objective optimization problem involves an objective function to be minimized and a number of equality/inequality constraints to be satisfied. It can be mathematically formulated as follows [1]:

$$\min f_{obj}(\mathbf{x}) \quad (2.1)$$

subject to:

$$\begin{aligned} g_k(\mathbf{x}) &= 0, \quad k = 1, \dots, n_{ec} \\ h_j(\mathbf{x}) &\leq 0, \quad j = 1, \dots, n_{ic} \end{aligned} \quad (2.2)$$

where \mathbf{x} is the vector of the optimization variables of the problem, f_{obj} is the objective function, g_k and h_j are the constraints and n_{ec} (n_{ic}) is the number of equality (inequality) constraints.

With reference to optimization problem model, important classes of optimization problems are linear and non-linear problems. In linear optimization problems the objective and all constraints are linear. Non-linear optimization is the term used to describe an optimization problem when the objective and/or the constraints are not linear [1].

Proposed single objective optimal operation strategies of BESS to furnish specific services in the grid including problem formulations, solving algorithms and numerical applications are separately reported in the following sections.

Obtained results of proposed strategies in numerical applications demonstrate technical and economic benefits that can be derived from the installation of BESS.

2.1. An advanced optimal operation strategy for load leveling

Load leveling is a service addressed to the distribution utility for reducing the fluctuations of the load demand along the day. This can be achieved by using demand side measures which reduce the peak demand or by using storage systems able to store energy during light load hours and discharge it during peak load hours. In this case, the installation of a BESS at the secondary side of the transformer of a distribution substation allows for a minimization of the difference between the mean and peak power requests. One of the main advantages for the distribution system operator is related to avoid new investments in transmission and distribution facilities [2-6].

2.1.1. State of the art

In the relevant literature several proposals have appeared dealing with BESS application for load leveling [7-13]. In [7] a BESS scheduling procedure was proposed, which provides a daily pattern that optimizes the load factor (i.e. the ratio of the mean and peak values of the load demand) with the aim of determining the optimal installation site and capacity of the BESS. In [8] an economic dispatch procedure is applied to BESSs for maximizing the fuel-cost savings of thermal plants and performing load leveling. In [9] an optimal BESS charge/discharge strategy is proposed to reduce the penalties paid to the transmission network for unforeseen demand beyond a maximum value at a metering point of a distribution substation. In [10] a load leveling control procedure is proposed to furnish both an active and a reactive power reference signals to the BESS during the discharging stage. Reference [11] proposed a simple, fast, and effective algorithm for finding optimal charge/discharge intervals of BESS and their associated rates without the need of processor intensive techniques often required by most optimization techniques. The core of the method is based on reshaping the aggregated load profile seen from the main distribution substation such that it gets close to the average load profile during a utilization period. In [12] load leveling for reducing transmission and distribution (T&D) losses based on shifting a fraction of the load from peak hours to off-peak hours through BESS in order to decrease the net resistive losses is proposed. In [13], an optimal operating strategy of BESS based on dynamic programming is proposed which provides the use of BESS in conjunction with photovoltaic (PV) generation units in order to level the load.

2.1.2. Proposed strategy

In this thesis, an innovative two-step procedure (day-ahead scheduling and very short time predictive control) is proposed which optimally controls a BESS connected to a distribution substation in order to perform load leveling (figure 2.1). Proposed BESS control strategy operates to provide energy during peak load hours and store energy during low demand hours. In the first step of the proposed strategy (day-ahead scheduling), starting from the day-ahead forecast of the active power at the distribution substation, an optimal profile of the power imported from the transmission network is obtained performing a day-ahead scheduling of the BESS power aimed at leveling the above profile.

In the second step (very short time predictive control), starting from a new forecast of the active power at the distribution substation, an optimal control of the BESS power is effected with the aim of approaching the actual power profile to the forecasted profile obtained in the first step.

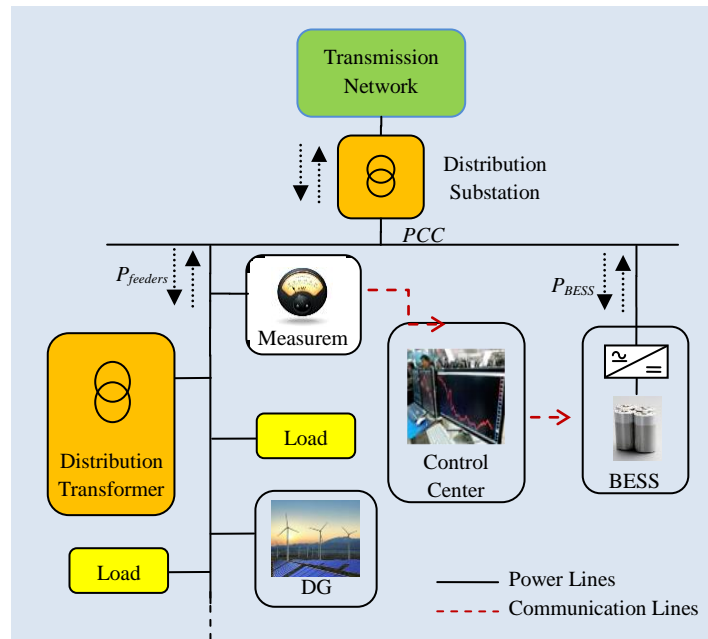


Figure 2.1: Grid architecture.

Adequate constraints are considered in both steps of the procedure in order to optimize the charge/discharge cycles and maximize the battery lifetime. In particular, the charge/discharge efficiency, DOD, the ramp rate and the number of charge/discharge daily cycles of the BESS are properly considered [14-16]. The load forecast is resulted by using a Feed Forward Neural Network (FFNN) which was considered particularly suitable for both day-ahead and real-time forecasts [17, 18].

It should be noted that two-step procedures based on day-ahead scheduling and very short time predictive control were traditionally used for solving important problems in power systems [19]. A proper coordination between the steps seems to be also a promising approach in the SG context where the need to integrate among distributed generation, loads, storage systems and market operation makes grid management a complex issue [20]. Moreover, two-step procedures referring to the optimal control of a BESS were proposed in [14, 21] but they did not refer to the problem of load leveling. In this thesis, according to the following considerable reasons, the two-step procedure control strategy in order to furnish a load leveling service is proposed:

- *Day-ahead scheduling* (i) allows a more detailed formulation of the optimization model thanks to the absence of computational efforts constraints; (ii) makes available the expected profile of the substation power that should be imported during the next day from the transmission network, whose knowledge is of great importance in helping the transmission system operator to optimally operate the system [22].
- *Very short time predictive control* (i) is particularly needed when dealing with variable loads and RESs (such as photovoltaic and wind sources) whose values can be highly variable and hard to predict with high accuracy in the day-ahead; and (ii) requires models whose solution involves low computational effort, because the optimization problem has to be rapidly solved several times a day.

It is also worth noting that the two steps of the procedure can be used separately for solving problems related to scheduling (e.g. unit commitment) or real-time operations (e.g. on-line

power dispatch or real time balancing market). Moreover, by shifting into the industrial customer's point of view, the proposed procedure can be easily applied for performing the DR services which are also presented in subsections 2.1.2 and 2.1.3.

2.1.3. Problem formulation and solving procedure

Let us consider the system shown in figure 2.1, where a distribution substation with HV/MV transformers connects the HV transmission grid to some MV feeders (for the sake of conciseness, in figure 2.1 only one feeder is shown); the feeders supply MV loads, MV/LV distribution transformers and distributed generation units. A BESS is connected to the MV bus of the HV/MV transformers.

The control center performs an optimal strategy consisting of BESS charging/discharging power control in order to level the power exchanged with the HV grid¹. We propose to perform the optimal strategy on the basis of following two multi-period optimization steps:

- *Day-ahead scheduling*: that identifies an optimal profile of the substation power whose peak value has been minimized; this profile is obtained thanks to an optimal day-ahead scheduling of the BESS charging/discharging powers.
- *Very short time predictive control*: that predicts a few minutes ahead BESS charging/discharging power with the aim of approaching the substation power to the optimal profile obtained in the day-ahead scheduling.

The figure 2.2 provides a flowchart of the two-step procedure. The multi-period optimization problems are discussed in the next subsections. In both steps, a single-objective constrained minimization problem is formulated as (2.1).

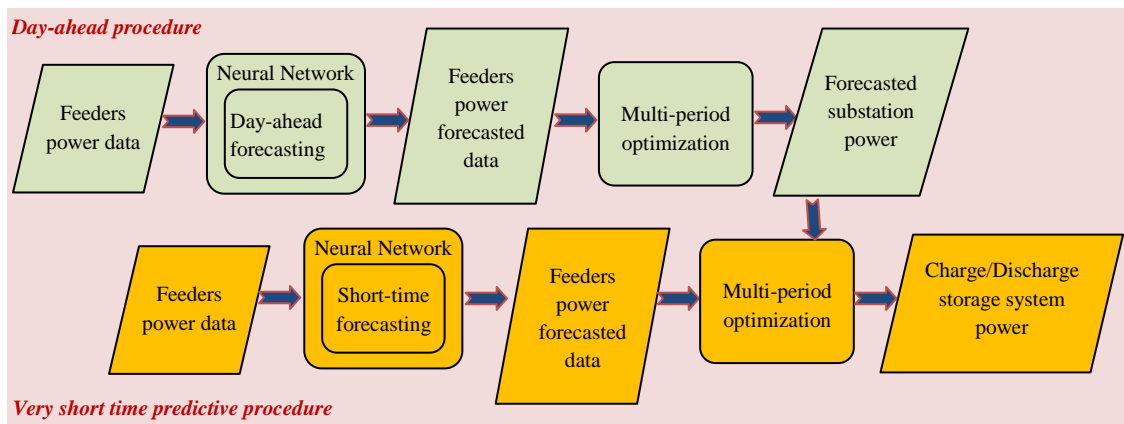


Figure 2.2: Flowchart of the two-step procedure.

The day is split in time intervals of length Δt . During each time interval, the feeder power is assumed constant and equal to its mean value. The choice of the time interval length depends on a compromise between accuracy and computational efforts. In order to maximize the BESS lifetime, a control on the number of charge/discharge cycles is imposed. Here, without loss of generality, this number is limited to one cycle/day and divide the day into two contiguous time periods: the discharging period and the charging period. Moreover, for the sake of clarity it is assumed that the first time interval is the beginning of the discharging

¹ Hereinafter the difference between the load demand and DG production will be referred to as “feeder power.” The total power of the substation that takes into account both feeder power and BESS power will be referred to as “substation power.”

period and the last time interval is the end of the charging period. Thus, the time intervals of the day refer to the indices $i \in [n_{in}^{dis} = 1, \dots, n_{fin}^{dis}, n_{in}^{ch}, \dots, n_{fin}^{ch} = n_t]$, where n_{in}^{dis} and n_{fin}^{dis} (n_{in}^{ch} and n_{fin}^{ch}) are the indices associated to the first and last time intervals, respectively, in which the BESS is allowed to discharge (charge).

Day-ahead scheduling

As previously evidenced, the day-ahead scheduling is performed once a day for the next day, with the aim of identifying an optimized profile of the substation power imported from the transmission network in the next day.

Input data of the scheduling are the BESS state of charge at the beginning of the day and the forecasted daily profile of the feeder power. The BESS state of charge at the beginning of the day is the output of the procedure applied in the preceding day while the forecasted daily profile of the feeder power is obtained through a FFNN trained by historical data.

Output of the scheduling is the profile of the substation power in the next day, which is the input of the very short time predictive control algorithm (figure 2.2). Hereinafter, this quantity will be referred to as day-ahead forecasted substation power.

The day-ahead scheduling is based on the solution of a linear multi-period optimization problem. The linear optimization problem aims to minimize the upper value of the substation power. This is obtained by considering a theoretical leveling value (P_{lev}) (figure 2.3) and assuming that when the requested power is greater than P_{lev} the BESS can discharge the stored energy, and when the requested power is lower than P_{lev} the BESS can charge. In this way, the expected daily profile of the substation power is leveled.

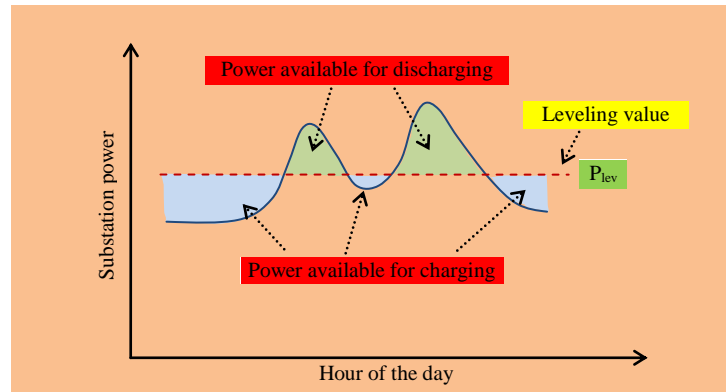


Figure 2.3: Load leveling schematic view.

Then, the objective function (2.1) to be minimized is:

$$f_{obj}^{da} = P_{lev} \quad (2.3)$$

Equality constraints refer to the BESS state of charge at the beginning of the day and at the end of the charging stage. In more detail, the BESS state of charge at the end of the charging stage has to reach a specified value:

$$C_{in}^{sp} - \frac{1}{\eta_{dis}} \Delta t \sum_{i=1}^{n_{fin}^{dis}} P_{b,i}^{da} - \eta_{ch} \Delta t \sum_{i=n_{in}^{ch}}^{n_t} P_{b,i}^{da} = C_{fin}^{sp} \quad (2.4)$$

where $P_{b,i}^{da}$ is the day-ahead BESS power at time interval i , η_{ch} (η_{dis}) is the BESS efficiency during the charge (discharge) mode, C_{fin}^{sp} is the specified value of the BESS charge when the charge ends and C_{in}^{sp} is the BESS state of charge at the beginning of the day. In a typical day the two states of charge (C_{in}^{sp} and C_{fin}^{sp}) should have the same value. However, due to particular events, the expected load demand can be very different from the forecasted one and, consequently, different values for the states of charge could be suitable. Obviously, C_{in}^{sp} and C_{fin}^{sp} cannot exceed the battery size.

The value of n_{in}^{ch} can be either fixed or dynamically evaluated. In the first case an opportune time of the day can be chosen on the basis of specific needs of the application. In the second case, the multi-period optimization is repeatedly performed until the value of n_{in}^{ch} , corresponding to the minimum value of P_{lev} , is found. Also a genetic algorithm (GA) can be used for evaluating, n_{in}^{ch} , which is a discrete variable.

The inequality constraints impose that the BESS can have only one charge/discharge cycle/day:

$$-P_{max} \leq P_{b,i}^{da} \leq 0, \quad i \in [n_{in}^{ch}, \dots, n_{fin}^{ch}] \quad (2.5)$$

$$0 \leq P_{b,i}^{da} \leq P_{max}, \quad i \notin [n_{in}^{ch}, \dots, n_{fin}^{ch}] \quad (2.6)$$

where P_{max} is the BESS maximum charge/discharge power. By imposing P_{max} equal to the BESS power rate, the ramp rate constraint could be also considered [15].

A further inequality constraint imposes that the state of charge cannot be lower than a minimum value (based on the admissible depth of discharge) during the discharge stage, that is²:

$$C_{in}^{sp} - \frac{1}{\eta_{dis}} \Delta t \sum_{j=1}^i P_{b,j}^{da} \geq C_{min}, \quad i \notin [n_{in}^{ch}, \dots, n_{fin}^{ch}] \quad (2.7)$$

where C_{min} is the admissible minimum value of the state of charge.

Finally, an inequality constraint is imposed on the day-ahead forecasted substation power ($P_{sub,i}^{da}$) which has to be bounded by the minimized leveling power (P_{lev}); this result in:

$$P_{sub,i}^{da} = P_{l,i}^{da} - P_{b,i}^{da} \leq P_{lev}, \quad i \in [1, \dots, n_t] \quad (2.8)$$

where $P_{l,i}^{da}$ is the day-ahead forecasted feeder power.

With reference to the feeder power forecasting, a FFNN with delay lines and one hidden layer is used to implement the NARX model [17, 18]. To have proper forecasting, different network

² It should be noted that a further inequality constraint should be included to impose that the state of charge cannot exceed the size of the battery during the charging stage. However, this constraint is intrinsically satisfied if constraints (2.4) and (2.5) are considered [23].

configurations were tried by varying the number of hidden neurons and the number of delays as well as various percentages of samples for training, validation and test.

Very short time predictive control

The very short time predictive control procedure is repeatedly performed at all the time intervals of the day. The main output of the procedure is the BESS charge/discharge power for each control interval $i \in [1, \dots, n_t]$. Aim of the procedure is to minimize the difference between the substation power calculated at this step and that evaluated in the previous step (i.e. the day-ahead forecasted substation power).

Input data of the procedure performed at each time interval $i-1$ are the forecasts of the feeder power (output of a FFNN) from the i^{th} time interval to the last time interval of the day, the day-ahead forecasted substation power values obtained in the day-ahead scheduling, and the BESS state of charge at the beginning of the i^{th} time interval (output of the optimization performed in the previous time interval).

Outputs of the procedure are the charge/discharge power and the state of charge at the end of the i^{th} interval (input for the next time interval).

The very short time predictive procedure is based on the solution of a non-linear multi-period optimization problem. The objective function (2.1) of the multi-period optimization for the i^{th} control interval is:

$$f_{obj,i}^{vst} = \sum_{j=i}^{n_t} (P_{sub,j}^{vst} - P_{sub,j}^{da})^2 \quad (2.9)$$

where $P_{sub,j}^{vst}$ is the substation power calculated by the very short time predictive control procedure (hereinafter referred as very short time forecasted substation power).

The first equality constraint to be satisfied refers to the power balance at each time interval:

$$P_{l,j}^{vst} - P_{b,j}^{vst} = P_{sub,j}^{vst}, \quad j \in [i, \dots, n_t] \quad (2.10)$$

where $P_{b,j}^{vst}$ is the very short time predictive BESS power and $P_{l,j}^{vst}$ is very short time forecast of the feeder power, both at time interval j .

Moreover, relationship (2.4) is modified according to the considered control interval: when the control interval falls into the discharging stage it is:

$$C_i - \frac{1}{\eta_{dis}} \Delta t \sum_{j=i}^{n_{fin}^{dis}} P_{b,j}^{vst} - \eta_{ch} \Delta t \sum_{j=n_{in}^{ch}}^{n_t} P_{b,j}^{vst} = C_{fin}^{sp}, \quad i \in [n_{in}^{dis}, \dots, n_{fin}^{dis}] \quad (2.11)$$

where C_i is the BESS state of the charge at the beginning of the i^{th} time interval; when the control interval falls into the charging stage, it is:

$$C_i - \eta_{ch} \Delta t \sum_{j=i}^{n_t} P_{b,j}^{vst} = C_{fin}^{sp}, \quad i \in [n_{in}^{ch}, \dots, n_{fin}^{ch}] \quad (2.12)$$

The inequality constraints (2.5) and (2.6) are still considered, while constraint (2.7) is modified as follows:

$$C_i - \frac{1}{\eta_{dis}} \Delta t \sum_{j=i}^{n_{fin}^{dis}} P_{b,j}^{vst} \geq C_{min} , \quad i \in [n_{in}^{dis}, \dots, n_{fin}^{dis}] \quad (2.13)$$

Regarding the feeder power forecasting, the same FFNN configuration of the day-ahead forecast can be used.

2.1.4. Numerical application

In this section, the proposed two-step procedure is applied to a distribution substation supplying both commercial and domestic loads. A one-year period of substation power measurements was available in the form of mean values evaluated at time steps of $\Delta t = 10$ min. In this application, to perform the load leveling service, a 6 MW-5 hours BESS is supposed to be connected to the secondary side of the transformer. The BESS efficiency is considered 90% in charging and 93% in discharging operations, and the admissible DOD is 80% [24]. In order to maximize the BESS lifetime and to avoid capacity reduction, charge and discharge power cannot exceed the BESS rate [15].

In the most general case, the feeder power forecasting depends upon factors such as substation power values and weather conditions (temperature, humidity, pressure, etc.). However, in this application only the substation power historical data were available and were selected as input and target to train the FFNN. Eleven neurons and four delays were chosen for the FFNN configuration. In all the experiment days, a mean absolute percentage error (MAPE) resulted whose values were within 1.0-8.7%.

The optimal two-step strategy shown in previous section was applied to several days. In the following subsections, for the sake of conciseness, only the results will be shown with reference to a single day of the year, in particular, December 1, 2010. Similar results were obtained when considering other days.

Day-ahead scheduling results

With the aim of evaluating the accuracy of the forecast, in figure 2.4 the day ahead forecasted feeder power profile and the values of the actual measurements are reported, with reference to a time interval of 10 minutes.

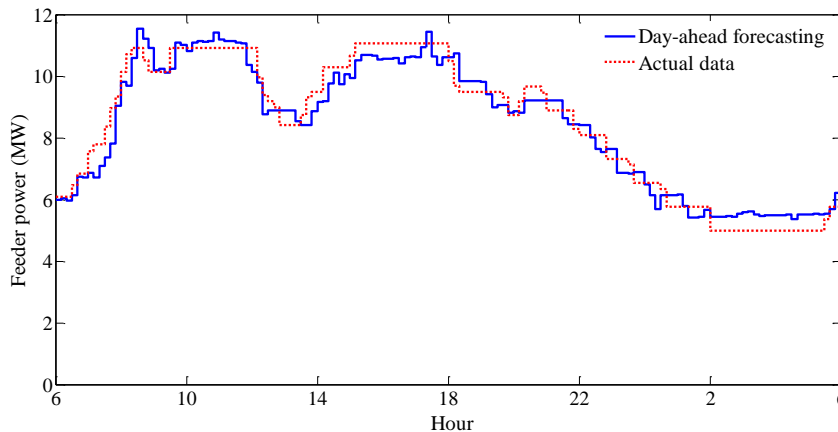


Figure 2.4: Day-ahead forecasting (feeder power).

MAPE resulted in 5.20% with a maximum percentage error of about 14%. In figure 2.5 the forecasted feeder power and the forecasted substation power are reported. Obviously, in cases of absence of BESS, these power profiles would assume the same values. The leveling value of the power requested to the transmission network resulted equal to 8.74 MW, whereas the maximum value of the forecasted feeder power was 11.52 MW.

In order to verify the satisfaction of the BESS constraints, the charging/discharging pattern resulted from the day ahead procedure is shown in figure 2.6, whereas in figure 2.7 the energy stored during the day is reported. The start of the battery-charging period resulted at 9:40 p.m.

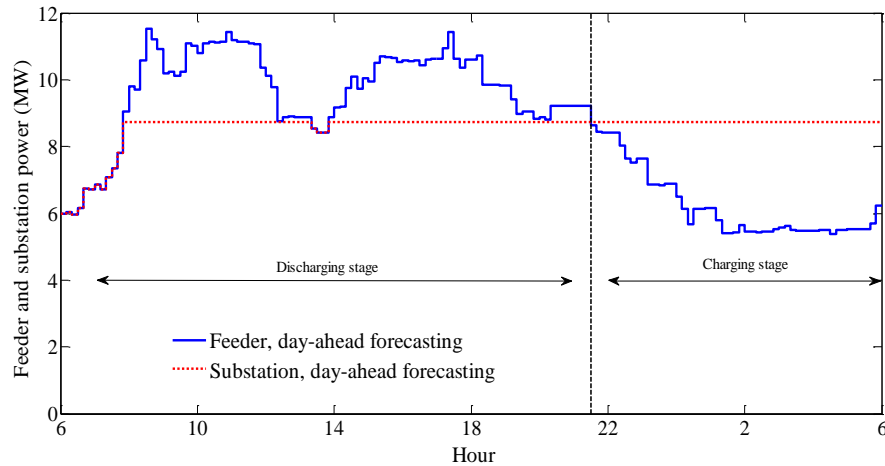


Figure 2.5: Day-ahead scheduling (feeder and substation powers).

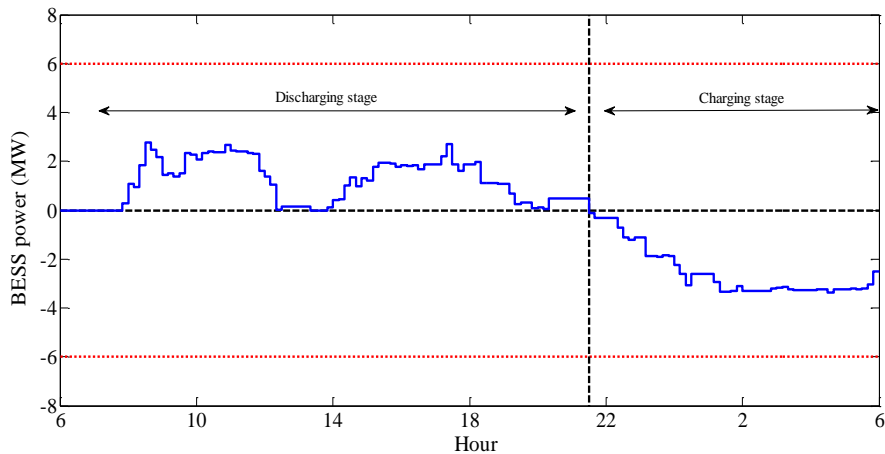


Figure 2.6: Day-ahead scheduling (BESS power).

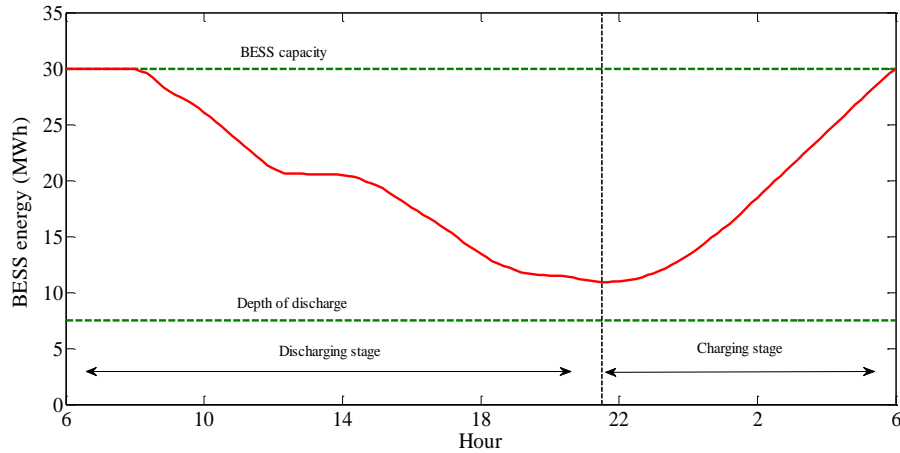


Figure 2.7: Day-ahead scheduling (BESS energy).

Very short time predictive control results

Very short time predictive control procedure was applied to all the time intervals of the day. The MAPE between power forecasted and actual measured values is about 3%, while the maximum percentage error resulted 12%. In order to reduce the effect of the maximum forecasting error on the load leveling procedure, the BESS reference signals were calculated every 20 minutes instead of every 10 minutes. It is calculated based on average value of the two very short time optimized BESS powers at time intervals i and $i+1$. For example, when the forecasted powers for time intervals i and $i+1$ are 5 kW and 10 kW, respectively, then average forecasted power of the two sequential time intervals will be 7.5 kW. More accurate BESS reference signals were experimented in this way.

Figure 2.8 shows the day-ahead forecasted (output of the day ahead scheduling) and the very short time predictive control forecasted substation power (output of the very short time predictive procedure). In order to verify the satisfaction of the constraints, the resulting charging/discharging patterns are shown in figure 2.9 whereas the energy stored during the day is reported in figure 2.10. To verify the effectiveness of the proposed procedure, in figure 2.11 the very short term predictive forecasted substation power profile is compared with its actual profiles with and without BESS (the power without BESS is equal to the actual profile of the actual feeder power).

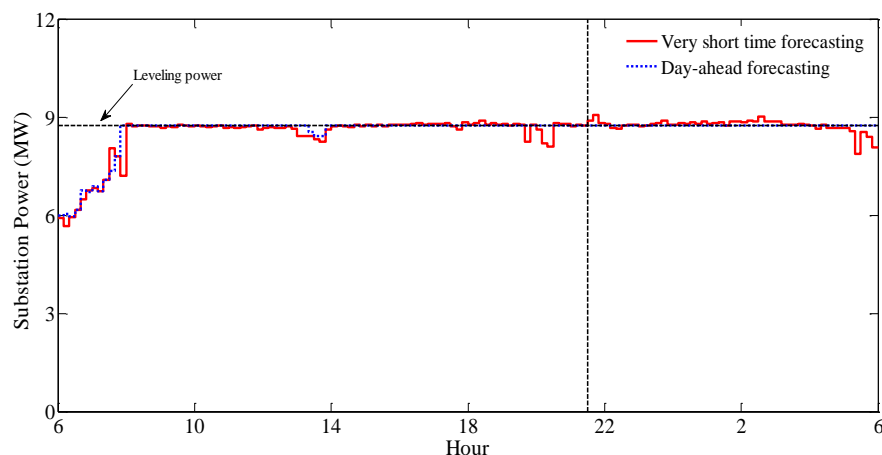


Figure 2.8: Very short term predictive control (substation power).

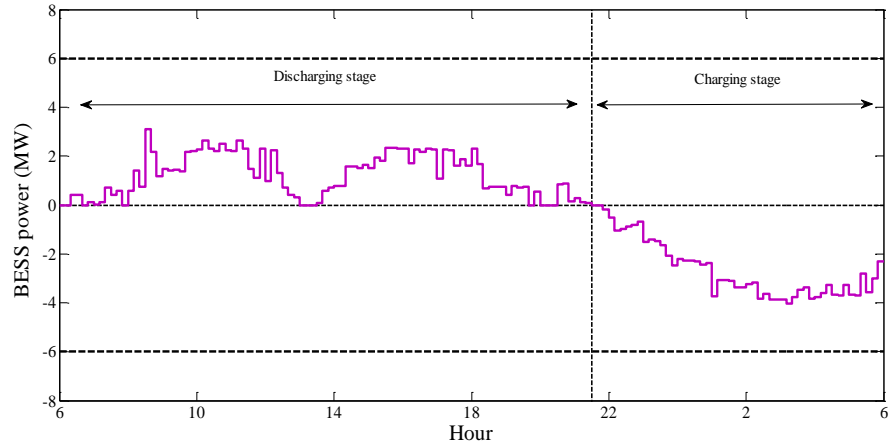


Figure 2.9: Very short term predictive control (BESS power).

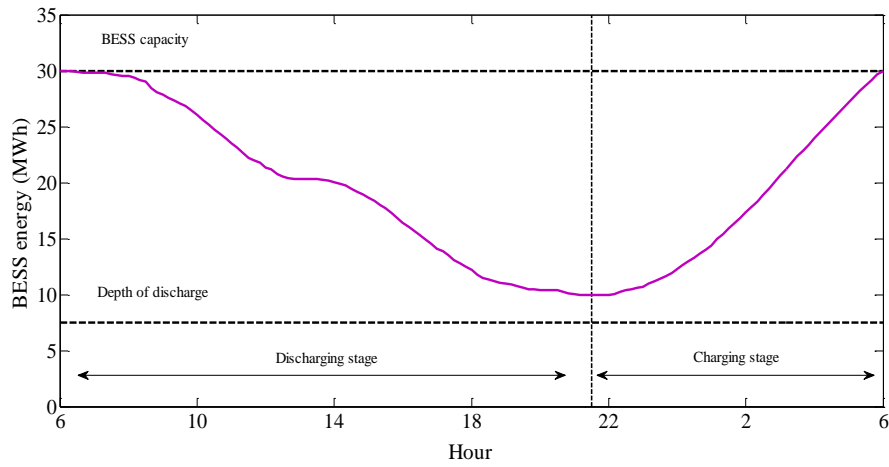


Figure 2.10: Very short term predictive control (BESS energy).

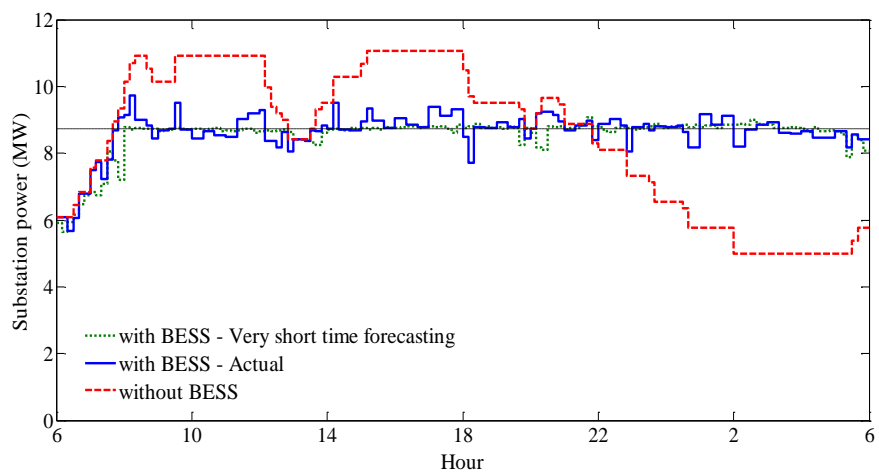


Figure 2.11: Very short term predictive control (substation power).

In table 2.1 the peak value and the load factor of the substation power without BESS and with BESS (day-ahead forecasting, real-time forecasting and actual values) are reported.

Case study	Peak value (MW)	Load factor
Without BESS	11.52	0.730
With BESS, Day-ahead	8.74	0.981
With BESS, Very short time	9.07	0.941
With BESS, Actual values	9.72	0.888

Table 2.1: Peak value and load factor of the substation power with and without BESS.

The analysis of the results reported in figure 2.11 and table 2.1 clearly reveals: (i) a decrement of the peak power of about 15%; (ii) an improvement of the load factor of about 20% (the ideal load factor is 1); (iii) a not negligible influence of the feeder power forecasting errors both in day-ahead and in real-time stages; and (iv) that the negative influence of the forecasting errors is concentrated at only a few points around the leveling power. Then, the proposed two-step procedure shows clear good performance and further improvements are expected in the presence of most performance forecasting of feeder power.

2.2. An advanced optimal operation strategy for demand response under real time pricing

DR is defined as changes in electric usage by end-use customers from their normal consumption patterns in response to changes in the price of electricity over time, or to incentive payments designed to induce lower electricity use at times of high wholesale market prices or when system reliability is under the risk [25]. It is offered by utilities and can be classified as:

- *Price-based*: gives customers time varying rates that reflect the value and cost of electricity in different time periods such as RTP, TOU, CPP and EDC. With this information, customers tend to use less electricity at times when electricity prices are high.
- *Incentive-based*: gives participating customers incentives to reduce load during the peak periods. The incentives may be in the form of explicit bill credits or payments for pre-contracted or measured load reductions. Customer enrollment and response are voluntary.

In the frame of price-based DR program, several electricity bill schemes can be applied in practical cases. Possible schemes are TOU, RTP, CPP and EDC tariffs which are described in the first chapter of this thesis in more details [25].

This subsection focused on DR service under the RTP electricity bill scheme which gives customers time varying rates that reflect the value and cost of electricity in different time periods. It is worth noting that, while DR can be easily applied to residential and commercial users, this application can have some limitations for industrial facilities since industrial production cannot deal with time shifting or interruptions easily. Then, installation of storage systems can be an interesting solution to furnish DR service. BESSs can be ideal candidate to perform DR, specifically in case of industrial loads, when they can provide the possibility of absorbing energy from the grid in the charging condition (i.e., load mode) and of supplying the

loads in discharging operating conditions (i.e., generator mode) and have the ability to change their operating condition very quickly [26, 27].

2.2.1. State of the art

The recent technical literature includes a wide range of work related to DR under different pricing tariffs, in particular DR under RTP. [28] develops a model for DR by utilizing consumer behavior modeling considering different scenarios and levels of consumer rationality. Consumer behavior modeling has been done by developing extensive demand-price elasticity matrices for different types of consumers. An optimal load scheduling strategy for participating industrial loads is formulated in [29] in a scenario in which DR is implemented through RTP scheme. The objective function is the minimization of energy cost (linear function of consumption over periods) with a set of linear constraints such as amount of electrical energy required to reach production target, bounds on energy consumption in an hour. More details about the RTP with the possible revenues for their implementation are discussed in [30, 31]. [30] describes how retail electricity demand can be made price-responsive through either dynamic, time-based retail pricing or DR programs offered by utilities. [31] investigate the difference of the consumer response, depending on what particular type of RTP is used. DR service for residential applications is considered in [32-34]. Reference [32] proposed DR optimization for smart home scheduling under the RTP. Authors in [33] proposed a method of scheduling power usage by various appliances in a home in a scenario in which RTP signals are sent from the utility to the customers. [34] presented the real-time price-based DR management for residential appliances via stochastic optimization and robust optimization approaches.

2.2.2. Proposed strategy

A real time control strategy of BESSs in the frame of dynamically varying energy pricing is proposed in this subsection. The battery, which is supposed to operate in a large industrial facility, is managed in order to reduce the daily costs sustained by the industry owner for the energy consumption. Different configurations of the battery system (i.e., one and more battery banks in a multi-battery configuration) are taken into account and an optimization model is formulated and solved including technical constraints that guarantee the adequate storage-system behavior. The RTP tariff scheme is considered. A numerical application based on real data of an industrial facility located in the South of Italy demonstrates the effectiveness and advantages of the proposed strategy.

2.2.3. Problem formulation and solving procedure

With reference to the most general case, this subsection presents an optimal operation strategy for the very short time predictive control of the charging/discharging power of a multi-battery system to be installed in an industrial facility. The multi-battery system includes n_b battery banks ($n_b=1$ corresponds to the case of one battery system). Each battery bank can operate in charging and discharging modes independently of the operating mode of the other banks. The strategy objective is the minimization of the costs sustained by the industrial owner for the energy consumption and is tailored for the RTP tariff scheme; batteries technical constraints and maximization of their lifetime are taken into account. The proposed strategy is based on a

multi-period single-objective optimization that minimizes a linear cost function on the basis of a 24 hour forecasting of load demand and RTP.

The 24 hours are split in n_t time intervals of length Δt . During each time interval, the load and battery powers are assumed constant. In order to maximize the battery lifetime, a control on the number of charge/discharge cycles is imposed to each battery bank and it is limited to one cycle/day. Further, in the procedure also the charge/discharge efficiency is taken into consideration.

The real time procedure is repeated at each i^{th} time interval of all the time intervals of the optimization period (24 hours) and it furnishes the optimal profile for the battery charging/discharging powers of the next 24 hours that minimizes the objective function satisfying the constraints along all the optimization period. Obviously, only the output results (battery powers) obtained for the first next ($i^{th} + 1$) time interval are used as the reference signals for all converters interfacing the batteries.

Main input data of the procedure are the batteries' state of charge at the beginning of the $i^{th}+1$ time interval (output of the procedure at the previous step), the forecasted profile of the facility load power and the price of energy for the next 24 hours. The load power forecasts can be obtained through a neural network [18, 35]. For RTP, the price signal is assumed to be sent to the customers either an hour or a day-ahead [36]. Thus, in the first case, the forecast of price for 23 hours is needed (once again a neural network can be applied); while in the second case no forecast is needed for the price profile. Moreover, in order to better highlight the differences between the use of one or two-battery systems, two different RTP profiles are taken into account in the numerical applications. The first RTP profile is characterized by significant differences in the values of the prices of narrow time bands (one hour) while the second profile is a typical day-ahead price profile.

For each bank of the multi-battery system, the day is split in sub-intervals in order to impose only one charge/discharge cycle per day. As an example related to a generic bank, in figure 2.12 the first interval refers to the charging stage, the second interval to the discharging stage and the third interval still refers to a charging stage. It is interesting to observe that it is possible to interchange the charging/discharging stages of the battery banks. For example, in the two-battery case, the charging stage of the first battery can correspond to the discharging stage of the second battery and vice-versa.

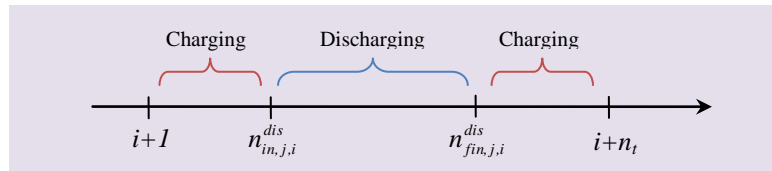


Figure 2.12: Time steps during 24 hours.

Under the above assumptions, the objective function of the optimization problem to be solved at i^{th} time interval is:

$$f_{obj}(\mathbf{x}) = \sum_{k=i+1}^{i+n_t} (Pr_{En,k} \cdot P_{grid,k}) \Delta t \quad (2.14)$$

where $P_{grid,k}$ and $Pr_{En,k}$ are the forecasted values of total power requested by the facility to the grid and RTP at the k^{th} time interval, respectively.

The equality constraints refer to the power balance and to the battery state of charge at the beginning of the first time interval and at the end of each charging stage (figure 2.12). The power balance imposes that the expected total power requested by the facility to the grid ($P_{grid,k}$) is equal to the sum of the battery powers and facility load power, at all the time intervals of the following 24 hours:

$$P_{grid,k} = P_{l,k} - \sum_{j=1}^{n_b} P_{b,k,j}, \quad k \in [i+1, \dots, i+n_t] \quad (2.15)$$

where n_b is the number of battery banks, $P_{l,k}$ and $P_{b,k,j}$ are the facility load power forecasting and the j^{th} battery power at the k^{th} time interval, respectively.

Another equality constraint imposes that state of charge of all the battery banks at the beginning of the discharging stage assumes a specified value. With reference to the battery stages sequence reported in figure 2.12 which refers to the j^{th} battery, this constraint can be expressed as follows:

$$C_{j,i+1} - \sum_{k=i+1}^{n_{in,j,i}^{dis}-1} \eta_{ch,j} P_{b,k,j} \Delta t = C_{in,j}^{dis} \quad (2.16)$$

where $C_{j,i+1}$ is the state of charge of the j^{th} battery at the begin of the $i^{th}+1$ time interval, $\eta_{ch,j}$ is its efficiency during the charge and $C_{in,j}^{dis}$ is the state of charge of the j^{th} battery when its discharge starts. Further equality constraints are imposed with reference to the state of charge at the end of the 24 hours which has to reach a specified value. Always with reference to the battery stages sequence reported in figure 2.12, this constraint is:

$$C_{j,i+1} - \sum_{k=i+1}^{n_{in,j,i}^{dis}-1} \eta_{ch,j} P_{b,k,j} \Delta t - \sum_{k=n_{in,j,i}^{dis}}^{n_{fn,j,i}^{dis}} \frac{1}{\eta_{dis,j}} P_{b,k,j} \Delta t - \sum_{i=n_{fn,j,i}^{dis}+1}^{i+n_t} \eta_{ch,j} P_{b,k,j} \Delta t = C_{j,i}^{sp} \quad (2.17)$$

where $C_{j,i}^{sp}$ is the specified value of the j^{th} battery state of charge at the end of the 24 hours ($i^{th}+n_t$ time interval) and $\eta_{dis,j}$ is the discharge efficiency of the j^{th} battery during the discharge. In (2.17) the value of $C_{j,i}^{sp}$ can be chosen on the basis of specific requirements of the end-user, and, in case of no requirements, $C_{j,i}^{sp}$ can be assumed equal to $C_{j,i+1}$.

The inequality constraints impose that the battery banks have to furnish power during discharging stages and absorb power during the charging stages:

$$-P_{max,j} \leq P_{b,k,j} \leq 0, \quad k \notin [n_{in,j,i}^{dis}, \dots, n_{fn,j,i}^{dis}] \quad (2.18)$$

$$0 \leq P_{b,k,j} \leq P_{max,j}, \quad k \in [n_{in,j,i}^{dis}, \dots, n_{fn,j,i}^{dis}] \quad (2.19)$$

where $P_{max,j}$ is the maximum charge/discharge power of the j^{th} battery which is based on the battery power rate [15].

The inequality constraints involve also the state of charge that cannot exceed the size of the battery banks during the charging stage and cannot be lower than the maximum DOD during the discharging stage, that is:

$$C_{j,i+1} - \sum_{h=1}^k \eta_{ch,j} P_{b,j,h} \Delta t \leq C_{max,j} , \quad k \in [i+1, \dots, n_{in,j,i}^{dis} - 1] \quad (2.20)$$

$$C_{j,i+1} - \sum_{h=1}^{n_{in,j,i}^{dis}-1} \eta_{ch,j} P_{b,j,h} \Delta t - \sum_{h=n_{in,j,i}^{dis}}^{n_{fin,j,i}^{dis}} \frac{1}{\eta_{dis,j}} P_{b,j,h} \Delta t - \sum_{h=n_{fin,j,i}^{dis}+1}^k \eta_{ch,j} P_{b,j,h} \Delta t \leq C_{max,j} , \quad k \in [n_{fin,j,i}^{dis} + 1, \dots, i + n_t] \quad (2.21)$$

where $C_{max,j}$ is the capacity of the j^{th} battery. Eventually, the state of charge cannot be lower than the minimum value of DOD during the discharging stage, that is:

$$C_{j,i+1} - \sum_{h=1}^{n_{in,j,i}^{dis}-1} \eta_{ch,j} P_{b,j,h} \Delta t - \sum_{h=1}^k \frac{1}{\eta_{dis,j}} P_{b,j,h} \Delta t \geq C_{min,j} , \quad k \in [n_{in,j,i}^{dis}, \dots, n_{fin,j,i}^{dis}] \quad (2.22)$$

where $C_{min,j}$ is evaluated on the basis of the maximum DOD of the j^{th} battery.

Note that also the above inequality constraints have been reported with reference to the charging/discharging stages sequence of the j^{th} battery reported in figure 2.12. Of course, when referring to a different battery bank (with different charging/discharging stages), the above constraints will be modified accordingly.

2.2.4. Numerical application

The proposed optimization strategy is applied at a GETRA facility which is located in the south Italy. GETRA's scheme as an industrial facility is reported in figure 2.13. Its electrical distribution system includes four, low-voltage electrical lines ("tanks and boxes manufactory", "tests", "assembly" and "winding and coils" lines) fed by two MV/LV transformers. Each electrical line is dedicated to a different manufacturing process. Based on the actual measured data of the industrial loads, this procedure is applied for numerical simulations in this section where, for the sake of simplicity and without loss of generality, only the results obtained at the first control interval are reported. The 24 hours forecasted load power has been assumed; the time step is 10 minutes (i.e., $n_t=144$). It is also assumed that the price of a specified hour of the day is sent 24 hours ahead. In order to better highlight the differences between the use of one or two-battery systems, two different RTP profiles are taken into account (figure 2.14): the first profile (*case a*) is characterized by significant differences in the values of the prices of narrow time bands (figure 2.14.a) while the second profile (*case b*) is a typical day-ahead price profile (figure 2.14.b). The multi-battery system consists of two Lithium-ion batteries, connected to -

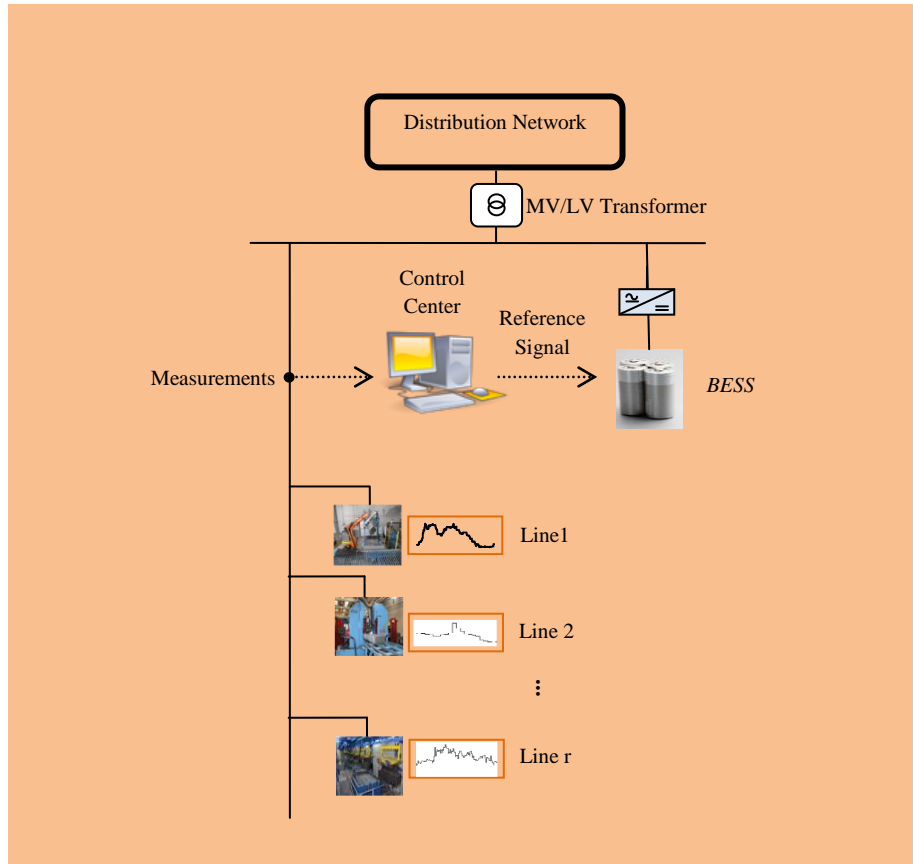


Figure 2.13: Industrial Facility.

the secondary side of the MV/LV transformer interfacing the facility with the distribution grid. A centralized control system performs the proposed optimization procedure and sends the charge/discharge control signals to the battery converters. The size of both battery banks is $60kW$ with a discharging time of 2.5 hours. The batteries charging efficiency is 0.90 and the discharging efficiency is 0.93, both these values including the interfacing converter efficiency. A maximum DOD of 80% is assumed in order to maximize the battery life cycle [24].

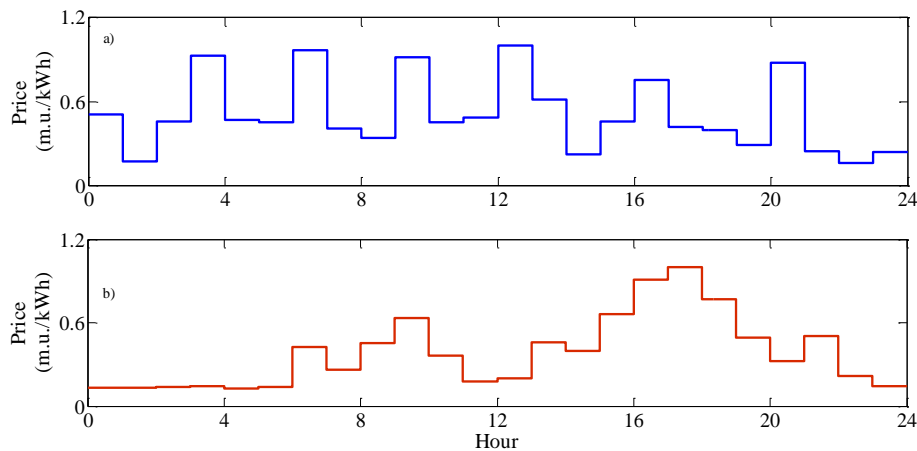


Figure 2.14: Energy price profile.

In the following subsections the above mentioned cases (*case a* and *case b*) are shown. In both cases, the two batteries operate as follows: the first battery discharging mode starts at the 12th hour and ends at the 24th hour while the second battery discharging mode starts at the first time

interval and ends after 12 hours. It is also assumed that the energy charge level of the first battery bank, at the beginning of the first time interval, assumes the minimum value. The second battery bank is initially fully charged and, at the end of the charging stage (24th hour), it is imposed that the battery bank is again fully charged.

Moreover, the results of both cases are also compared with the case of a 120 kW-2.5 hours single battery system, where it is imposed a maximum number of cycles per day equal to one.

Case a)

The charge/discharge power profiles of the two battery banks are reported in figure 2.15. Figure 2.16 shows the battery banks energy profiles. The analysis of figure 2.15 shows that the constraints on upper and lower limits (size of the battery banks) are always satisfied. The power profiles of figure 2.15 are also compatible with the constraints imposed on the battery energy (figure 2.16). Since only the results obtained for the first next time interval ($i^{th} + 1$) are used as reference signals, then the reference signals for both the two battery banks are equal to zero kW. The total stored energy in the battery banks (i.e. the sum of the energy stored in the two banks) is also reported in figure 2.16. It can be observed that, for each battery bank, the constraint on the number of charge/discharge cycles per day is fully satisfied. Moreover, the analysis of the total stored energy profile clearly reveals that, if only one battery bank would be applied, more than one cycle per day would be required.

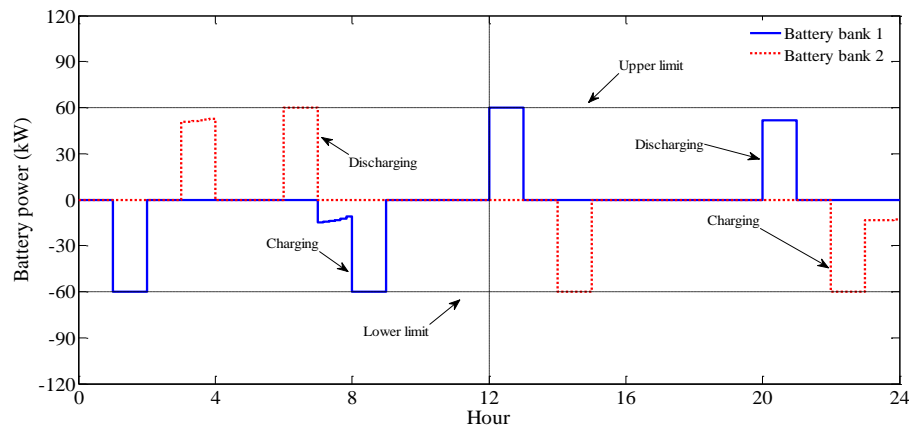


Figure 2.15: Battery power profile (case a).

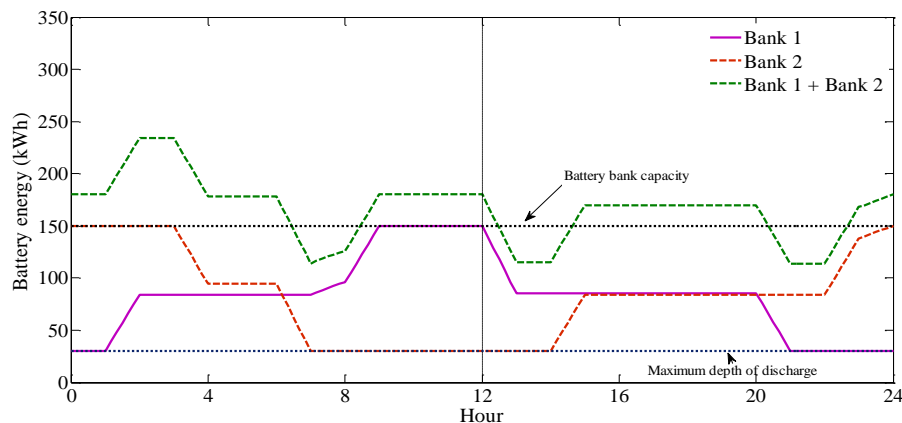


Figure 2.16: Battery energy profile (case a).

In figure 2.17 the power that the industrial facility is expected to request to the grid (“grid power forecasting”) is reported and compared with the load power forecast. Figure 2.17 shows that the optimization procedure doesn’t perform peak shaving. In fact, it allows decreasing the industrial power requests when the energy price is higher even if the load demand is low and increasing the power when the price is lower, even in high load demand periods. This is evidenced in figure 2.18 where the plot of the energy price is reported together with the plot of ΔP (that represents the difference between the load and grid power forecasting, i.e. the total power of the batteries). As mentioned, the batteries charge when price is lower and discharge when price is higher. It is worth to note that, to shave the peak power request, an upper limit at the imported power should be included in the optimization problem (e.g., the MV/LV transformer size), as shown in [37].

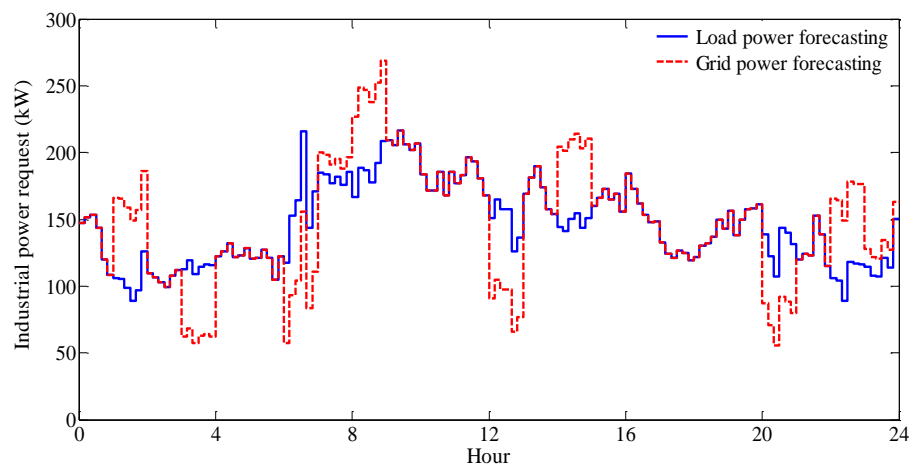


Figure 2.17: Load and grid powers (*case a*).

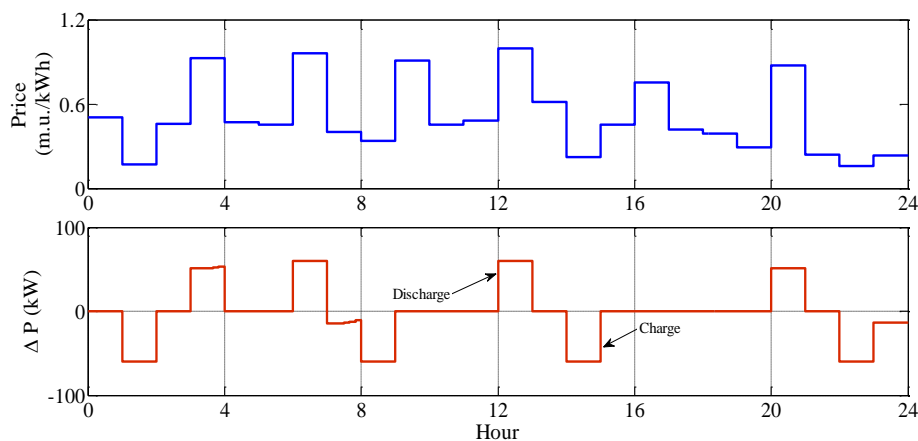


Figure 2.18: Energy price and total power of the batteries (*case a*).

Case b)

The results of the simulation considering the energy price profile of figure 2.14.b are reported in figures 2.19-2.22. Once again the power profiles of the two battery banks (figure 2.19) satisfy the constraints on upper and lower limits (size of the battery banks); the reference signals for the next time interval is 60 kW for the battery bank 1 (which operates in charging mode) and zero for the battery bank 2 (which operates in discharging mode). These power

profiles are also compatible with the constraints imposed on the battery energy (figure 2.20). The constraint on the number of charge/discharge cycle per day is satisfied for each battery bank, even though the total stored energy profile (figure 2.20) clearly presents more than one cycle per day.

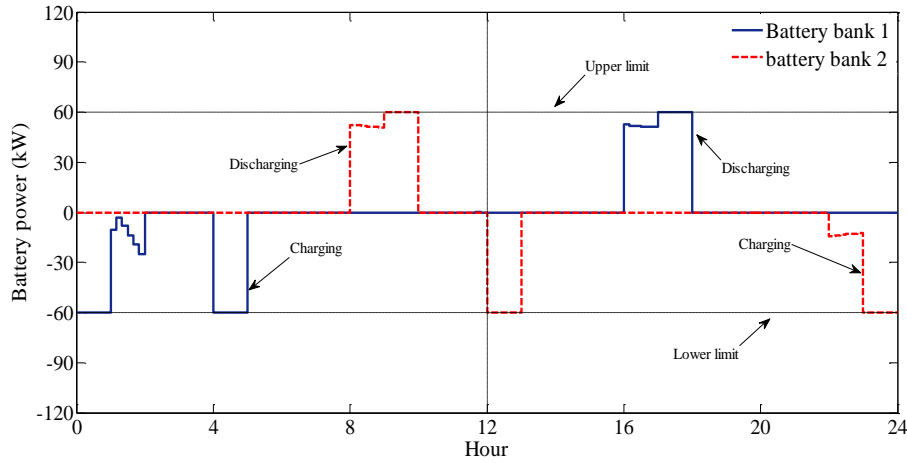


Figure 2.19: Battery power profile (case b).

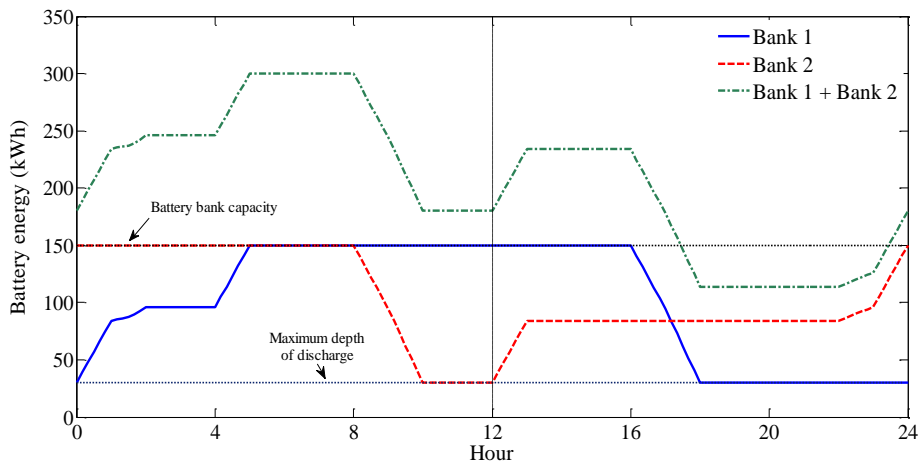


Figure 2.20: Battery energy profile (case b).

In figure 2.21 the power that the industrial facility is expected to request to the grid is reported and compared with the load power forecasting, showing the same features of figure 2.17.

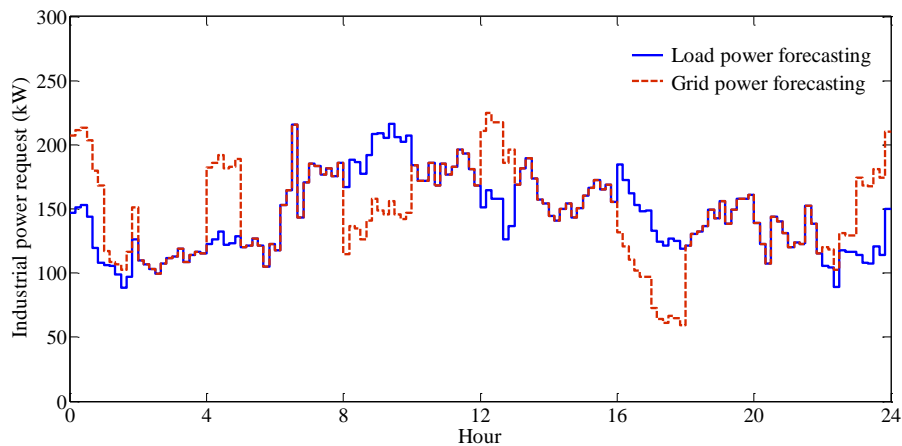


Figure 2.21: Load and grid powers (case b).

Figure 2.22 shows the plot of the energy price together with the plot of ΔP . Also in this case the batteries charge when price is lower and discharge when price is higher.

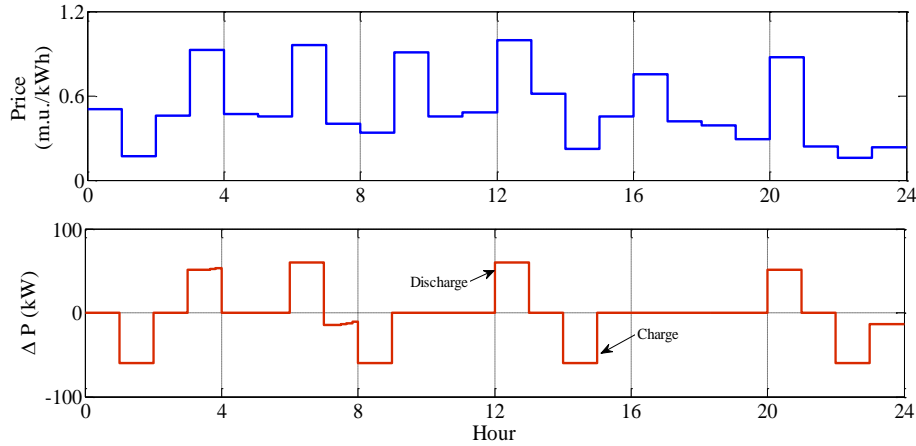


Figure 2.22: Energy price and total power of the batteries (*case b*).

Eventually, in order to show the feasibility of the proposed strategies, in table 2.2 the percentage reduction of the value assumed by the objective cost function (2.14) in cases *a*) and *b*), with respect to the case of no-battery installed, are reported. The reductions obtained in both the two cases are also compared with the reductions obtained with a 120 kW-2.5 hours single battery system.

Battery system configuration	Objective function reduction (%)	
	case a	case b
Two batteries	8.12	9.12
One battery	7.53	12.82

Table 2.2: Objective function reduction.

The analysis of table 2.2 clearly demonstrates that the use of storage systems always allows reducing the energy cost sustained by the industrial owner. Moreover, the use of multi-battery system seems particularly advantageous in case of the energy price profiles of figure 2.14.a where more than one charging/discharging cycle per day are allowed by the procedure. In case of price profiles of 2.14.b, the use of a single battery seems to be the most adequate choice, even with the constraint of one charging/discharging cycle per day.

2.3. An advanced optimal operation strategy for demand response under energy demand charge

This subsection is focused on DR service under the EDC tariff which involves a structure directly linked to both the consumed energy and the peak load.

Customers can be expected to vary their usage in response to this price information and manage their energy costs by shifting their usage to a lower cost period [38, 39]. In addition to charges based on usage, an electricity bill may include a demand charge, which is determined by the maximum capacity available to a customer, whether or not it is actually

used. The demand charge is billed as a fixed rate that is calculated on a per kW basis. This charge is based on the premise that commercial customers and other large users should pay a share of the infrastructure costs associated with the maintenance of capacity [39, 40].

2.3.1. State of the art

In the technical literature numerous works to apply DR under dynamic pricing, especially with reference to EDC tariff, are investigated. [41] presents an overview on DR in the electricity market. The definition and a classification of demand response, different potential benefits as well as cost components of demand response are considered. The use of storage facilities to apply price-based DR was analyzed in [32, 34, 42] with reference to residential applications. The application of price-based DR in industrial loads also has been considered in [23], where a BESS that was able to provide energy to the industrial loads during high-price/peak-demand periods was considered. In [38] scaling distributed energy storage for grid peak reduction based on EDC tariff is proposed, where the tariff involves energy prices varying hourly taking also into account the peak value of the power. In [39] charge scheduling of an ESS under TOU pricing and EDC is considered. A real-coded genetic algorithm is used to schedule the charging of an energy storage system (ESS), operated in tandem with renewable power by an electricity consumer who is subject to time-of-use pricing and a demand charge. [43] formulated similar problem of [39] but [39] aims to optimize a daily, rather than a monthly, bill.

2.3.2. Proposed strategy

In this subsection, with reference to an industrial customer, an advanced optimal control strategy to perform price-based DR by optimally controlling a BESS installed in the industrial facility's substation is proposed. The control strategy minimizes the electricity bill acting on both consumed energy and peak load. It is based on a two-step procedure that minimizes the problem of forecasting errors. The first step is a day-ahead scheduling for evaluating the peak value of the power that the facility must request from the grid and for determining the periods when the battery is allowed to charge and discharge. The second step is a very short-time predictive procedure for the real time optimal control of the BESSs' powers. The aim of the entire procedure is the reduction of the electricity costs related to the energy charge, by shifting the load times, and the reduction of the electricity costs associated with demand charge, by providing peak-shaving service. The procedure takes into account also the battery's efficiency and lifecycle by imposing limits on the depth of discharge and the number of charging/discharging cycles.

As it is presented in subsection 2.1.1, two-step procedures for BESS power optimal control were proposed to furnish load leveling service which allows reducing the difference between the mean power and the peak power, thereby avoiding or deferring new investments in transmission and distribution facilities.

There are important reasons why also in case of DR the two-step optimal control approach can be used:

- First, in order to identify the time intervals related to the charging and discharging of the battery, a discrete variable procedure is needed that typically involves the use of algorithms that require high computational effort (e.g., genetic algorithm, dynamic

programming); thus, the procedure should be performed off line (in this case, the day before).

- Second, once the optimal charging/discharging intervals have been established, accurate power-forecast information is needed for performing a very short-time control of the BESS's power, which can only be performed on line and at small time intervals (the very short-time predictive control).

It is outlined that the forecast of the peak value of the power which the facility must request from the grid can be performed easily in the day-ahead scheduling and, then, also this quantity can be assumed to be assigned in the second step of the procedure.

Summarizing the advantages of the two-step procedure are that:

- it minimizes the influence of the forecasting errors on the load demand taking into account that the forecast in the very short time predictive control is able to highly improve the day ahead forecast of the first step;
- it avoids the problem of computational efforts of the very short time predictive control, by evaluating both the desired peak value of the facility power and the battery charging/discharging periods in the day ahead scheduling.

More detailed discussion on the advantages obtained by applying the two-step procedure is reported in numerical application which is on an actual industrial application.

2.3.3. Problem formulation and solving procedure

In this application, the generalization of the EDC tariff is considered, where the tariff involves energy prices varying hourly taking also into account the peak value of the power [38]. In this case, the generalized energy demand charge tariff (f_{GEDC}) has the following structure:

$$f_{GEDC} = Pr_{peak} \cdot \max_{i \in \Omega} \{P_{grid,i}^{da}\} + \sum_{i=1}^{n_t} (Pr_{En,i} \cdot P_{grid,i}^{da}) \Delta t, \quad \Omega = [1, \dots, n_t] \quad (2.23)$$

where $P_{grid,i}^{da}$ is the expected power requested by the facility to the grid at the i^{th} time interval, n_t is the number of time intervals in which the day is divided, $Pr_{En,i}$ and Pr_{peak} are the energy charge at the i^{th} time interval and demand charge, respectively.

The proposed optimal control strategy for minimizing the electricity costs of the industrial facility given by (2.23) is based on the solution of two different optimization problems:

- *Day-ahead scheduling*: it evaluates the peak value of the power that the facility must request from the grid and the periods in which the battery is allowed to charge and discharge;
- *Very short time predictive control*: it evaluates the BESS's charging/discharging power for real-time operation.

Day-ahead scheduling

Day-ahead scheduling is performed once a day, for the next day. Input data of the scheduling are the BESS's state of charge at the beginning of the day, the daily forecasted profile of the facility's load, and the hourly energy-price profile for the next day. The outputs of day-ahead

scheduling are the time periods in which the BESS is allowed to charge/discharge and the maximum power that the industrial facility can extract from the grid.

In order to maximize the battery's lifetime, as mentioned in the subsection 2.1.2, a maximum number of charge/discharge cycles per day is imposed [44]. To do that, the day is divided into specific time periods, i.e., charging periods (when the battery only is allowed to charge) and discharging periods (when the battery only is allowed to discharge). Figure 2.23 shows a day on which the battery was allowed to charge in the early morning hours and the night hours. This figure is similar to the figure 2.12 where, the indices change at every time interval ($n_{in,j,i}^{dis}$, $n_{fin,j,i}^{dis}$), since the optimization period dynamically varies during the day. But in this case, instead, the whole day is considered at the same time and these bounds (n_{in}^{dis} , n_{fin}^{dis}) are fixed (figure 2.23).

If the tariff scheme has a limited number of price levels (e.g., "off-peak" and "on-peak"), it is easy to specify the charging and discharging periods; in fact, it is obvious that the more profitable result can be obtained by fixing the discharge period during the peak price hours and the charge period during the non-peak price hours. In case of numerous price levels during the day (e.g., the case in which the price varies hourly), determining the most profitable charging and discharging time periods is very difficult. This proposed optimization problem is focused on this last, more general case.

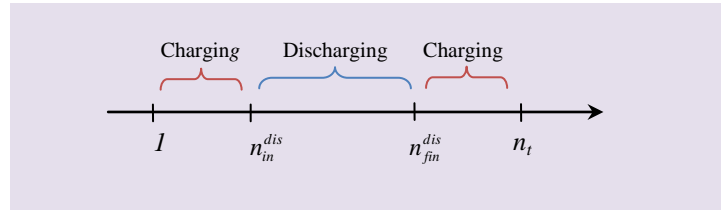


Figure 2.23: Time intervals during the day (indices refer to the day ahead).

In the proposed formulation, the day is divided into n_t time intervals of length Δt , e.g., in the numerical application, 10 minutes. During each time interval, the load and battery powers are assumed to be constant. The BESS's charging/discharging periods during the day are defined uniquely when the initial and final time intervals of discharging (n_{in}^{dis} , n_{fin}^{dis}) are specified (figure 2.23). Thus, the scheduling is based on the solution of an optimization problem including both integer variables and real variables. The battery's power and energy are real variables, whereas the initial/final time intervals of the discharging periods are integer variables.

In case of mixed integer optimization problems for the BESS's operation, some solving procedures have been proposed in the literature based on dynamic programming (DP) [14, 45, 46]. However, DP handles discrete variables, thus requiring a discretization so that it also can deal with continuous variables (e.g., the battery's charge level); obviously, the required computational time increases when the discretization is thinner.

In this thesis, a hybrid solving procedure is proposed to solve the day-ahead scheduling problem. The procedure includes a genetic algorithm (GA) for handling the discrete variables (i.e., charging/discharging time intervals) and a linear optimization algorithm (LOA) for the real variables (i.e., the battery's power). The proposed procedure does not require any discretization, so a more accurate minimization of the objective function is obtained.

In the following, the scheduling optimization model is presented with reference to the mixed GA and LOA implementation. Figure 2.24 depicts a flowchart of the proposed procedure. The GA is aimed at identifying the initial and final discharging time interval, while the inner LOA-

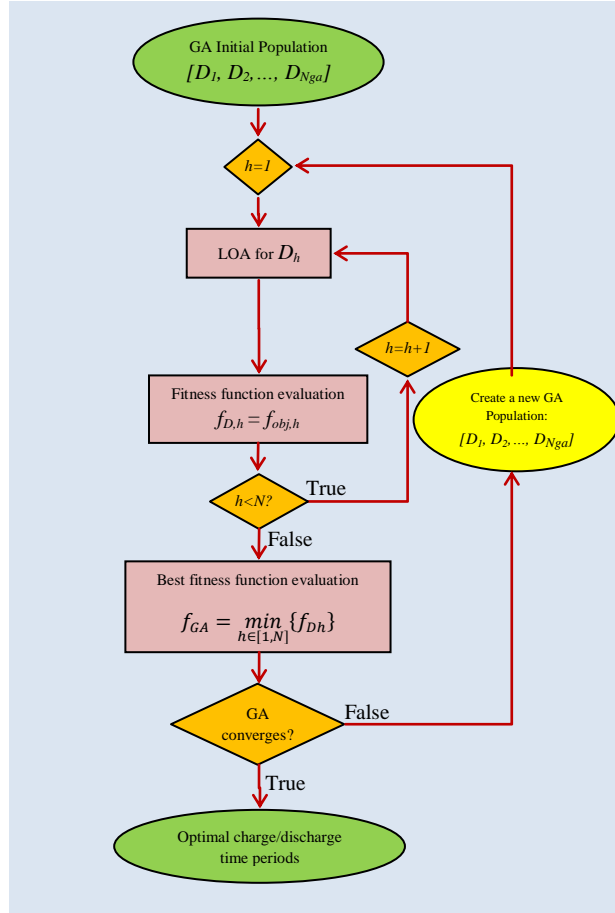


Figure 2.24: Flowchart of the scheduling procedure.

is aimed at determining the daily charge/discharge power profile of the battery that minimizes the electricity costs sustained by the facility. The GA is able to create the initial population, which includes N_{ga} individuals (or chromosomes). The individuals consist of two elements (or genes); the first element is the initial step of the discharging period (n_{in}^{dis}), and the second is the final step of the discharging period (n_{fin}^{dis}). According to these considerations, then D_h denotes the h^{th} ($h=1, \dots, N_{ga}$) individual. For each individual, the following trivial inequality constraints are applied:

$$\begin{aligned}
 1 &\leq n_{in}^{dis} \leq n_t \\
 1 &\leq n_{fin}^{dis} \leq n_t \\
 n_{in}^{dis} &\leq n_{fin}^{dis}
 \end{aligned} \tag{2.24}$$

The inner LOA is performed for each individual according to the sequence of the flowchart shown in figure 2.24. Note that the value of each individual's fitness function is equal to the optimal value of the objective function of the LOA that corresponds to that individual (f_{Dh}^{LOA}). The best fitness function of the current population f_{GA} is the one that corresponds to the

individual characterized by the minimum f_{Dh}^{LOA} . The GA converges when the value of the best fitness function remains constant over an assigned number of generations or when a maximum number of iterations is reached [47]. Otherwise, the GA generates a new population based on proper evolutionary operators (e.g., selection, recombination, mutation).

The inner LOA solves a constrained, single-objective minimization problem aimed at determining the daily charge/discharge power profile of the battery that minimizes the electricity costs sustained by the industrial facility. The optimization variable is constituted by the BESS's power at each time step of the day.

The objective function is defined as³:

$$f_{obj}(\mathbf{x}) = f_{GEDC} \quad (2.25)$$

with f_{GEDC} given by (2.23).

The equality constraints refer to the power balance and the BESS state of charge at the beginning of the day and at the end of the charging stage.

Comparing with the power balance equation for the previous application (2.15) which is considered at each time interval for the following 24 hours, here, similar power balance equation imposes that the expected power value requested by the facility to the grid (hereinafter referred to as “day-ahead forecasted facility power”) is equal to the algebraic sum of the BESS power and facility load power, at all the time intervals of the day.

A further equality constraint can be considered which imposes that the BESS state of charge at the beginning of the discharging stage has to reach a specified value:

$$C_{in}^{sp} - \sum_{i=1}^{n_{ch}^{dis}-1} \eta_{ch} P_{b,i}^{da} \Delta t = C_{in}^{dis} \quad (2.26)$$

where C_{in}^{sp} is the BESS state of charge at the beginning of the day, $P_{b,i}^{da}$ is the BESS power at time interval i , η_{ch} is the BESS efficiency during the charge and C_{in}^{dis} is the state of charge of the BESS when the discharge of the battery starts.

An equality constraint has to be imposed also with reference to the state of the charge at the end of the day:

$$C_{in}^{sp} - \sum_{i=1}^{n_{ch}^{dis}-1} \eta_{ch} P_{b,i}^{da} \Delta t - \sum_{i=n_{ch}^{dis}}^{n_{fin}^{dis}} \frac{P_{b,i}^{da}}{\eta_{dis}} \Delta t - \sum_{i=n_{fin}^{dis}+1}^{n_t} \eta_{ch} P_{b,i}^{da} \Delta t = C_{fin}^{sp} \quad (2.27)$$

where C_{fin}^{sp} is the specified value of the state of the charge of the BESS at the end of the day and η_{dis} is the BESS efficiency during the discharge.

Equation (2.27) is similar to (2.4) and (2.17). Equation (2.17) is formulated at each time interval for specific value of the state of charge at the end of the following 24 hours ($i^{th} + n_t$ time interval). Equation (2.4) is formulated for a only one discharging and charging periods where

³ Note that the objective function (2.25) does not have the form of a standard linear optimization problem, but it can be transformed readily to an equivalent, linear-program form [1].

(2.27) is for charging, discharging and charging periods, thus the first summation in (2.27) is not considered in (2.4).

The inequality constraints impose that the BESS has to furnish power during discharging stages and absorb power during the charging stages:

$$-P_{max} \leq P_{b,i}^{da} \leq 0, \quad i \notin [n_{in}^{dis}, \dots, n_{fin}^{dis}] \quad (2.28)$$

$$0 \leq P_{b,i}^{da} \leq P_{max}, \quad i \in [n_{in}^{dis}, \dots, n_{fin}^{dis}] \quad (2.29)$$

where P_{max} is the maximum charge/discharge power of the BESS [14]. These constraints are according to inequalities which are formulated in (2.5-2.6) for load leveling application and (2.18-2.19) for demand response application.

Similar to the inequalities in (2.20-2.22), which guarantee that in case of multi battery system the state of charge cannot exceed the size of the battery banks during the charging stage and cannot be lower than the maximum DOD during the discharging stage, here, the inequality constraints (2.30-2.32) are also considered. They are:

$$C_{in}^{sp} - \sum_{j=1}^i \eta_{ch} P_{b,j}^{da} \Delta t \leq C_{max}, \quad i \in [1, \dots, n_{in}^{dis} - 1] \quad (2.30)$$

$$C_{in}^{sp} - \sum_{j=1}^{n_{fin}^{dis}-1} \eta_{ch} P_{b,j}^{da} \Delta t - \sum_{j=n_{in}^{dis}}^{n_{fin}^{dis}} \frac{P_{b,j}^{da}}{\eta_{dis}} \Delta t - \sum_{j=n_{fin}^{dis}+1}^i \eta_{ch} P_{b,j}^{da} \Delta t \leq C_{max}, \quad i \in [n_{in}^{dis} + 1, \dots, n_t] \quad (2.31)$$

$$C_{in}^{sp} - \sum_{j=1}^{n_{in}^{dis}-1} \eta_{ch} P_{b,j}^{da} \Delta t - \sum_{j=1}^i \frac{1}{\eta_{dis}} P_{b,j}^{da} \Delta t \geq C_{min}, \quad i \in [n_{in}^{dis}, \dots, n_{fin}^{dis}] \quad (2.32)$$

where C_{max} is the capacity, C_{min} is the minimum value of the energy that can be stored in the battery based on the allowable depth of discharge and η_{dis} is the BESS discharge efficiency.

When the inner linear optimization problem converges, the value assumed by the objective function represents also the value of the fitness function related to each individual of the GA.

Very short time predictive control

Very short time predictive control is performed n_t times per day, with reference to each interval i ($i=1, \dots, n_t$) of the day. This procedure is aimed at providing the power that the battery has to absorb or furnish during the controlled time interval starting from more accurate forecasts. In more detail, the procedure that refers to the generic interval i is performed during the preceding interval. Obviously, for the first interval, the procedure is performed during the last interval of the day before, and the procedure performed during the last interval of the current day refers to the first interval of the following day.

Input data for the procedure are the very short time forecasts of the load power from the controlled time interval i up to the last time interval of the day, the maximum value of the day-ahead forecasted power required by the facility, the charge/discharge time intervals of the BESS, with the last two being outputs of the day-ahead optimization, and the state of charge of the battery at the beginning of the i^{th} interval, that is the output of the optimization

performed in the previous time interval.

Outputs of the procedure are the charge/discharge power and the final state of charge, both evaluated with reference to the i^{th} time interval. The final state of charge of the battery is an input for the next time interval.

The optimization procedure of the very short time predictive control at the i^{th} time interval is based on the solution of the linear optimization problem (2.1) that is solved during the preceding interval.

With reference to a generic controlled time interval i , the values of the BESS's power at each time interval, starting from the controlled time interval i up to the last time interval of the day are optimization variables. In this subsection, the interval $[i, \dots, n_t]$ will be called the rest of the day.

The objective function for the i^{th} time interval is:

$$f_{LOA}^{vst} = \sum_{j=i}^{n_t} (Pr_{En,j} \cdot P_{grid,j}^{vst}) \Delta t \quad (2.33)$$

where $P_{grid,j}^{vst}$ is the power requested by the facility from the grid resulting from the very short time procedure at j^{th} time interval.

The power balance imposes that the facility power $P_{grid,j}^{vst}$ is equal to the algebraic sum of the BESS's power and the forecasted load power of the facility at all of the time intervals of the rest of the day:

$$P_{grid,j}^{vst} = P_{l,j}^{vst} - P_{b,j}^{vst}, \quad j=i, \dots, n_t \quad (2.34)$$

where $P_{l,j}^{vst}$ is the forecast of the load power demand at the j^{th} time interval.

An equality constraint is imposed on the battery's state of charge, i.e., at the end of the day, the state of charge must be equal to a specified value. For the generic controlled interval, this constraint is:

$$C_i - \sum_{j=i}^{n_t} (k_j P_{b,j}^{vst} \Delta t) = C_{fin}^{sp} \quad k_j = \begin{cases} \eta_{ch} & \text{if } P_{b,j}^{vst} > 0 \\ 1/\eta_{dis} & \text{if } P_{b,j}^{vst} \leq 0 \end{cases} \quad (2.35)$$

where C_i is the BESS's state of charge at the beginning of the controlled time interval, and C_{fin}^{sp} is the final state of charge.

Inequality constraints involve peak shaving, i.e., the facility's power must be lower than a maximum value:

$$P_{grid,j}^{vst} \leq P_{grid,max}^{da} \quad j=i, \dots, n_t \quad (2.36)$$

where $P_{grid,max}^{da}$ is the maximum value of facility's power requirement that has been forecasted the day-ahead. Technical constraints also impose that the battery's power cannot exceed the rate at which the battery can be discharged or charged. When $i < n_{in}^{dis}$, these constraints are:

$$0 \leq P_{b,j}^{vst} \leq P_{max}^{dis}, \quad j = n_{in}^{dis}, \dots, n_{fin}^{dis} \quad (2.37)$$

$$-P_{max}^{ch} \leq P_{b,j}^{vst} \leq 0, \quad j = i, \dots, (n_{in}^{dis} - 1), (n_{fin}^{dis} + 1), \dots, n_t \quad (2.38)$$

when $n_{in}^{dis} \leq i \leq n_{fin}^{dis}$, they are:

$$-P_{max}^{dis} \leq P_{b,j}^{vst} \leq 0, \quad j = i, \dots, n_{fin}^{dis} \quad (2.39)$$

$$0 \leq P_{b,j}^{vst} \leq P_{max}^{ch}, \quad j = n_{fin}^{dis} + 1, \dots, n_t \quad (2.40)$$

when $i > n_{fin}^{dis}$, only the constraint for the charging is applied:

$$0 \leq P_{b,j}^{vst} \leq P_{max}^{ch}, \quad j = i, \dots, n_t \quad (2.41)$$

Due to inaccurate forecasting, it could happen that constraints cannot be satisfied, so the optimization procedure does not converge. In this case, lower values of the battery's state of charge at end of the last time interval, as well as higher values of the maximum peak power, are allowed, and the problem is solved iteratively until it converges.

The battery's technical constraints also impose that the level of the stored energy during the charging periods cannot exceed the battery's capacity:

$$C_i - \eta_{ch} \sum_{j=1}^{n_{in}^{dis}-1} (P_{b,j}^{vst} \Delta t) \leq C_{max} \quad (2.42)$$

The inequality constraints also involve the BESS's state of charge, which cannot be lower than a specific minimum value during the discharging stage, i.e.:

$$C_i - \sum_{j=i}^{n_{fin}^{dis}} (k_j P_{b,j}^{vst} \Delta t) \geq C_{min} \quad k_j = \begin{cases} \eta_{ch} & \text{if } P_{b,j}^{vst} > 0 \\ 1/\eta_{dis} & \text{if } P_{b,j}^{vst} \leq 0 \end{cases} \quad (2.43)$$

2.3.4. Numerical application

The results refer to the application of the procedures to the GETRA industrial facility located in South Italy, whose scheme is reported in figure 2.13. The BESS, which consists of a lithium-ion battery connected to the power grid through a pulse width modulation (PWM)-controlled AC/DC converter, installed at the secondary side of the MV/LV transformer of the facility. A control system performs the optimization procedures and sends the charge/discharge control signals (i.e. the output of the very short time control procedure) to the BESS. The size of the battery was 60 kW with a discharging time of 5 h. The BESS's charging efficiency was 0.90, and the discharging efficiency was 0.93. The admissible DOD was 80% [24]. The load forecasting profile of the load demand of the industrial facility, should be obtained through neural network approaches based on historical measurement data,. However, due to the lack of available historical data, in this application the load forecasting profile was obtained based on random variations into the measured available daily profile.

Figure 2.25 shows the day-ahead forecast of the load power that was obtained and the actual,

measured profile. Regarding the energy prices, an hourly energy charge was assumed according to the profile of figure 2.26, where the prices are expressed in $m.u./kWh$. The energy charge profile refers to data of a typical Italian day-ahead market. The demand charge was assumed to be 100 times greater than the energy charge (i.e., $100 m.u./kwh$) [48].

In the following sections, some of the results of the simulations that were performed are reported. In the simulations, it was assumed that the battery was charged to 80% of its full capacity at the beginning of the day and that the same charge level was imposed at the end of the day.

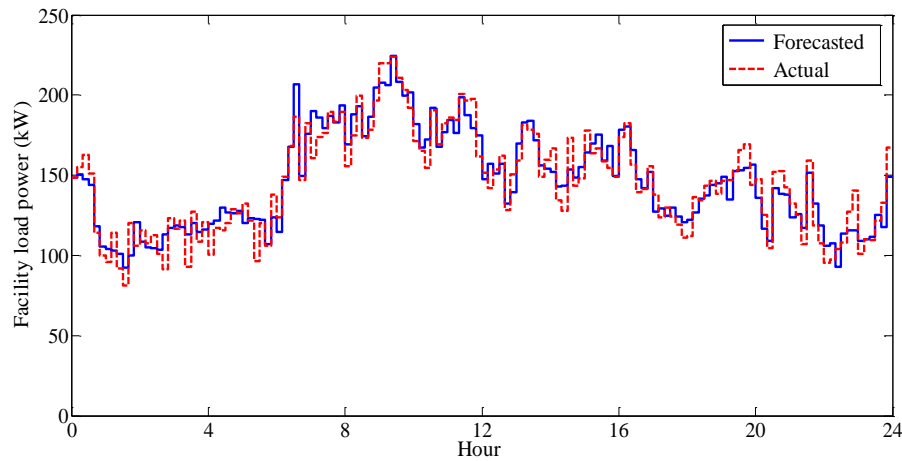


Figure 2.25: Day-ahead forecasted values and actual values of load.

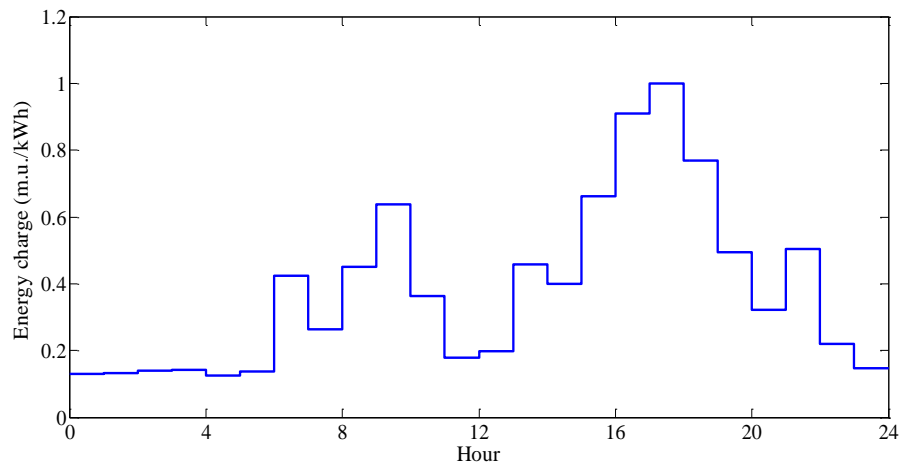


Figure 2.26: Energy charge.

Day-ahead scheduling results

Figure 2.27 shows the facility's load profile obtained with day-ahead scheduling. For comparative purposes, the same profile was reported for the case in which there was no BESS. Compared to the day-ahead forecast of the power requested from the grid in the absence of a BESS, the forecasted peak demand reduction was of about $54 kW$, which corresponds to a reduction of 32%. Figure 2.28 shows the battery's power during the day and that the BESS started discharging at 5:10 a.m. and stopped discharging at 6:10 p.m. The results shown in Figures 2.27 and 2.28 illustrate that the BESS was discharged at about 9:00 a.m., which was during the hours of peak demand. The figures also show that the BESS was discharged about

5:00 p.m., during the hours in which the energy charge was high (figure 2.26). Charging of the BESS occurred mainly during the initial and final hours of the day, when the energy cost was lower. Thus, the entire power demand of the industrial facility resulted in a more-leveled daily profile, as well as periods of increased power demand during the early morning and late night hours.

The diagrams reported in figures 2.28 (battery power during the day) and 2.29 (battery energy during the day) also show that the technical constraints of the battery were satisfied completely in terms of the desired value of energy stored at the beginning and end of the day, maximum and minimum capacity, desired number of cycles per day (only one), and the BESS's size limits. The reduction in terms of the objective function value between the cases with and without the BESS was about 13%. However, this is a theoretical value that cannot be attained due to forecasting error.

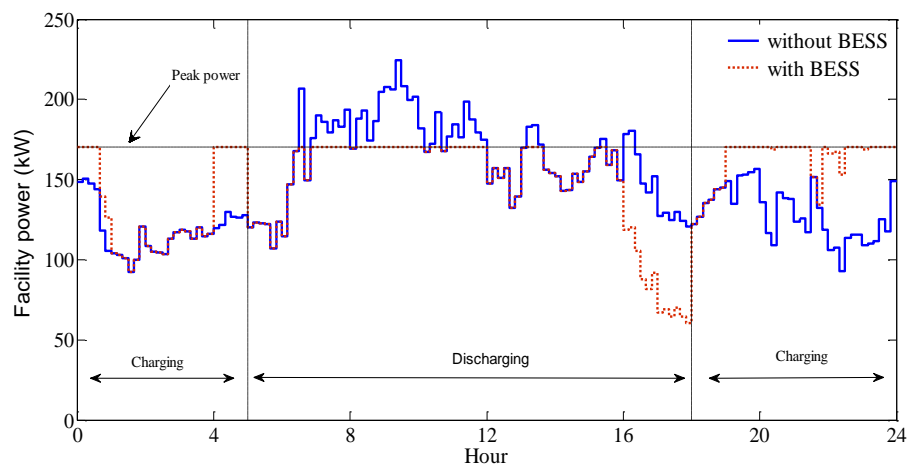


Figure 2.27: Day-ahead power profile of the facility with and without the BESS.

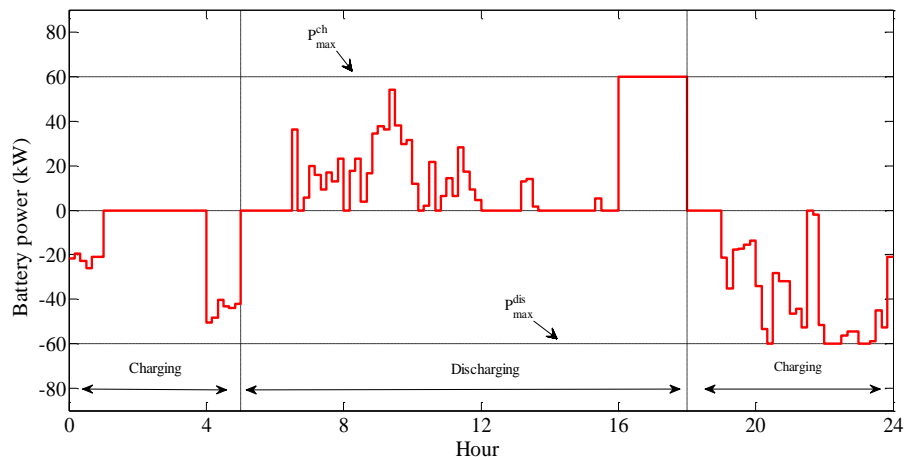


Figure 2.28: Day-ahead profile of the BESS's power.

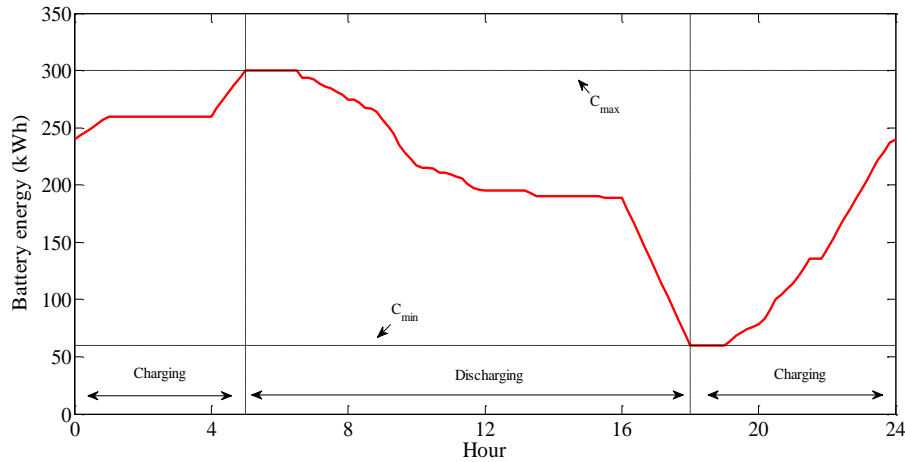


Figure 2.29: Day-ahead profile of the BESS's energy.

The results of day-ahead scheduling, which are inputs to the very short time procedure, are the discharge time interval of the BESS (5:10 a.m. and 6:10 p.m.) and the maximum peak demand (170 kW).

Very short time predictive control results

As evidenced before, the inputs of the very short time procedure are the discharge stage periods of the BESS (5:10 a.m. and 6:10 p.m.) and the desired peak value of the power requested from the grid (170 kW), both output of the day-ahead scheduling. At each control interval, other inputs of the very short time procedure are the power forecast of the load demand, starting from the control interval up to the last interval of the day.

The very short time procedure was performed for all the time intervals of the day, and its outputs are the signal of the power that the BESS must furnish/absorb at each controlled interval. With reference to the entire day, the control signal for the BESS is reported in figure 2.30, while, in figure 2.31, the corresponding actual state of the charge is shown.

Figures 2.30 and 2.31 show that the battery's technical constraints were satisfied in terms of minimum and maximum capacity of the battery, the desired number of cycles per day, and the limits of the battery's power size. In order to satisfy these constraints, the final state of charge of the battery (236 kWh) did not perfectly match the desired value (240 kWh).

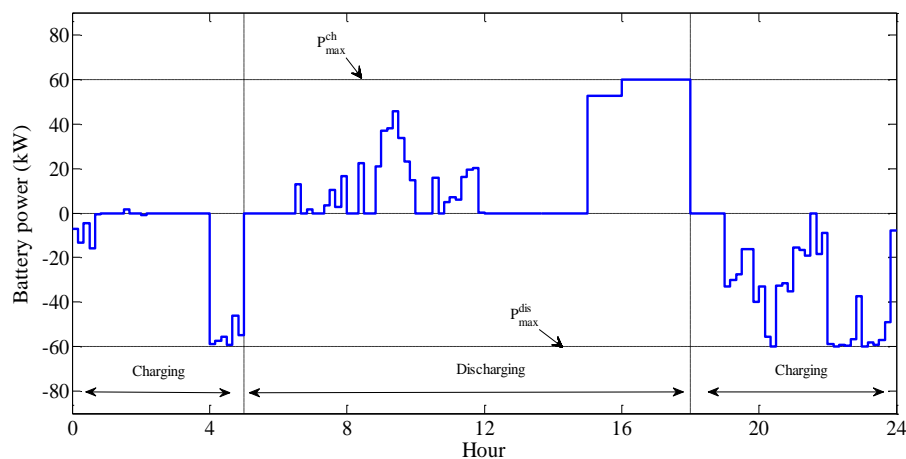


Figure 2.30: BESS's reference power signal.

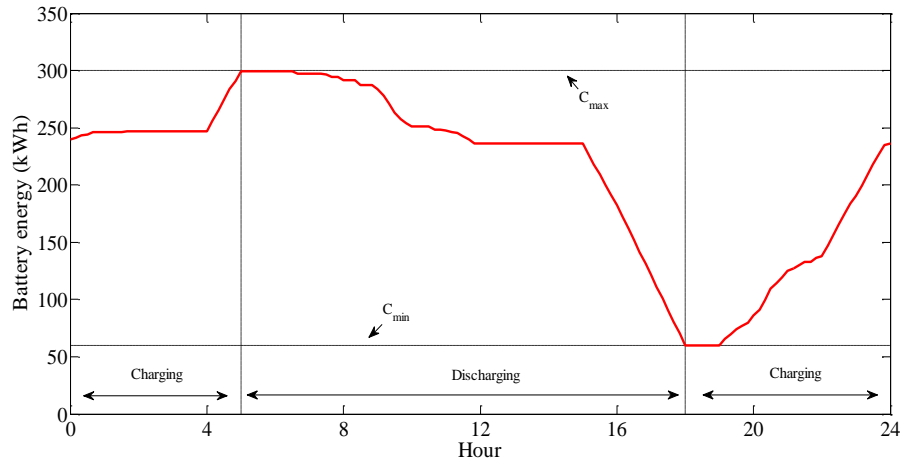


Figure 2.31: Actual energy stored in the BESS.

As discussed in [49] this happens due to forecasting errors and thus lower values of the battery's state of charge at end of the last time interval, as well as higher values of the maximum peak power, were allowed.

The power that the facility should request from the grid on the basis of very short time predictive control is reported in figure 2.32. In the figure the actual load demand (i.e., the power requested from the grid when a BESS was not installed) and the desired peak value are also reported. Figure 2.32 shows that the forecasting errors produce a difference between the expected reductions of peak power (i.e., the reduction corresponding to the desired peak value obtained in day-ahead scheduling) and the actual reduction of peak power. In fact, based on day-ahead scheduling, the desired peak power was 170 kW, while the actual peak value was 185 kW. In terms of percentages, the actual peak power reduction ΔP_{act} corresponded to about 17% than that in the case without BESS.

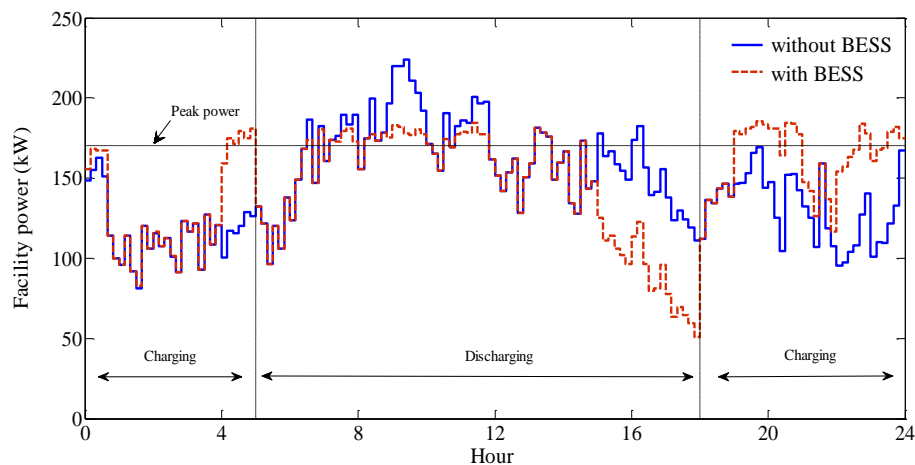


Figure 2.32: Actual power profile of the facility with and without a BESS.

In order to verify the effectiveness of the two-step procedure, the case of the BESS operated without the very short time procedure (i.e., the reference signal for the BESS only was evaluated with the scheduling procedure) also should be considered. Figure 2.33 shows the profiles of day-ahead scheduling and very short time procedure. The gap between the maximum peak values in the two cases is apparent in the figure. As expected, the reduction of

peak power was lower than the reduction obtained in case of the BESS controlled by the very short time procedure. In fact, without the short time procedure, the peak power was 195 kW. Moreover, in the case without the very short time procedure, the reduction of the objective function with respect to the case without the BESS was 9%, while it was about 11.5% when the very short time procedure was used.

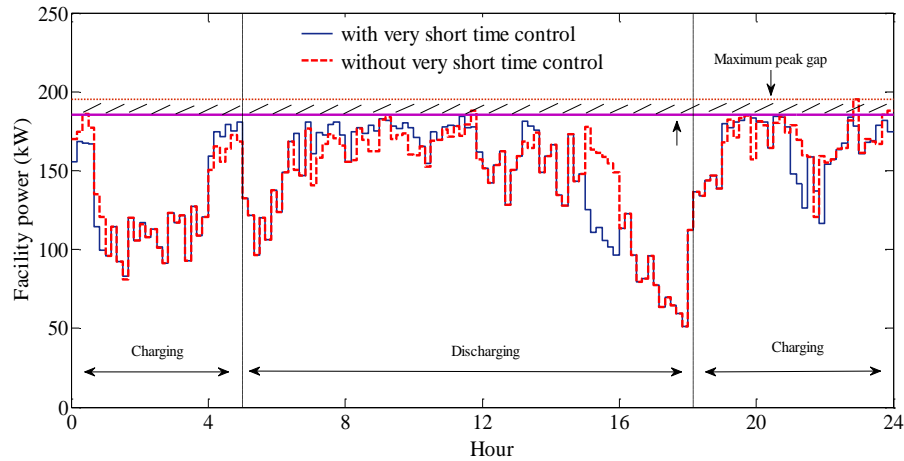


Figure 2.33: Actual power profile of the facility with and without very short time predictive control.

Impact of forecasting errors

In order to verify the need for and usefulness of the second step, different simulations also were performed with different forecasting errors; the results are reported in table 2.3. In more detail, three different errors for very short time forecast (i.e., 1%, 2%, and 6%) were considered. The results reported in table 2.3 show that (i) the forecasting errors penalize the ability of the proposed method to reduce the peak power requests and (ii) the use of the two-step procedure obtained better results.

Interesting results also were observed with reference to the correspondence of the values of the objective function with the different values of the forecasting errors. In fact, while significant reduction of the objective function values occurred in the case of the low error of the very short time forecast, less significant results were obtained with high forecasting errors, approaching the results obtained by using only the day-ahead procedure. Moreover, for low short time forecast error (1%) and high day-ahead forecast error (6%), slightly better results were obtained than with low short time forecast error (1%) and low day-ahead forecast errors (3%). This was due to the strong influence of the very short time forecast on the final results. Once again, this confirms the need for the very short time step, which should be characterized by low forecasting errors.

Day-ahead forecasting error (%)	Very short time forecasting Error (%)	Without very short time procedure		With very short time procedure	
		Δf_{obj} (%)	ΔP_{peak} (%)	Δf_{obj} (%)	ΔP_{peak} (%)
6	6	8.81	12.88	8.84	8.60
	2			11.46	17.13
	1			11.95	19.36
3	3	9.76	16.02	10.04	14.25
	2			11.13	18.51
	1			11.73	20.28

Table 2.3: Performance of the very short time procedure.

2.4. An advanced optimal operation strategy for microgrid scheduling

μ Gs typically involve a cluster of loads, DG units and storage systems. These electrical components must be integrated and controlled to maximize the technical and economic benefits they provide.

Study of optimal operation strategy for μ Gs in the presence of new type of loads such as plug-in electrical vehicles (PEVs) and datacenters (DCs) and their impact on the correct and secure operation of power systems is one of the most crucial challenges for the researchers and employers in the electric power industries, since the number of these loads is expected to significantly increase in the next future [50, 51]. Moreover, it is generally accepted that the operation of these loads can have also beneficial effects in the context of SGs. The availability of storage on board of PEVs as well as storage used inside the UPS of DCs, in fact, can be suitable as distributed resources able to furnish several services to the grid, if they are optimally managed and integrated with other energy resources [52, 53, 54].

Different strategies of energy management can be implemented in order to pursue a specific service while guaranteeing the correct operation of distribution systems as well as the primary goal of each storage device (i.e., to furnish energy for mobility, in case of PEVs, or to serve as back-up, in case of the UPS). These strategies can be related to the energy efficiency (e.g., to minimize the power losses), power quality (e.g., to improve the voltage profile), economical operation (e.g., peak shaving) and services to provide to upstream grids (e.g., load leveling). However, while a service is furnished in order to pursue a specific objective, the large amount of energy requested by PEVs or DCs can dramatically affect other grid performances. As an example, if the grid operation is performed by minimizing the operation costs, this strategy could result in a degradation of the power quality or energy efficiency.

2.4.1. State of the art

In the relevant literature the optimal operation of μ Gs, including PEV fleet aggregators, has been analyzed in several research works [37, 55-60]. In [37], the scheduling of the active and reactive power of the aggregators and DG units in a μ G was performed with the aim of minimizing the total daily cost of energy incurred by the μ G while meeting the technical constraints on the grid's currents and voltages. Peak-shaving service also was considered. A review of the available single-objective, optimization models for the optimal control of EVs' charging in a μ G is presented in [55, 56]. In [57, 58], peak-shaving service was performed by smart management of the charging of the vehicles connected to a distribution network while minimizing losses. In [59], charging/discharging strategies for EVs were proposed with the aim of managing congestion in the μ Gs. In [60], optimal scheduling of both active power and the combination of active and reactive power was proposed in order to pursue different objectives, such as minimizing the costs incurred by the aggregators for charging and improving the voltage profile.

Recently, the relevant literature has indicated that there also is increasing interest in the optimal operation of data centers where the models proposed in the technical literature are related mainly to the control of only the data centre's energy consumption in order to improve efficiency and to give them the potential for participating in a demand-response program [61-65]. Reference [61] presented benefits of integrating data centers into demand response schemes. The data centers were assumed to be able to perform the mechanisms required to reshape power consumption during the day. In [62], a model was proposed for determining

the optimal, hourly and demand-response capability of individual data centers by optimally shifting cloud service tasks among distributed data centers. In [63], a model for evaluating the data centre's energy cost was proposed in order to avoid the coincident peak and to reduce expenditures for energy by using workload shifting and local power generation. In [64], a load-control method for data centers was presented that was based on both the data network and the electrical network with the aim of controlling power usage associated with participation in the demand-response program. In [65], an approach was proposed to enable electrical energy buffering in batteries to predictably minimize data centers' electricity costs in smart grids. In this approach, the batteries are charged when the price of electricity is low, and they are discharged to power servers when the price of electricity is high. Also, the problems of using different technologies for storage and of placing storage systems at different levels of the power hierarchy were analyzed extensively. [53] focused on the use of data centers and EV aggregators as demand response resources. A new model for the optimal operation of a μ G that includes DG units, EV fleets and the data centre's storage systems has been proposed. The procedure is based on a non-linear, constrained, optimization model with the aim of minimizing the total cost of energy and simultaneously shaving peak power.

2.4.2. Proposed strategy

In this thesis, different single-objective strategies are presented which are able to manage the operation of a microgrid characterized by the presence of DCs, PEVs and DGs. The battery energy storage inside the UPS equipping a DC is used in order to absorb/supply power from/to the grid based on control signals received by the centralized control system (CCS) of the microgrid. The reference signals are evaluated according to the needs of the grid itself, the requirements devoted to prolong the lifetime of the battery and the features of the privileged loads serviced by the UPS [53]. The needs of the grid are related to the satisfaction of the operation limits (e.g., the currents have to be lower than line capacities) or to specific services that have to be supplied. In order to prolong the battery lifetime, a specific number of charging/discharging cycles per day has to be satisfied (typically one), as well as a maximum DOD cannot be exceeded, thus imposing a limit to the minimum value of the energy stored in the battery. The minimum value of the energy stored in the battery also depends on the energy needed to supply the privileged loads during the power grid outages until diesel generators can be brought on-line (from few seconds to two minutes) [54]. As a consequence, the minimum value of the energy stored is the maximum between the values due to the DOD and that to the back-up service.

Here, it is supposed that a charging strategy is implemented by the CCS able to charge the vehicles according to the grid needs as well as the drivers' needs [55, 56]. In order to do this, the grid interacts with a PEV fleet through an aggregator. Based on the forecasted requirements of the vehicles plugged-in, that is the initial energy stored in the batteries, and the hour, in which each battery has to be fully charged, the aggregator evaluates the total energy that has to absorb from the grid during the following day. Based on the data provided by each aggregator, the day is divided in a specific number of intervals characterized by specified value of contracted energy that the aggregator has to absorb from the grid [53, 56]. During these time intervals, the power supplied to the aggregator can vary according to the needs of the grid or services to be pursued.

Based on single-objective formulations, the proposed strategies allow operating these resources in order to gain some services such as cost minimization, power quality or energy savings.

The following section is aimed at providing strategies for grid operation which are able to control the active powers of aggregators and battery of a DC's UPS. Moreover, the strategies can control the reactive power of the converters used to connect PEV fleets, DCs and DG units to the grid.

2.4.3. Problem formulation and solving procedure

The proposed strategies refer to a microgrid in the presence of DCs, DG units and fleets of PEVs connected to the grid by means of aggregators. A CCS controls and coordinates these resources by calculating and sending control signals. These signals refer to the reactive power of the resources connected to the grid by means of converters, the active power of PEV fleets and UPS' battery. These powers are calculated by an optimization model whose inputs are the PEV fleets' requirements, the forecast of the loads' power and DG units' generation; outputs are the active powers of PEV fleets, battery of DCs and the reactive power of the converters connected to the grid.

The optimization model is formulated as a single-objective, multi-period, non-linear constrained minimization problem. The day is divided in n_t time slots, each one of duration Δt , and the optimization problem is solved for all the n_t time slots, simultaneously. The objective function refers to the specific service that has to be pursued. This research study considered following functions with the corresponding objective functions to be minimized:

- *Squared voltage deviation*

$$f_{obj,1} = \frac{1}{n_t} \sum_{t=1}^{n_t} \left[\frac{1}{n} \sum_{i=1}^n (V_{i,t} - V_{i,t}^{sp})^2 \right] \quad (2.44)$$

where $V_{i,t}$ is the voltage at busbar i at time slot t , $V_{i,t}^{sp}$ is its desired value and n is the number of grid busbars; in this case, the performed service is aimed at increasing the power quality.

- *Power losses minimization*

$$f_{obj,2} = \sum_{t=1}^{n_t} P_{loss,t} \quad (2.45)$$

where $P_{loss,t}$ is the power losses at time slot t ; in this case, the performed service is aimed at improving the energy efficiency.

- *Security margin*

$$f_{obj,3} = \frac{1}{n_t} \sum_{t=1}^{n_t} \left(1 - \min_{l \in \Omega_l} \left| \frac{I_{l,t} - I_l^r}{I_l^r} \right| \right) \quad (2.46)$$

where $I_{l,t}$ is the current through the l^{th} line at time t , I_l^r is its rating and Ω_l is the set of all the lines of the grid; in this case, the performed service is aimed at improving the secure operation, since it unable the system to better support unexpected loads and DG variations [66, 67].

- *Energy cost*

$$f_{obj,4} = \sum_{t=1}^{n_t} Pr_{en,t} P_{1,t} \Delta t \quad (2.47)$$

where $Pr_{en,t}$ is the energy price during the time slot t , $P_{1,t}$ is the active power imported from the upstream grid; in this case, the performed service is aimed at reducing the operation cost.

- *Load leveling*

$$f_{obj,5} = \frac{1}{n_t} \sum_{t=1}^{n_t} (P_{1,t} - P_{1,\mu})^2 \quad (2.48)$$

where $P_{1,\mu}$ is the mean value of active power absorbed from the upstream grid during the day. In this case, the performed service is aimed at leveling the active power at the interconnection bus.

The equality constraints to be satisfied are:

- The load flow equations

$$P_{i,t} = V_{i,t} \sum_{k=1}^n V_{k,t} [G_{i,k} \cos(\delta_{i,t} - \delta_{k,t}) + B_{i,k} \sin(\delta_{i,t} - \delta_{k,t})] \quad (2.49)$$

$$Q_{i,t} = V_{i,t} \sum_{k=1}^n V_{k,t} [G_{i,k} \sin(\delta_{i,t} - \delta_{k,t}) - B_{i,k} \cos(\delta_{i,t} - \delta_{k,t})] \quad (2.50)$$

$$i \in \Omega_{grid}, \quad t = 1, 2, \dots, n_t$$

where $P_{i,t}$ ($Q_{i,t}$) is the net active (reactive) power injected in the bus i at time t , $V_{i,t}$ ($\delta_{i,t}$) is the magnitude (argument) of the voltage, $G_{i,k}$ ($B_{i,k}$) is the (i, k)-term of the system's conductance (susceptance) matrix and Ω_{grid} is the set of all buses. In case of load bus, both active and reactive powers are specified values (i.e., $P_{i,t} = -P_{i,t}^{sp}$ and $Q_{i,t} = -Q_{i,t}^{sp}$); in case of DG bus, the active power is a specified value (i.e., $P_{i,t} = P_{i,t}^{sp}$) and the reactive power is an optimization variable; in case of PEVs, both active and reactive powers are optimization variables; in case of DCs, the active power is given by the algebraic sum of two terms: the first refers to the load demand (that is a negative, and specified value), the second term refers to the power of battery (that is an optimization variable which will be positive, if it refers to the discharge, or negative, otherwise), while the reactive power is an optimization variable (obviously the efficiencies of both battery and converter have to be considered) [53].

- The voltage (magnitude and angle) at the slack is specified.

- The grid has to supply a specified value of energy to the PEV fleet aggregators ($E_{i,j}^{sp}$) during specified time intervals of the day:

$$\sum_{t=n_j^{start}}^{n_j^{end}} P_{i,t} \Delta t = -E_{i,j}^{sp} \quad i \in \Omega_{PEV}, \quad j = 1, 2, \dots, N_c \quad (2.51)$$

where Ω_{PEV} is the set of buses where PEV fleet aggregators are installed, N_c is the number of time intervals, n_j^{start} (n_j^{end}) are the first (last) slot of each interval.

- The energy stored in the UPS battery must be the same at the beginning and at the end of the day:

$$\sum_{t=1}^{n_t} \gamma_{i,t} P_{i,t}^b \Delta t = 0, \quad \gamma_{i,t} = \begin{cases} \eta_i^{batt} & \text{if } (P_{b,j,i,t} \geq 0) \\ 1/\eta_i^{batt} & \text{if } (P_{b,j,i,t} < 0) \end{cases} \quad t = 1, 2, \dots, n_t, \quad i \in \Omega_{DC} \quad (2.52)$$

where $P_{i,t}^b$ is the power supplied/absorbed by the battery, $\gamma_{i,t}$ refers to the efficiency of the battery in both charging and discharging modes and Ω_{DC} is the set of buses where data centers are installed.

The inequality constraints to be satisfied are:

- The current through the lines $I_{l,t}$ has to be lower than the rated value I_l^r :

$$I_{l,t} \leq I_l^r \quad t = 1, 2, \dots, n_t, \quad l \in \Omega_l \quad (2.53)$$

- The voltage magnitude at the busbars of the grid has to fall into admissible ranges:

$$V^{min} \leq V_{i,t} \leq V^{max} \quad t = 1, 2, \dots, n_t, \quad i \in \Omega_{grid} \quad (2.54)$$

where V^{min} (V^{max}) are the minimum (maximum) admissible magnitudes of the bus voltage.

- The active power of the PEV fleet aggregators has to fall into admissible ranges:

$$P_i^{min} \leq P_{i,t} \leq P_i^{max} \quad t = 1, 2, \dots, n_t, \quad i \in \Omega_{PEV} \quad (2.55)$$

where P_i^{min} (P_i^{max}) is the minimum (maximum) power allowable at the aggregator bus.

- The active power of the UPS battery cannot exceed a specified value in both charging and discharging mode:

$$\begin{aligned} -P_{i,ch}^{max} \leq P_{i,t}^b \leq 0, \quad t \in \Omega_{CH} \\ 0 \leq P_{i,t}^b \leq P_{i,dch}^{max}, \quad t \in \Omega_{DCH}, \quad i \in \Omega_{DC} \end{aligned} \quad (2.56)$$

where $P_{i,ch}^{max}$ ($P_{i,dch}^{max}$) is the maximum power that can be absorbed (supplied) by the battery, Ω_{CH} and Ω_{DCH} are the set of time slots in which the UPS storage system is allowed to charge and discharge, respectively. These last two intervals are consecutive, thus allowing the battery to have only one charging/discharging cycle per day.

- The apparent power flowing through the power converters are bounded by the converters' sizes:

$$\sqrt{(P_{i,t})^2 + (Q_{i,t})^2} \leq S_i^{max} \quad t = 1, 2, \dots, n_t, \quad i \in \Omega_{CONV} \quad (2.57)$$

where S_i^{max} is maximum apparent power of converters and Ω_{CONV} is the set of buses equipped by converters.

- The energy stored in the battery of the UPS has to be within an admissible range:

$$E_{i,ch}^{in} - \sum_{t \in \Omega_{CH}} \gamma_{i,t} P_{i,t}^b \Delta t \leq E_i^{max}, \quad i \in \Omega_{DC} \quad (2.58)$$

$$E_{i,dch}^{in} - \sum_{t \in \Omega_{DCH}} \gamma_{i,t} P_{i,t}^b \Delta t \geq E_i^{min}, \quad i \in \Omega_{DC} \quad (2.59)$$

where $E_{i,ch}^{in}$ ($E_{i,dch}^{in}$) is the initial stored energy at the beginning of the charging (discharging) periods, E_i^{max} is the size of the battery and E_i^{min} is the minimum value of the energy to be stored in the battery, evaluated as:

$$E_i^{min} = \max\{E_{i,DOD}, E_{i,UPS}\}, \quad i \in \Omega_{DC} \quad (2.60)$$

where $E_{i,DOD}$ is the minimum stored energy according to the allowable depth of discharge, and $E_{i,UPS}$ is the value of energy needed for the UPS service (back-up).

2.4.4. Numerical application

To verify and compare the proposed approaches, the MV test system of figure 2.34 is studied [68]. The test system is constituted by 17 busses and it is connected to a HV transmission network by means of an 18 MVA transformer. The data of the system are reported in tables 2.4 and 2.5. The system includes three DG systems (a 500 kW- wind turbine and two 1 MW- photovoltaic systems), two PEV fleet aggregators (1 MW maximum power) and two DCs, having 1 MW-privileged loads. All these devices are connected to the grid by means of interfacing power converters. Each DC is equipped with a UPS system made by two Li-ion batteries of 500 kW, which are able to supply the privileged loads for 20 minutes. The batteries have a maximum DOD of 80%, can charge during the central hours of the day and discharge otherwise, thus allowing only one charging/discharging cycle per day; it is also assumed that the minimum allowable state of charge is large enough for the back-up service. Regarding to the PEV fleets, the energy requests by the aggregators are reported in table 2.6, and it is assumed that the grid supplies power to the aggregators (grid to vehicle mode), while the vice versa (vehicle to grid mode) is not allowed.

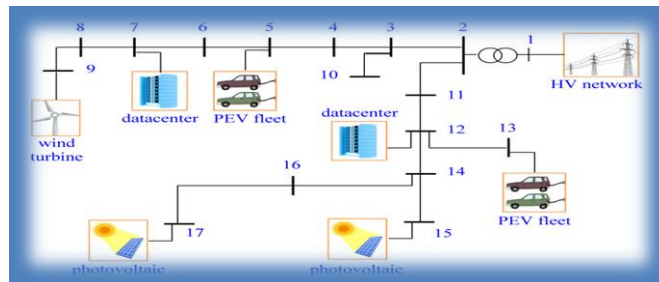


Figure 2.34: MV test system.

Line		R (p.u.)	X_L (p.u.)	X_C (p.u.)
1	2	0.00312	0.06753	0
2	3	0.00431	0.01204	0.000035
3	4	0.00601	0.01677	0.000049
4	5	0.00316	0.00882	0.000026
5	6	0.00896	0.02502	0.000073
6	7	0.00295	0.00824	0.000024
7	8	0.01720	0.02120	0.000046
8	9	0.04070	0.03053	0.000051
3	10	0.01706	0.02209	0.000043
2	11	0.02910	0.03768	0.000074
11	12	0.02222	0.02877	0.000056
12	13	0.04803	0.06218	0.000122
12	14	0.03985	0.05160	0.000101
14	15	0.02910	0.03768	0.000074
14	16	0.03727	0.04593	0.000100
16	17	0.02208	0.02720	0.000059

Table 2.4: Test system data.

Node	P_c (p.u.)	Q_c (p.u.)	$\cos\phi$
1	0	0	-
2	0	0	-
3	0.02	0.012	0.86
4	0.04	0.025	0.85
5	0.15	0.093	0.85
6	0.30	0.226	0.80
7	0.08	0.05	0.85
8	0.02	0.012	0.86
9	0.10	0.062	0.85
10	0.05	0.031	0.85
11	0.10	0.062	0.85
12	0.03	0.019	0.84
13	0.02	0.012	0.86
14	0.08	0.05	0.85
15	0.05	0.031	0.85
16	0.10	0.062	0.85
17	0.02	0.012	0.86

Table 2.5: Load base values ($P_{BASE}=10$ MVA).

Time period	Aggregator at bus #5	Aggregator at bus #13
	Energy requested (MWh)	Energy requested (MWh)
[00.00-08.00]	3.60	1.00
[08.00-12.00]	0.80	2.50
[12.00-14.00]	0.50	1.00
[14.00-18.00]	1.00	0.80
[18.00-24.00]	3.00	0.75

Table 2.6: Energy requests by the aggregators.

For all the objective functions (2.44)-(2.48) the scheduling was performed by solving the corresponding optimization problem by dividing the day in 24 time slots of 1 hour. As an example of the inputs, the forecasted daily profiles of a load (bus #6) and DG (bus #15), privileged load demand of a DC (bus#7) and the energy price are reported in figure 2.35.

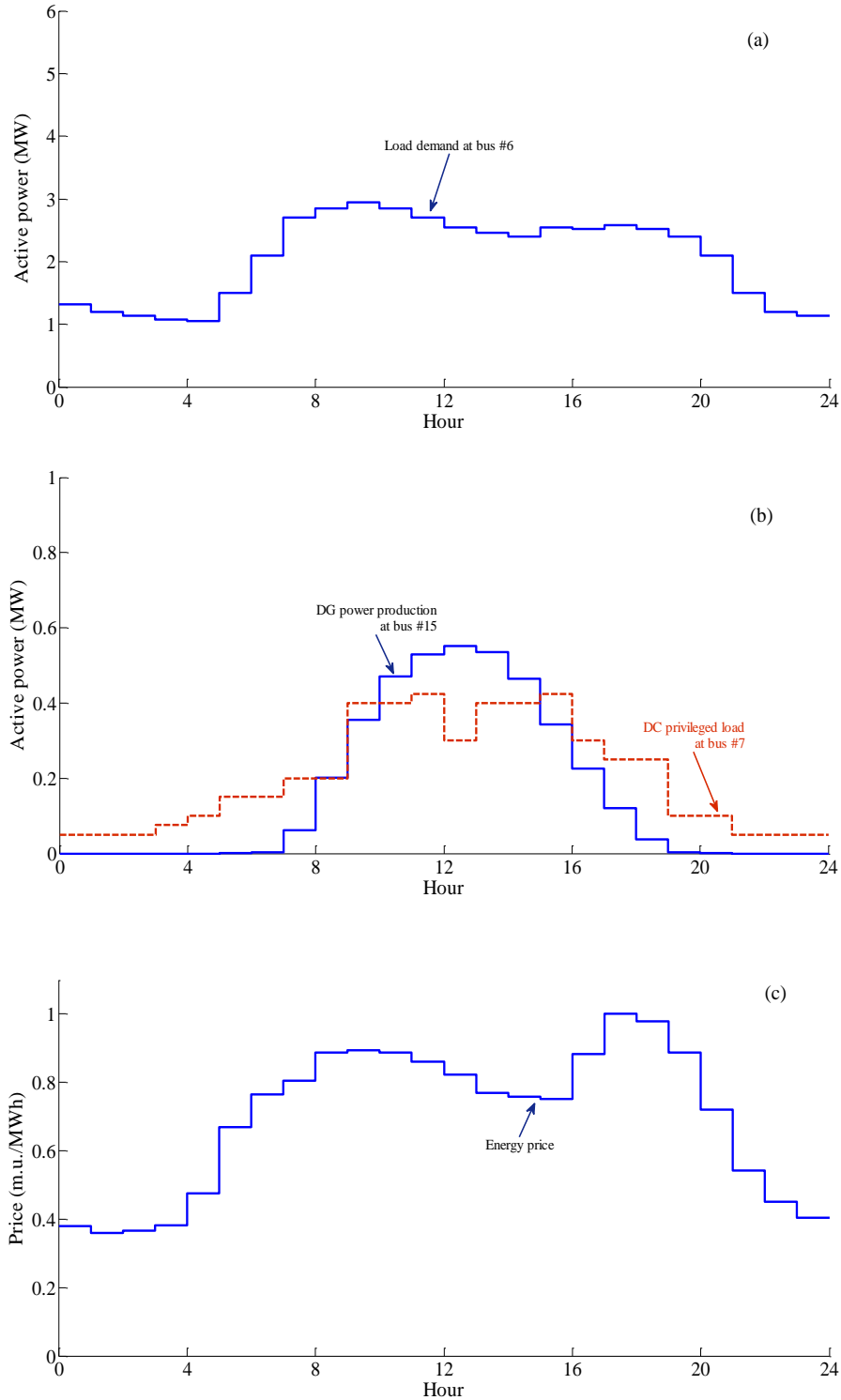


Figure 2.35: Load demand at bus#6 (a). DG power production at bus#15 and DC privileged load demand at bus#7 (b). Energy price (c).

For the sake of brevity, some detailed results are reported only with reference to the load leveling case. In particular, the graphs in figure 2.36 refer to the power imported by the grid from the upstream HV grid (i.e. the power at the HV/MV substation), the active power of the aggregator connected at the bus #13 and the active power of the battery equipping the UPS of the DC connected at the bus #7.

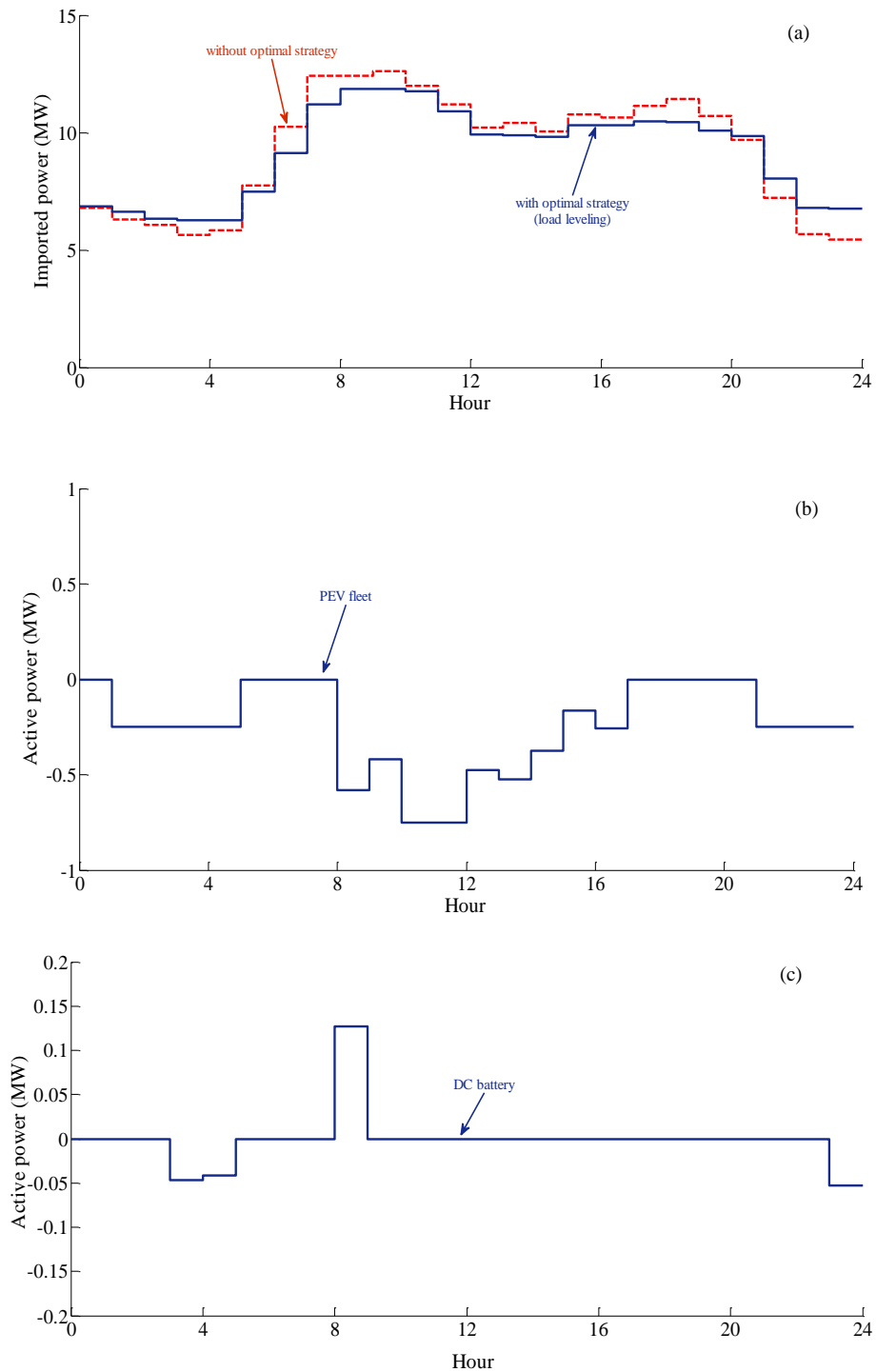


Figure 2.36: Active power imported from the HV grid (a). Active power of the aggregator at bus #13 (b). Active power of a battery of DC bus #7 (c).

For comparative purposes, in figure 2.36(a), also the power imported from the HV grid, when no-control actions are applied is reported. In this case, that is considered as no-strategy case, it is assumed that the PV units are operated with a unitary power factor, the PEV fleets are charged with a constant power during each interval and the batteries of UPSs are used only for back-up services. As it can be observed, a useful improvement in terms of leveling power is obtained. In fact, when the optimal strategy is applied, a peak reduction of about 6% is gained as well as the difference between the minimum and maximum value is reduced of about 22%.

The graph in figure 2.36(b) shows that the significant power requested by the aggregator assumes a profile aimed at leveling the substation power: as an example, at 9.00, the power supplied to the PEV is slightly reduced, thus shaving the substation peak power (figure 2.36(a)); during the interval [18.00-24.00], instead, the power requested for charging the PEVs is higher during the hours of light loads, thus filling the valley of substation power profile (2.36(a)). In the graph of figure 2.36(c), it is interesting to observe that the battery is mainly used in order to supply power to the grid in the periods in which the loads are increasing (i.e. at the 8.00); instead, the battery charges during the light load hours. Regarding the reactive power support, significant values of power are provided by all resources, in particular during the hours of peak power demand. The profiles of the reactive power, here not reported for the sake of conciseness, and of the active power met the constraints imposed by the size of each converter.

The results of the five strategies (i.e., squared voltage deviation, power losses, security margin, energy cost and load leveling) are reported in table 2.7: in a specific row, the values of each objective function obtained by applying a specific strategy are reported, and in a specific column the values obtained for a specific objective function by applying different strategies are reported. For comparison purposes, the results obtained in the no strategy case are also reported. As expected, the results reported in table 2.7 shows that the minimum of each function is obtained when it is used as objective of the strategy. By analyzing table 2.7, it emerges that the functions of load leveling and energy cost are the most conflicting with the other functions, because, when minimized, almost always, negatively affects the other functions. This, with the exceptions of the strategy for losses, that gives the worst result in terms of energy cost, and the strategy for voltage deviation, that gives the worst result in terms of load leveling. Moreover, in terms of security margin, the strategy for both load leveling and energy cost are worse than the case of no-strategy. On the other hand, the strategy that always gives results inside the best and the worst, in terms of the other functions, is the strategy for security margin.

Strategy	Objective function values				
	$f_{obj,1}$ (%)	$f_{obj,2}$ (p.u.)	$f_{obj,3}$ (p.u.)	$f_{obj,4}$ (m.u.)	$f_{obj,5}$ (p.u.)
Voltage	0.0041	0.4357	0.4700	16.2243	0.0448
Losses	0.0543	0.3681	0.4383	16.3138	0.0415
Security margin	0.0101	0.4186	0.4319	16.2219	0.0430
Cost	0.0774	0.5807	0.6176	16.0625	0.0416
Load leveling	0.2455	0.5660	0.5473	16.1563	0.0372
No strategy	0.6057	0.5834	0.5331	16.6526	0.0602

Table 2.7: Objective function values for different strategies.

2.5. References

- [1] S. Boyd, and L. Vandenberghe, "*Convex optimization*," New York, USA, Cambridge University Press, 2004.
- [2] A. Oudalov, D. Chartouni, C. Ohler, and G. Linhofer, "Value analysis of battery energy storage applications in power systems," in *Proc. IEEE Power Systems Conference and Exposition*, Atlanta, GA, USA, 29 October-1 November, 2006.
- [3] S. Yoda, and K. Ishihara, "The advent of battery-based societies and the global environment in the 21st century," *Journal of Power Sources*, vol. 81-82, pp. 162-169, September 1999.
- [4] G. Carpinelli, G. Celli, S. Mocci, F. Mottola, F. Pilo, and D. Proto, "Optimal integration of distributed energy storage devices in smart grids," *IEEE Trans. on Smart Grids*, vol. 4(2), pp. 985-995, June 2013.
- [5] K. S. Tam, "A comparison of alternatives to enhance the utilization of transmission lines," *Electric Power Systems Research*, vol. 41(2), pp. 133-140, May 1997.
- [6] R. C. Leou, "An economic analysis model for the energy storage system applied to a distribution substation," *Electrical Power and Energy Systems*, vol. 34(1), pp. 132-137, January 2012.
- [7] K. H. Jung, H. Kim, and D. Rho, "Determination of the installation site and optimal capacity of the battery energy storage system for load leveling," *IEEE Trans. on Energy Conversion*, vol. 11(1), pp. 162-167, March 1996.
- [8] C. H. Lo, and M. D. Anderson, "Economic dispatch and optimal sizing of battery energy storage systems in utility load-leveling operations," *IEEE Trans. on Energy Conversion*, vol. 14(3), pp. 824-829, September 1999.
- [9] F. A. Chacra, P. Bastard, G. Fleury, and R. Clavreul, "Impact of energy storage costs on economical performance in a distribution substation," *IEEE Trans. on Power Systems*, vol. 20 (2), pp. 684-691, May 2005.
- [10] I. Papic, "Simulation model for discharging a lead-acid battery energy storage system for load leveling," *IEEE Trans. on Energy Conversion*, vol. 21(2), pp. 608-615, June 2006.
- [11] A. Rahimi, M. Zarghami, M. Vaziri, and S. Vadhva, "A simple and effective approach for peak load shaving using battery storage systems," in *Proc. North American Power Symposium, NAPS 2013*, Manhattan, KS, USA, 22-24 September, 2006.
- [12] A. Nourai, V. I. Kogan, and C. M. Schafer, "Load leveling reduces T&D line losses," *IEEE Trans. on Power Delivery*, vol. 23 (4), pp. 2168 - 2173, April 2008.
- [13] B. H. Chowdhury, "Central-station photovoltaic plant with energy storage for utility peak load leveling," in *Proc. 1989 Energy Conversion Engineering Conference, IECEC-89*, Washington, DC, USA, 6-11 August, 1989.
- [14] X. Dong, G. Bao, Z. Lu, Z. Yuan, and C. Lu, "*Optimal battery energy system charge scheduling for peak shaving application considering battery lifetime*," Berlin, Germany, Springer Verlag, 2011.
- [15] S. S. Choi, and H. S. Lim, "Factors that affect cycle-life and possible degradation mechanisms of a Li-ion cell based on LiCoO₂," *Journal of Power Sources*, vol. 111(1), pp. 130-136, September 2002.

- [16] W. Waag, S. Käbitz, and D. U. Sauer, "Experimental investigation of the lithium-ion battery impedance characteristic at various conditions and aging states and its influence on the application," *Applied Energy*, vol. 102, pp. 885-897, February 2013.
- [17] H. A. Maleki, N. B. Karayiannis, and M. Balasubramanian, "Short-Term electric power load forecasting using fed forward neural networks," *Expert Systems*, vol. 21(3), pp. 157-167, July 2004.
- [18] M. Cococcioni, E. D. Andrea, and B. Lazzerini, "24 hour-ahead forecasting of energy production in solar PV systems," in *Proc. International Conference Intelligent Systems Design and Applications, ISDA 2011*, Córdoba, Spain, 22-24 November, 2011.
- [19] E. Hirst, (2001). Real-time balancing operations and markets. [Online]. Available: <http://www.ksg.harvard.edu/hepg/Papers/Hirst%204-01.rtmreport.pdf>
- [20] T. Logenthiran, D. Srinivasan, A. M. Khambadkone, and H. N. Aung, "Multi-agent system for real time operation of a microgrid in real time digital simulator," *IEEE Trans. on Smart Grid*, vol. 3(2), pp. 925-933, June 2012.
- [21] G. Carpinelli, S. Khormali, F. Mottola, and D. Proto, "Load leveling with electrical storage systems: a two-step optimization procedure," *International review of electrical engineering*, vol. 8(2), pp. 729-736, March /April 2013.
- [22] P. Havel, "Utilization of real-time balancing market for transmission system control under uncertainty," *IEEE Trans. on Power Systems*, vol. 29(1), pp. 450-457, January 2013.
- [23] G. Carpinelli, S. Khormali, F. Mottola, and D. Proto, "Optimal operation of electrical energy storage systems for industrial applications," in *Proc. IEEE Power and Energy Society General Meeting*, Vancouver, BC, Canada, 21-25 July, 2013.
- [24] K. H. Ahlert, and C. Van Dinther, "Sensitivity analysis of the economic benefits from electricity storage at the end consumer level," in *Proc. 2009 IEEE Power Tech Conference*, Bucharest, Romania, 28 June-2 July, 2009.
- [25] M. M. Eissa, "Demand side management program evaluation based on industrial and commercial field data," in *Proc. 14th International Middle East Power Systems Conference, MEPCON 2010*, Cairo, Egypt, 19-21 December, 2010.
- [26] G. Carpinelli, S. Khormali, F. Mottola, and D. Proto, "Multi-battery management under real-time pricing for industrial facility applications," in *Proc. 12th International Conference on Environment and Electrical Engineering, IEEEIC 2013*, Wroclaw, Poland, 5-8 May, 2013.
- [27] R. S. Walawalkar, "Economics of emerging electric energy storage technologies and demand response in deregulated electricity markets," *Ph.D. Dissertation*, Carnegie Mellon University, May 2008.
- [28] N. Venkatesan, J. Solanki, and S. K. Solanki, "Residential demand response model and impact on voltage profile and losses of an electric distribution network," *Applied Energy*, vol. 96, pp. 84-91, August 2012.
- [29] J. G. Roos and I. E. Lane, "Industrial power demand response analysis for one-part real-time pricing," *IEEE Trans. on Power Systems*, vol. 13, pp. 159-164, February 1998.
- [30] S. Braithwait, "Behavior modification," *IEEE Power and Energy Magazine*, Vol. 8(3), pp. 36-45, May/June 2010.

- [31] A. K. David, and Y. Z. Li, "A comparison of system response for different types of real time pricing, " in *Proc. IET International Conference on Advances in Power System Control, Operation and Management*, Hong Kong, 5-8 November, 1991.
- [32] K. M. Tsui, and S. C. Chan, "Demand response optimization for smart home scheduling under real-time pricing," *IEEE Trans. on Smart Grid*, vol. 3(4), pp. 1812-1821, December 2012.
- [33] G. Xiong, C. Chen, S. Kishore and A. Yener, "Smart (in-home) power scheduling for demand response on the smart grid, " in *Proc. Innovative Smart Grid Technologies (ISGT 2011)*, Anaheim, CA, USA, 17-19 January, 2011.
- [34] Z. Chen, L. Wu, and Y. Fu, "Real-Time price-based demand response management for residential appliances via stochastic optimization and robust optimization," *IEEE Trans. on Smart Grid*, vol. 3(4), pp. 1822-1831, December. 2012.
- [35] P. Mandal, T. Senjyu, and T. Funabaschi, "Neural networks approach to forecast several hour ahead electricity prices and loads in deregulated market," *Energy Conversion and Management*, vol. 47, pp. 2128-2142, July 2006.
- [36] S. Borenstein, M. Jaske, and A. Rosenfeld, (2002). Dynamic pricing, advanced metering and demand response in electricity markets. Center for the Study of Energy Markets. Berkeley, CA. [Online].Available: <http://www.escholarship.org/uc/item/11w8d6m4>.
- [37] G. Carpinelli, F. Mottola, D. Proto, and A. Bracale, "Single-objective optimal scheduling of a low voltage microgrid: a minimum-cost strategy with peak shaving issues," in *Proc. 2012 11th International Conference on Environment and Electrical Engineering*, Venice , Italy, 18-25 May, 2012.
- [38] A. Mishra, D. Irwin, P. Shenoy, and T. Zhu, "Scaling distributed energy storage for grid peak reduction," in *Proc. 2013 Fourth International Conference on Future Energy Systems*, Berkeley, Ca, USA, 21–24 May, 2013.
- [39] Y. Yoon, and Y.H. Kim, "Charge scheduling of an energy storage system under time-of-use pricing and a demand charge," *The Scientific World Journal*, vol. 2014, pp. 1-9, August 2014.
- [40] J. L. Neufeld, "Price discrimination and the adoption of the electricity demand charge," *The Journal of Economic History*, vol. 47(3), pp. 693-709, September 1987.
- [41] M. H. Albadi, and E. F. EL-Saadany, "Demand response in electricity markets: an overview, " in *Proc. IEEE Power and Energy Society General Meeting*, Tampa, FL, USA, 24-28 June, 2007.
- [42] L. Huang, J. Walrand, and K. Ramchandran, "Optimal demand response with energy storage management," in *Proc. 2012 IEEE Third International Conference on Smart Grid Communications (SmartGridComm)*, Tainan, Taiwan, 5-8 November, 2012.
- [43] T. Lee, "Operating schedule of battery energy storage system in a time-of-use rate industrial user with wind turbine generators: a multipass iteration particle swarm optimization approach, " *IEEE Trans. on Energy Conversion*, vol. 22(3), pp. 774-782, September 2007.
- [44] G. Carpinelli, A. R. di Fazio, S. Khormali, and F. Mottola, "Optimal sizing of battery storage systems for industrial applications when uncertainties exist," *Energies*, vol. 7(1), pp. 130-149, January 2014.

- [45] G. Bao, C. Lu, Z. Yuan, and Z. Lu, "Battery energy storage system load shifting control based on real time load forecast and dynamic programming," in *Proc. 2012 8th IEEE International Conference on Automation Science and Engineering*, Seoul, South Korea, 20-24 August, 2012.
- [46] G. Carpinelli, F. Mottola, and L. Perrotta, "Energy management of storage systems for industrial applications under real time pricing," in *Proc. 2013 International Conf. Renewable Energy Research and Applications*, Madrid, Spain, 20-23 October, 2013.
- [47] M. Safe, J. Caballido, I. Ponzoni, and N. Brignole, "On stopping criteria for genetic algorithms: in *Advances in artificial intelligence*," Berlin, Germany, Springer, 2004.
- [48] M. P. Johnson, A. Bar-Noy, O. Liu, and Y. Feng, "Energy peak shaving with local storage," *Sustainable Computing: Informatics and Systems*, vol. 1(3), pp. 177-188, September 2011.
- [49] G. Carpinelli, S. Khormali, F. Mottola, and D. Proto, "Demand response and energy storage systems: an industrial application for reducing electricity costs. part I: theoretical aspects," in *Proc. International Symposium on Power Electronics, Electrical Drives, Automation and Motion, SPEEDAM 2014*, Ischia, Italy, 18-20 June, 2014.
- [50] L. Rao, X. Liu, M. D. Ilic, and J. Liu, "Distributed coordination of internet data centers under multiregional electricity markets," *Proceedings of the IEEE*, vol. 100(1), pp. 269-282, January 2012.
- [51] A. Brooks, E. Lu, D. Reicher, C. Spirakis, and B. Wehl, "Demand dispatch," *IEEE Power and Energy Magazine*, vol. 8(3), pp. 20-29, May./June. 2010.
- [52] W. Kempton, and J. Tomic, "Vehicle-to-grid power fundamentals: calculating capacity and net revenue," *Journal of Power Sources*, vol. 144(1), pp. 268-279, June 2005.
- [53] G. Carpinelli, F. Mottola, and D. Proto, "Optimal scheduling of a microgrid with demand response resources," *IET Generation, Transmission & Distribution*, in press, DOI: 10.1049/iet-gtd.2013.0758.
- [54] S. Govindan, A. Sivasubramaniam, and B. Uргаonkar, "Benefits and limitations of tapping into stored energy for datacenters," in *Proc. 2011 International Symposium on Computer architecture, ISCA'11*, San Jose, CA, USA, 4-8 June, 2011.
- [55] A. Andreotti, G. Carpinelli, F. Mottola, and D. Proto, "A review of single-objective optimization models for plug-in vehicles operation in smart grids - part I: theoretical aspects," in *Proc. IEEE Power and Energy Society General Meeting*, San Diego, CA, USA, 22-26 July, 2012.
- [56] A. Andreotti, G. Carpinelli, F. Mottola, and D. Proto, "A review of single-objective optimization models for plug-in vehicles operation in smart grids - part II: numerical applications to vehicles fleets," in *Proc. IEEE Power and Energy Society General Meeting*, San Diego, CA, USA, 22-26 July, 2012.
- [57] A. S. Masoum, S. Deilami, P. S. Moses, M. A. S. Masoum, and A. Abu-Siada "Smart load management of plug-in electric vehicles in distribution and residential networks with charging stations for peak shaving and loss minimisation considering voltage regulation," *IET Generation, Transmission & Distribution Journal*, vol. 5(8), pp. 877-888, August 2011.

- [58] S. I. Vagropoulos, and A. G. Bakirtzis, "Optimal bidding strategy for electric vehicle aggregators in electricity markets," *IEEE Trans. on Power Systems*, vol. 28(4), pp. 4031-4041, August 2013.
- [59] M. A. Lopez, S. Martin, J. A. Aguado, and S. de la Torre, "V2G strategies for congestion management in microgrids with high penetration of electric vehicles," *Electric Power Systems Research*, vol. 104, pp. 28-34, November 2013.
- [60] L. Carradore, R. Turri, L. M. Cipcigan, and P. Papadopoulos, "Electric vehicle as flexible energy storage systems in power distribution networks," in *Proc. International Conference on Ecologic Vehicles and Renewable Energies*, Monte Carlo, France, April 2010.
- [61] A. Berl, S. Klingert, M. T. Beck, and H. De Meer, "Integrating data centers into demand-response management: a local case study," in *proc. 39th Annual Conference of the IEEE Industrial Electronics Society, IECON 2013*, Vienna, Austria, 10-13 November, 2013.
- [62] Z. Chen, Z. L. Wu, and Z. Li, "Electric demand response management for distributed large-scale internet data centers," *IEEE Trans. on Smart Grid*, vol. 5(2), pp. 651-661, February 2014.
- [63] Z. Liu, A. Wierman, Y. Chen, B. Razon, and N. Chen, "Data center demand response: avoiding the coincident peak via workload shifting and local generation," *Performance Evaluation*, vol. 70(10), p.p 770-791, October 2013.
- [64] C. J. Tang, M. R. Dai, C. C. Chuang, Y. S. Chiu, and W. S. Lin, "A load control method for small data centers participating in demand response programs," *Future Generation Computer Systems*, vol. 32, , p.p 232-245, March 2014.
- [65] J. Yao, X. Liu, and C. Zhang "Predictive electricity cost minimization through energy buffering in data centers," *IEEE Trans. on Smart Grid*, 5(1), pp. 230-238, August 2013.
- [66] G. Carpinelli, P. Caramia, F. Mottola, and D. Proto, "Exponential weighted method and a compromise programming method for multi-objective operation of plug-in vehicle aggregators in microgrids," *International Journal of Electrical Power & Energy Systems*, vol. 56, pp. 374-384, March 2014.
- [67] Y. Hsiao, C. Chen, and C. Chien, "Optimal capacitor placement in distribution systems using a combination fuzzy-GA method," *International Journal of Electrical Power & Energy Systems*, vol. 26(7), pp. 501-508, September 2004.
- [68] W. M. Grady, M. J. Samotji, and A. H. Noyola, "Minimizing network harmonic voltage distortion with an active power line conditioner," *IEEE Trans. on Power Delivery*, vol.6(4), pp. 1690-1697, October 1991.

Chapter 3: Optimal Sizing of Battery Energy Storage Systems

BESS is an indispensable component for μ G due to the number and variety of services they can provide, as shown in the previous chapters. However, due to the high investment costs and, for some technologies, the short operational life of BESS, its large-scale application has been greatly restricted [1], so how to rational size BESS capacity while meeting the operational requirements of system has important practical significance. It is also known that small BESS may not provide significant economic benefits, desired flexibility or predefined reliability objectives in the μ G and the large BESS impose higher investment and maintenance costs [2]. Then, optimal operation and sizing of BESSs can play considerable role in order to satisfy economic and technical benefits. Since optimal operation of BESS, which is discussed in the second chapter, cannot only satisfy proposed benefits then the sizing of BESSs must be also performed in an optimized way in order to maximize the benefits related to their use. Subsequently, this chapter of the thesis presents optimal sizing procedures of BESS.

Optimal sizing methods are mainly divided into three categories: energy balance methods, fluctuations stabilize methods and the economic characteristics optimization methods [2]. An energy balance method can be proposed to determine optimal battery capacity to ensure continued supply and meet certain reliability indices where in fluctuations stabilize methods the goal is to smooth out the intermittent generation of wind and solar generators and obtain a dispatchable output. Economic characteristics optimization methods mainly focus on the sizing of BESS in order to reduce the electricity bill based on energy charge and demand charge [2]. This chapter deals with the latter methods.

It should be noted, moreover, that in the sizing framework, the engineer who is sizing the BESS can perform the sizing problem based on deterministic approaches or probabilistic approaches. In this thesis, optimal sizing of BESS with reference to both the approaches are considered. In case of deterministic approach, the BESS sizing problem is proposed based on a quick closed form procedure, where in case of probabilistic approach, the BESS sizing problem is based on decision theory. Moreover, since both sizing approaches require a cost analysis then investment costs, maintenance costs and benefits associated with the installation of the BESS are taken into account.

Obtained results of proposed optimal sizing approaches in numerical applications demonstrate technical and economic benefits that can be derived from the installation of optimized size of BESS.

3.1. Deterministic optimal sizing of battery energy storage system based on TOU tariff

Deterministic optimal sizing of BESS operates under the deterministic framework of the data associated with the problem. In this section, particularly, the optimal sizing of BESS under TOU tariff with the consideration of certain data from the end customer point of view to reduce electricity costs is presented.

As clearly evidenced in the previous chapters of this thesis, minimizing the electricity costs is one of the greatest challenges related to the use of batteries in modern smart grids. Focusing on the end customer point of view, residential homes and small/medium-sized industrial facilities

are expected to actively modify their energy spending patterns by adopting battery systems and optimizing their consumption. The key barrier to the use of such devices remains their high cost as batteries are still quite expensive. However, looking at the longer-term, the technological development is expected to play an important role in both cost reduction and performance's improvement, so making batteries increasingly competitive for these applications [3].

To evaluate the benefit of using batteries, several factors must be taken into account such as electricity rates, load profile, technical and economic constraints of the battery and grid connection policies. All the aforementioned factors are considered in experience, which discusses the economic analysis affected for sizing a battery system with the aim of reducing the cost sustained for the energy consumptions. In more detail, the users are expected to modify their energy spending patterns by adopting battery systems and optimizing their consumption in the frame of the applied energy tariff schemes. Obviously, only dynamic pricing programs can be considered at this purpose and, in particular, RTP and TOU. RTP reflects the actual wholesale energy market and can suffer of large price variations in narrow time bands; TOU tariffs are based on only two or three price levels. Even if RTP seems to have high potential in the highly automated grid of the next future, nowadays it has not been widely accepted or implemented, whereas TOU pricing has been used extensively [4,5].

In this thesis, a methodology is proposed to study the profitability of a battery system for a customer under TOU pricing. In particular, a simple closed form procedure is proposed to evaluate the size of the battery system which minimizes the total costs sustained by the customer. The proposed procedure is able to account for both the technical constraints of the battery and contractual agreements between the customer and the utility. In the numerical application, the methodology is applied with reference to both residential and small industrial customers and based on actual TOU tariffs. Some aspects that affect the profitability of the battery, such as technological limitations (e.g. the battery and converter efficiency) and economic barriers (e.g. capital cost and the rate of change of the cost) are also discussed [5].

3.1.1. State of the art

In literature, the evaluation of the benefits related to the use of batteries under TOU tariff schemes is usually referred to the problem of optimal sizing of the battery [6-8]. In [6], the sizing is based on the maximization of the economic benefit which is defined as the ratio between the annual electricity saved (i.e. the difference between the total annual electricity charge without and with battery system) and the capital cost of the battery system. In [7], different combinations of technologies and sizes of the battery system are analyzed. The comparative analysis is made by evaluating the return of investment function, which is defined as the ratio between the revenue of the battery system (i.e. the difference between the capital cost and the total profit) and its capital cost. In [8], the most beneficial battery combination (i.e. technology and size) was identified on the basis of a closed form inequality. In particular, to check the profitability of the battery systems, the costs with and without battery were compared.

The sizing procedure proposed in this thesis allows a closed form optimal sizing procedure of BESS and, compared to that proposed in [6], introduces also important technical constraints on the use of the battery (e.g., the depth of discharge). The net present values of all the costs were also included in the economic analysis.

Compared to the proposal in [7], constraints related to the contractual agreements between the customer and utility are included which refer to both the periods in which the battery charges and those in which it discharges. These constraints are taken into account in [8] only with reference to the discharging stage. The importance of taking into account these constraints leads to the high influence they have on the amount of energy exchanged with the grid.

Moreover, unlike this proposed sizing procedure, in [6-8] the trend variation of the load profile along the years is not taken into account. This application performs also a wide sensitivity analysis to consider different perspectives in terms of life span and future costs.

3.1.2. Problem formulation and solving procedure

In this subsection, problem formulation and solving procedure of proposed closed form optimal sizing of BESS in a deterministic framework are considered. First, economic analysis of using BESS is presented then, based on this analysis, the BESS sizing problem is solved.

i. Economic analysis

A thorough economic analysis in order to evaluate the benefits achievable using BESSs in terms of reduction of costs related to the electricity consumption is considered. The economic analysis is performed by considering a specific time period whose choice can be related to the lifecycle of the system where the BESS is installed.

The economic analysis considers all the costs related to the inclusion of the battery system in a residential area or in an industrial facility that hereinafter will be referred to as the customer. In both the cases it is assumed that it is not possible to sell energy to the grid. Then, the energy stored in the battery can be used only to supply the loads. In the case of industrial facility, it is also assumed that the inclusion of the BESS doesn't introduce any modifications in the manufacturing process and in the facility's infrastructures [5]. To evaluate the total customer costs related to the BESS adoption, capital, maintenance, replacement, disposal and energy costs are taken into account:

$$C_{LCC} = C_0 + C_{mt} + C_{rep} + C_{disp} + C_{en} \quad (3.1)$$

where C_{LCC} is the life cycle cost (or total customer cost), C_0 is the capital cost of the BESS, C_{mt} is the BESS maintenance costs, C_{rep} is the cost related to the replacement of the batteries, C_{disp} is the BESS disposal cost and C_{en} is the energy cost. The maintenance, replacement and energy costs refer to their sum over the specified time period in which the economic analysis is performed. The net present value of the maintenance, replacement and energy costs have to be calculated as:

$$C_k(n)_{npv} = C_k(n) \frac{(1+\alpha)^{n-1}}{(1+\beta)^{n-1}} \quad (3.2)$$

where $C_k(n)$ is the expected cost (energy, maintenance and replacement) to suffer in the year n , $C_k(n)_{npv}$ is its net present value, β is the assumed discount rate and α is the effective rate of change assumed for the cost in the years. It is worth note that the expected cost ($C_k(n)$) takes into account the variation of the costs at year n that is not depended on the discount rate and

effective rate of change. As an example, in case of the energy cost, $C_k(n)$ includes the increasing rate of the loads at n^{th} year.

BESS capital costs (C_0) in (3.1) include equipment purchase cost and installation cost. Both the cost of the battery system C_{batt} and the converter C_{conv} are considered:

$$C_0 = C_{batt} + C_{conv} \quad (3.3)$$

BESS maintenance costs (C_{mt}) in (3.1) include corrective maintenance and preventive maintenance costs [9]. They can also be included as percentage of capital costs [10].

BESS replacement costs (C_{rep}) have to be sustained for purchasing a new battery if the battery lifetime is lower than the time period considered in the economic analysis. The life time of the battery depends on the number of charging/discharging stages per day:

$$\text{Battery lifetime} = \frac{N_{cycles}}{365 \cdot v} \quad (3.4)$$

where N_{cycles} is the total number of charging/discharging cycles declared by the battery manufacturer and v is the number of daily charging/discharging cycles.

With reference to the BESS disposal costs (C_{disp}) in (3.1), it is assumed that they can take into account also the benefit derived from the recycling of the battery. This cost/benefit may vary depending on the country where the disposal is performed. Based on the expected development of recycling technology, disposal activity could also be assumed to represent a benefit rather than a cost [11].

Energy costs (C_{en}) in (3.1) are the costs sustained by the BESS's owner (i.e. the customer) related to the energy consumption. They include both the purchase of the energy required to supply its loads and that required to charge the battery. The benefit in terms of reduction of these costs is related to the discharge of the battery to supply the loads during peak price periods. In the evaluation of the energy costs both the variations of the price of energy due to the inflation and load variations caused by economic growth can be taken into account by imposing a percentage variation per year.

The Energy costs (C_{en}) can be evaluated as follows:

$$C_{en} = C_{load} + C_{ch} - C_{dch} \quad (3.5)$$

where C_{load} is the total electricity cost required to supply the loads without considering the presence of the BESS, C_{ch} is the electricity cost sustained for charging the battery, C_{dch} is that avoided by the customer as loads are supplied by the BESS. Both C_{ch} and C_{dch} depend on the energy tariff applied to the customer. Utilities usually propose different tariffs depending on the periods (season) of the year [4]. In the most general case, the cost required for supplying the loads is given by:

$$C_{load}(n) = \sum_{i=1}^{n_s} N_i \int_{T_{day}} Pr_{En,i,n}(t) P_{l,i,n}(t) dt \quad (3.6)$$

where $P_{l,i,n}(t)$ is the power requested by the loads at time t of a typical day of the i^{th} season of the n^{th} year, T_{day} is the duration of the day, N_i is the number of days of the i^{th} season, $Pr_{En,i,n}(t)$ is the price of energy (energy charge) at time t of the i^{th} season of the n^{th} year.

In order to gain economic advantage, the battery is allowed to charge during low price hours and it is allowed to discharge during the high price hours. Thus, the costs sustained for charging the battery (C_{ch}) and the cost avoided by the consumer as loads are supplied by the BESS (C_{dch}) can be evaluated as follows:

$$C_{dch}(n) = \sum_{i=1}^{n_s} N_i \int_{\Omega_{dch,i,n}} Pr_{En,i,n}(t) P_{b,i,n}(t) dt \quad (3.7)$$

$$C_{ch}(n) = \sum_{i=1}^{n_s} N_i \int_{\Omega_{ch,i,n}} Pr_{En,i,n}(t) P_{b,i,n}(t) dt \quad (3.8)$$

where $P_{b,i,n}(t)$ is the absolute value of the power of the battery at time t of the i^{th} season of the n^{th} year, $\Omega_{ch,i,n}$ and $\Omega_{dch,i,n}$ are the set of all the time intervals of the day, in which the battery is allowed to charge and discharge, respectively. With reference to the figure (2.23), $\Omega_{dch,i,n}$ refers to the set of time intervals within n_{in}^{dis} , n_{fin}^{dis} . Eventually, by substituting (3.5) in (3.1) the total customer cost will be:

$$C_{LCC} = C_0 + C_{mt} + C_{rep} + C_{disp} + C_{load} + C_{ch} - C_{dch} \quad (3.9)$$

ii. BESS sizing procedure under TOU pricing

The optimum value of the size of the battery is the one corresponding to the minimum total cost

$$\min (C_{LCC}) \quad (3.10)$$

subject to the following constraints:

1. the number of charging/discharging cycles per day has to be coherent with the specified tariff;
2. a maximum depth of discharge is allowed;
3. the energy discharged by the battery must be used only to supply the load (the customer is not allowed to sell energy to the grid);
4. the power absorbed by the customer cannot exceed a maximum value imposed by the contractual agreement;
5. the energy stored in the battery at the beginning and at the end of the day has to be the same.

The minimization problem (3.10), subjected to the constraints 1-5, can be solved by means of a classical optimization algorithm [12-14]. However, in case of TOU tariff, a simplified closed form procedure can be used which makes the evaluation more simple and straightforward. The details of the proposed closed form approach are given in the following.

In order to meet constraint 1 the number of daily charging/discharging cycles has to be evaluated. When the TOU tariff is made by two price periods, that is the on-peak hours (the hours of higher price) and the off-peak hours (the hours of lower price), it is trivial to allow

the charging of the battery during the off-peak hours, and the discharging during the on-peak hours. It follows also that, if this case is considered, the battery is subjected to only one charging/discharging cycle in 24 hours. This condition can be still valid in case of TOU tariff made by three price levels, which is the tariff that provide a specified price for the mid-peak hours. In fact, usually, mid-peak periods refer to few hours [4], thus a benefit can be achieved if the battery is idle during these hours.

In the following, only for the sake of simplicity and without loss of generality, it is supposed that TOU tariff doesn't vary along the years, hence the index n in $Pr_{En,i,n}(t)$ in (3.6)-(3.8), and in $\Omega_{ch,i,n}$ and $\Omega_{dch,i,n}$ in (3.7)-(3.8), can be neglected. With reference to $C_{dch}(n)$ relationship (3.7) reads:

$$C_{dch}(n) = \sum_{i=1}^{n_s} N_i Pr_{dch,i} E_{dch,i,n} \eta_{dch} \quad (3.11)$$

where $Pr_{dch,i}$ is the energy charge (i.e. the price for energy) during the on-peak hours, that is in the time intervals included in $\Omega_{dch,i}$, $E_{dch,i,n}$ is the daily energy supplied by the battery in the same time intervals and η_{dch} is the BESS discharge efficiency.

With reference to $C_{ch}(n)$, relationship (3.8) reads:

$$C_{ch}(n) = \sum_{i=1}^{n_s} N_i Pr_{ch,i} E_{ch,i,n} \frac{1}{\eta_{ch}} \quad (3.12)$$

where $Pr_{ch,i}$ is the energy charge during the off-peak hours, that is the time intervals included in $\Omega_{ch,i}$ and $E_{ch,i,n}$ is the daily energy requested by the battery in the same time intervals, both evaluated at the n^{th} year and η_{ch} is the BESS charge efficiency. When the energy tariff is assumed to vary along the years, formulas (3.11) and (3.12) can be easily extended. In order to calculate $E_{dch,i,n}$ in (3.11) and $E_{ch,i,n}$ in (3.12), the following considerations have to be made.

By taking into account the maximum allowable depth of discharge (constraint 2), the maximum amount of energy that can be theoretically charged/discharged from the battery is given by:

$$E^T = E_{size} \frac{\delta}{100} \quad (3.13)$$

where E_{size} is the size of the battery and δ is the percentage value of the maximum depth of discharge of the battery [15].

Equation (3.13), however, cannot be directly included in (3.11) and (3.12), because it gives only the theoretical value of the daily energy available for charging/discharging, since during the operation the practical value of the energy that can be discharged is limited by constraints 3 and the maximum energy that can be charged is limited by constraint 4.

With reference to constraint 3, if initially the energy limit imposed by (3.13) is not considered, $\Omega_{dch,i}$ (i.e. the interval in which the battery is allowed to discharge) includes two time periods:

- the first, $\Omega_{1,i,n}$, includes all the time intervals in which the maximum power that can be supplied by the battery is greater than the maximum power requested from the load (i.e. $(\Omega_{1,i,n} = \{t : P_{b,max} > P_{l,i,n}(t)\})$);

- the second, $\Omega_{2,i,n}$, includes all the time intervals in which the power requested from the load is greater than or equal to the maximum power that can be supplied by the battery (i.e. $(\Omega_{2,i,n} = \{t : P_{b,max} \leq P_{l,i,n}(t)\})$).

where $P_{l,i,n}(t)$ is the active power required by the load at time t of the i^{th} season, n^{th} year, and $P_{b,max}$ is the maximum power that can be supplied by the battery. Since the customer is not allowed to sell energy to the utility, during $\Omega_{1,i,n}$, the maximum energy that can be discharged by the battery is

$$E_{1,i,n} = \frac{1}{\eta_{dch}} \int_{\Omega_{1,i,n}} P_{l,i,n}(t) dt \quad (3.14)$$

whereas, during $\Omega_{2,i,n}$, the maximum energy that can be discharged by the battery is

$$E_{2,i,n} = \frac{1}{\eta_{dch}} \int_{\Omega_{2,i,n}} P_{b,max} dt \quad (3.15)$$

The maximum energy that can be discharged during $\Omega_{dch,i}$ is then given by:

$$E_{max,i,n}^{dch} = E_{1,i,n} + E_{2,i,n} \quad (3.16)$$

With reference to constraint 4, if initially the energy limit imposed by (3.13) is not considered, $\Omega_{ch,i}$ (i.e. the interval in which the battery is allowed to charge) includes two time periods:

- the first, $\Omega_{3,i,n}$, includes all the time intervals in which the sum of the power requested by the load and the maximum power that can be used by the battery for charging is lower than the maximum value of the power that can be imported from the grid which is imposed by the contractual agreement (i.e. $(\Omega_{3,i,n} = \{t : (P_{b,max} + P_{l,i,n}(t)) < P_{max}^{ca}\})$).
- the second, $\Omega_{4,i,n}$, includes all the time intervals in which the sum of the power requested by the load and the maximum power that can be used by the battery for charging is greater than or equal to the maximum value imposed by the contractual agreement (i.e. $(\Omega_{4,i,n} = \{t : (P_{b,max} + P_{l,i,n}(t)) \geq P_{max}^{ca}\})$).

where P_{max}^{ca} is the maximum value of the power that can be imported from the grid which is imposed by the contractual agreement. Since the customer is not allowed to absorb more than P_{max}^{ca} from the grid, the maximum energy that can be charged during $\Omega_{3,i,n}$ is

$$E_{3,i,n} = \eta_{ch} \int_{\Omega_{3,i,n}} P_{b,max} dt \quad (3.17)$$

and the maximum energy that can be charged during $\Omega_{4,i,n}$, is

$$E_{4,i,n} = \eta_{ch} \int_{\Omega_{4,i,n}} (P_{max}^{ca} - P_{l,i,n}(t)) dt \quad (3.18)$$

The maximum energy that can be charged during $\Omega_{ch,i}$ is then given by:

$$E_{max,i,n}^{ch} = E_{3,i,n} + E_{4,i,n} \quad (3.19)$$

Finally, based on the hypothesis that during the day the total energy charged and discharged is the same (constraint 5) and considering now the energy limit given by (3.13), it follows that $E_{dch,i,n}$ in (3.11) and $E_{ch,i,n}$ in (3.12) are given by:

$$E_{dch,i,n} = E_{ch,i,n} = \min\{E^T, E_{max,i,n}^{dch}, E_{max,i,n}^{ch}\} \quad (3.20)$$

The proposed procedure for the calculation of C_{ch} and C_{dch} (given by (3.11) and (3.12)) will be applied to different battery sizes; thus, for each of them, the total cost will be evaluated by means of (3.9). The optimum value of the size of the battery will be that corresponding to the minimum total costs.

3.1.3. Numerical application

Two case studies are presented in which the proposed approach was performed with reference to two different load profiles that are reported in figure 3.1: residential customer (figure 3.1.a) and industrial customer (figure 3.1.b).

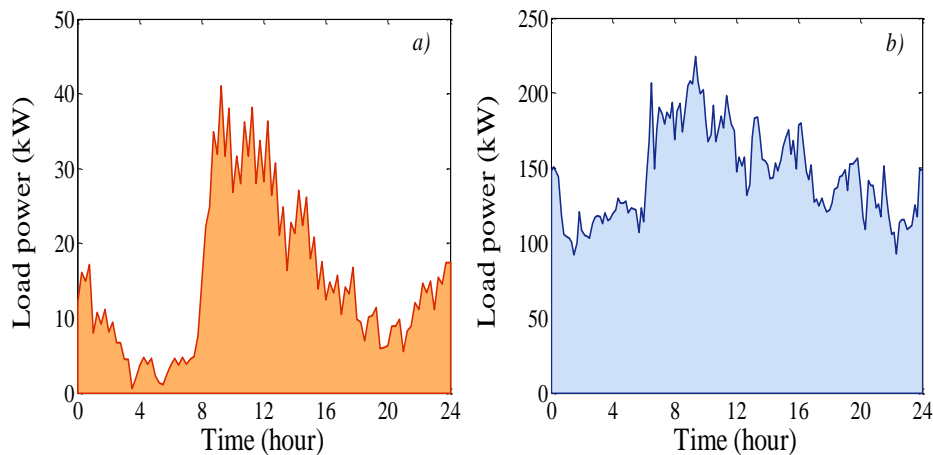


Figure 3.1: Residential load profile (a), Industrial load profile (b)

For both the residential and industrial loads, annual load variations of +1%, +3%, +5% were considered so including different possible trends of load growth versus years. Different combinations of the values assumed for the discount rate β and effective rate of change α were considered too, varying from 3% to 7% in order to evaluate different economic scenarios.

The BESS considered in this application includes a Lithium-ion battery which is connected to the power grid by a PWM-controlled AC/DC converter. In order to take into consideration both the nowadays technological status and the future perspectives, a sensitivity analysis was performed by considering for the BESS different charging and discharging efficiencies as well as different installation costs. The charging and discharging efficiencies were supposed to vary from 0.93 to 0.98 and from 0.96 to 0.98, respectively, whereas the installation cost was supposed to vary from 200 \$/kWh to 1000 \$/kWh. These costs include maintenance (2%) whereas the benefit deriving from the disposal of battery has been disregarded. A maximum

DOD of 80% is assumed which corresponds to a life cycle of about 4500 cycles [3]. By imposing one charging/discharging cycle per day, a life cycle of 12 years can be assumed for the battery; replacement costs are not considered.

Regarding the energy rates, TOU tariffs were considered with reference to the industrial and residential cases. For both the two cases the TOU tariff adopted by an actual utility was considered, whose values are reported in tables 3.1 and 3.2 [16]. The considered tariff is applicable to both small and medium industrial customers as well as for service in common areas in multifamily complexes.

Summer tariff	
On peak	12:00 noon to 6:00 p.m.
Part peak	8:30 a.m. to 12:00 noon and 6:00 p.m. to 9:30 p.m.
Off peak	9:30 p.m. to 8:30 a.m.
Winter tariff	
Part Peak	8:30 a.m. to 9:30 p.m.
Off Peak	9:30 p.m. to 8:30 a.m.

Table 3.1: Time of use tariff periods.

TOU periods	Summer tariff (\$/MWh)	Winter tariff (\$/MWh)
On peak	542.04	161.96
Part peak	252.90	
Off peak	142.54	132.54

Table 3.2: Time of use tariff prices.

Case a)

In this case study, the procedure was applied to a BESS of a residential load (figure 3.1.a). The total customer costs versus BESS sizes are reported in figure 3.2 with reference to different battery installation costs. The figure refers to the effective rate of change $\alpha=5\%$ and discount rate $\beta=5\%$, charge/discharge efficiencies of the BESS $\eta_{ch}=95\%$, $\eta_{dch}=98\%$, respectively. A 5% annual load variation was also supposed. In the figure the benefit obtained for each size can be deduced. For a specific battery size, in fact, the difference between the total cost and the cost corresponding to size zero (if negative) represents the economic advantage (i.e. the benefit) obtained with the use of that battery. If the difference is positive, no convenience exists to install the BESS. This consideration applies also for the following figures.

In figure 3.2, each curve is characterized by a minimum value of the total customer costs which corresponds to the optimal size of the BESS. Figure 3.2 shows that when the installation cost increases, the total cost increases as well and, at the same time, the optimal BESS size (if it exists) decreases. In addition, it is possible to observe that no benefits exist when the BESS installation cost is higher than 700 \$/kWh. In these cases, in fact, the total costs are always greater than the case of size zero.

Focusing on the case of installation cost equal to 600 \$/kWh, figure 3.3 reports the results of the analysis performed with reference to different annual load variations. Also in this case $\alpha=5\%$, $\beta=5\%$, $\eta_{ch}=95\%$, $\eta_{dch}=98\%$. The figure shows that, as expected, the total cost increases

when the annual load variation increases. The benefit provided by the use of BESS increases with the load variation and the optimal size of BESS increases from 160 kWh (for 1% and 3% annual load variations) to 170 kWh (5% annual load variation).

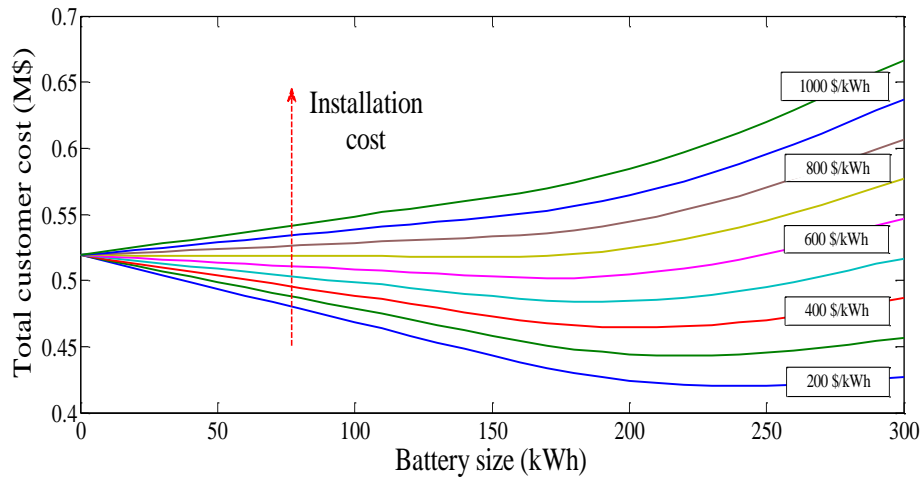


Figure 3.2: Total customer cost with $\alpha=5\%$, $\beta=5\%$, $\eta_{ch}=95\%$, $\eta_{dch}=98\%$, for 5% annual load variations and for different installation costs (residential load).

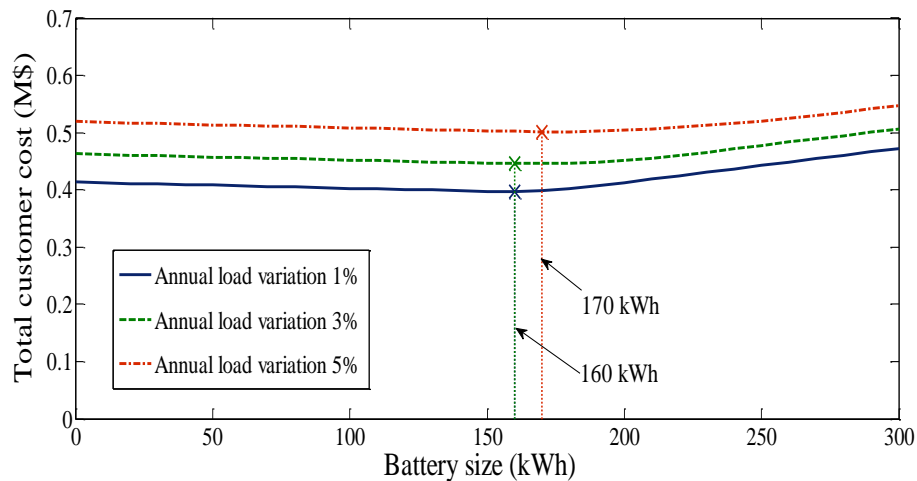


Figure 3.3: Total customer cost with $\alpha=5\%$, $\beta=5\%$, $\eta_{ch}=95\%$, $\eta_{dch}=98\%$, BESS installation cost = 600 \$/kWh, for different values of annual load variation (residential load).

Figure 3.4 shows the total cost and optimal sizes of battery under different values of the effective rate of change α and discount rate β with the annual load variation of 5%, and $\eta_{ch}=95\%$, $\eta_{dch}=98\%$.

In figure 3.4, it is interesting to note that the total cost increases when $\beta < \alpha$. On the other hand, when $\beta > \alpha$ the total cost decreases and, in the particular case reported in the figure ($\alpha=3\%$, $\beta=7\%$), the installation of BESS never provides any benefit, since the total cost for size zero is always lower than those obtained for all the other battery sizes. In case of $\beta \leq \alpha$, instead, a benefit is evidenced. Also, it can be observed that the values of α and β strongly affect the optimal size, since their variation results in very different values of total cost (up to 18%).

In figure 3.5, different BESS efficiencies are considered when the installation cost is 600 \$/kWh, $\alpha=5\%$, $\beta=5\%$ and the annual load variation is 5%. Obviously, the total cost decreases when efficiency increases, thus making the BESS even more profitable.

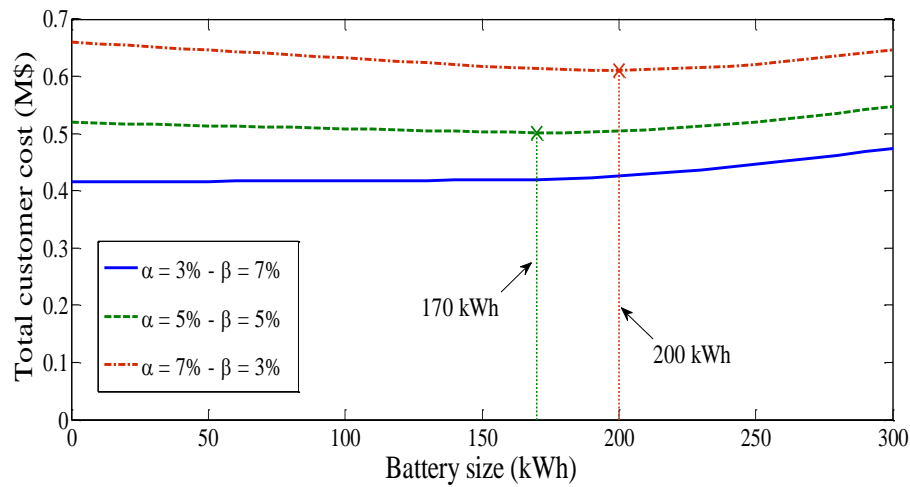


Figure 3.4: Total customer cost with an annual load variation of 5%, $\eta_{ch}=95\%$, $\eta_{dch}=98\%$, BESS installation cost = 600 \$/kWh, for different values of α and β (residential load).

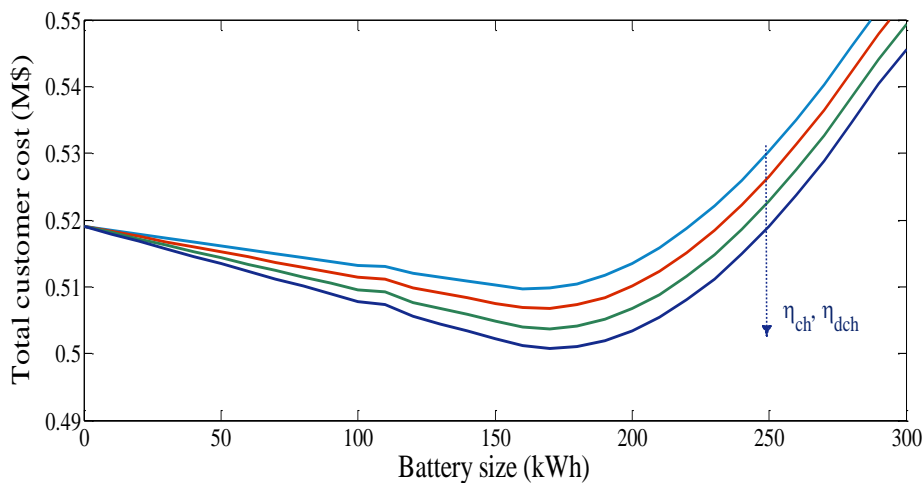


Figure 3.5: Total customer cost with $\alpha=5\%$, $\beta=5\%$, 5% annual load variation and different values of BESS efficiency (residential load).

Case b)

In this case study, the power profile of a small industrial facility was considered (figure 3.1.b). In figure 3.6 the results obtained for different installation costs are reported with $\alpha=5\%$, $\beta=5\%$, $\eta_{ch}=95\%$, $\eta_{dch}=98\%$ and annual load variations of 5%. The total cost for different annual load variations is shown in figure 3.7 when $\alpha=5\%$, $\beta=5\%$, $\eta_{ch}=95\%$, $\eta_{dch}=98\%$ and the installation cost is 600 \$/kWh.

Compared with those of case a, in both figures the values of the total cost and benefits are larger (because the load power request is larger). However, the same considerations reported with reference to the residential case are still valid. In particular, from the analysis of figure 3.6, it is very interesting to note that, even if the industrial load request is larger than the

residential, the maximum installation cost that makes the use of BESS profitable is about 700 \$/kWh, that is the same obtained in the residential case. As it can be observed in both figures (3.6 and 3.7), the optimal size of the battery increases with the load request. In the considered cases reported in figure 3.7, the optimal size of the battery is 1200 or 1250 kWh, thus highlighting a slight influence of the annual load variation on the battery sizing.

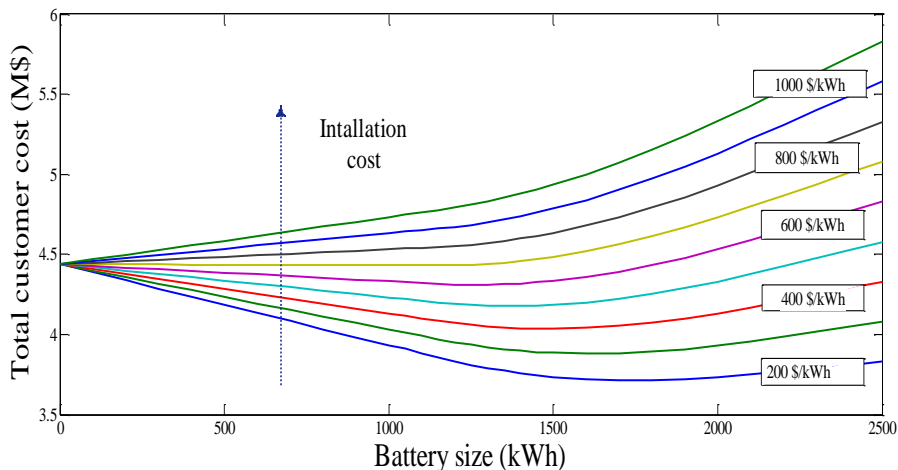


Figure 3.6: Total customer cost with $\alpha=5\%$, $\beta=5\%$, $\eta_{ch}=95\%$, $\eta_{dch}=98\%$, for 5% annual load variations (industrial load).

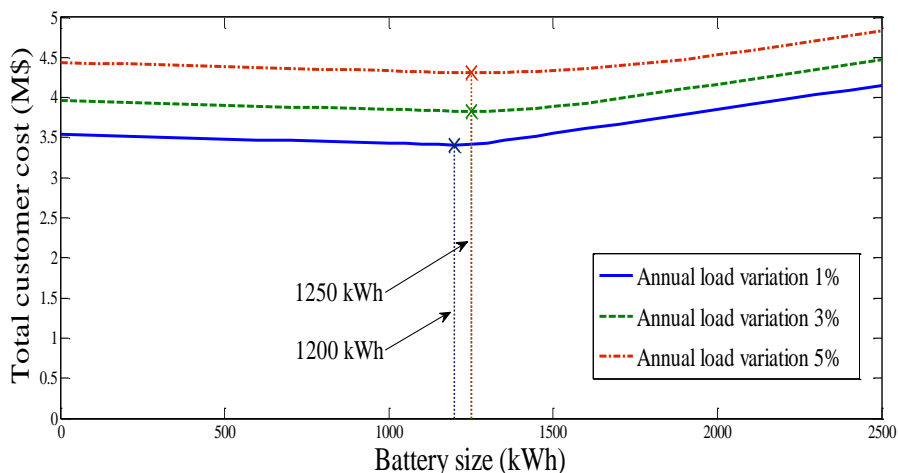


Figure 3.7: Total customer cost with $\alpha=5\%$, $\beta=5\%$, $\eta_{ch}=95\%$, $\eta_{dch}=98\%$, BESS installation cost = 600 \$/kWh, for different values of annual load variation (industrial load).

Figure 3.8 shows the total cost and optimal sizes of battery under different values of the effective rate of change α and discount rate β based on annual load variation of 5%, $\eta_{ch}=95\%$, $\eta_{dch}=98\%$ and installation cost 600 \$/kWh. Again, the same considerations reported with reference to the residential case (figure 3.4) are still valid. In particular, figure 3.8 shows that the total cost increases when $\beta < \alpha$, or decreases when $\beta > \alpha$ and, in the case reported in the figure ($\alpha=3\%$, $\beta=7\%$), the installation of BESS never provides any benefit. Benefits are evidenced when $\beta \leq \alpha$. Also, it can be observed that the values of α and β strongly affect the optimal size, since their variation results in very different values of the total cost (up to 16%).

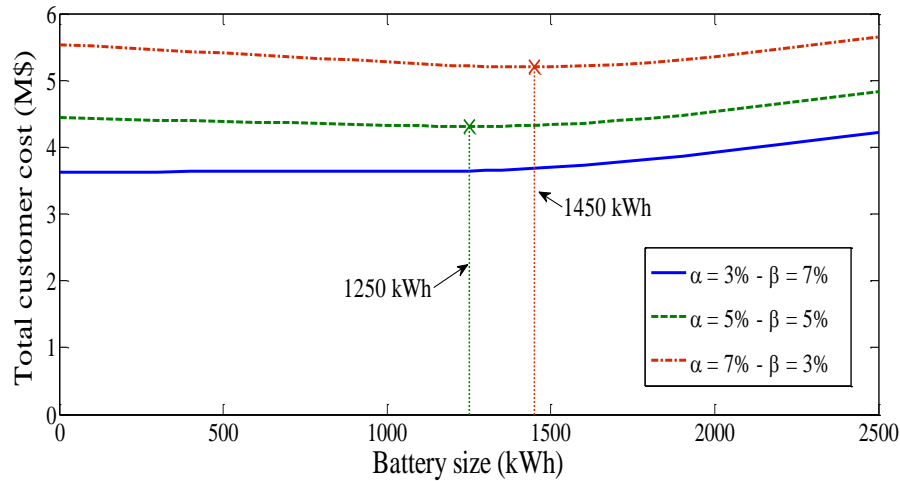


Figure 3.8: Total customer cost with a annual load variation of 5%, $\eta_{ch}=95\%$, $\eta_{dch}=98\%$, BESS installation cost = 600 \$/kWh, and for different values of α and β (industrial load).

Also in figure 3.9, where different BESS efficiencies are considered, based on installation cost of 600 \$/kWh, $\alpha=5\%$, $\beta=5\%$ and annual load variation of 5%, the same considerations on the profitability of BESS can be drawn. Figure 3.9, in fact, shows that the total cost decreases when efficiency increases.

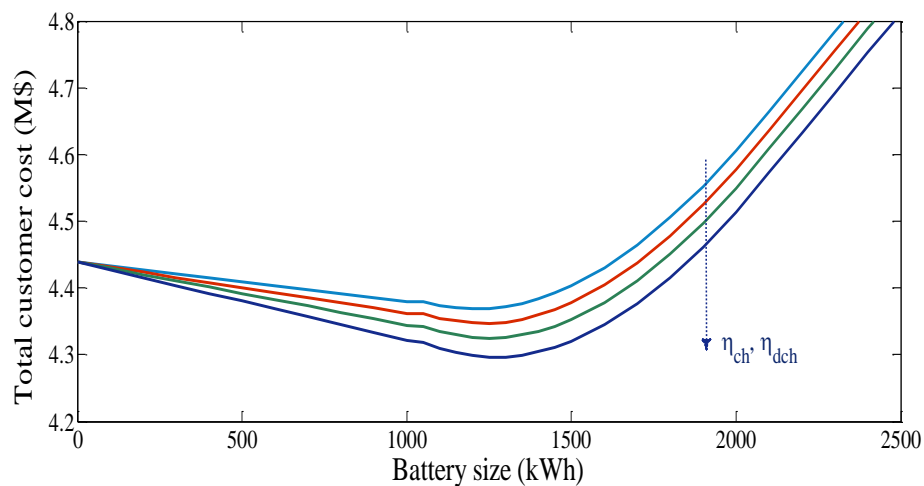


Figure 3.9: Total customer cost with $\alpha=5\%$, $\beta=5\%$, 5% annual load variation, BESS installation cost = 600 \$/kWh, and different values of BESS efficiency (industrial load).

3.2. Probabilistic optimal sizing of battery energy storage system based on decision theory

In defining the sizing framework, the engineer who is sizing the BESS (hereafter referred to as the “Decision Maker” or DM) can operate under the hypothesis of either a deterministic framework or under the uncertainty of the data associated with the problem. In the first case, which has been the more popular approach in the past and was analyzed in the previous section, certain conditions are assumed and used as input data. In the second case, uncertainties are introduced and modeled probabilistically. In this section, particularly, the optimal sizing of BESS under the decision theory is presented with the consideration of

unavoidable uncertainties which are introduced by the cost of electricity and the load demands of industrial facilities.

As is well known, possible applications of BESSs that seem particularly useful are load leveling, reducing end-user's electricity bills, improving end-user's power quality, reliability, and spinning reserve [17, 18]. In the frame of these applications, in this section we focus on the optimal sizing of a BESS installed in an industrial facility to reduce the facility's electricity bill. In the most general case, reducing the electricity bill can involve both energy (energy charge (EC)) and peak power charge (demand charge) [12, 19], as shown in chapter 2. This application refers only to the EC, so reducing the electricity bill means only the ability of the end-user to increase its energy required from the grid during the lower price hours and decrease the energy required from the grid when the price is higher.

In the probabilistic framework too, when sizing a BESS, a cost analysis should be conducted that takes into account costs and benefits associated with the installation of the BESS. These benefits depend on the control strategy performed during the operation of the BESS.

However, to apply any sizing procedure for reducing the electricity bill, we must have some input data ("sizing framework"). In particular, the load demand of the industrial facility and the relationships that quantify the electricity bill, *i.e.*, the way in which the electricity bill is calculated and the way in which it depends on electricity use at each time of day, must be known.

We contend that the problem of sizing storage systems to be installed to reduce the electricity bills of an industrial facility can be successfully solved assuming uncertain input data related to the problem. This position is based on the fact that in this way the DM can properly include both short-term and long-term factors in the sizing procedure. Of course, future systems will be subject to random perturbations that unavoidably result in uncertainties in the sizing calculations. Thus, traditional, deterministic paradigms, in some cases can lead to uneconomic or unreliable solutions.

This section deals with the probabilistic optimal sizing of a BESS installed in an industrial facility to reduce electricity costs applying a four-step procedure, based on decision theory, with the aim to obtain a good solution for the sizing problem, even when facing uncertainties. The numerical applications performed on an actual industrial facility provided evidence of the effectiveness of the proposed procedure.

3.2.1. State of the art

In the relevant literature some research works presented the probabilistic sizing of storage systems to reduce the uncertainties associated with wind power and photovoltaic power [20-27]. With reference to wind power, in [20], a stand-alone system was considered, and the storage was calculated for different levels of mean load. In [21], dynamic sizing based on probabilistic forecasts and a real market situation was proposed, considering the degree of risk that a power producer would find acceptable. In [22, 23], the possible smoothing effect of a BESS was simulated with an exponential moving average. In [24], a probabilistic reliability assessment method was proposed for determining the adequate size of an on-site energy storage system and determining the transmission upgrades required to connect wind generators' output power with the power system. In [25], a probabilistic method for sizing energy storage systems was proposed based on wind power forecast uncertainty; the proposed sizing methodology permitted the estimation of the size as a function of unserved energy.

With reference to photovoltaic power, in [26], a probabilistic approach was used to size both the PV system and the battery storage system for three selected sites in Italy, characterized by different values of solar radiation. In [27], a probabilistic approach for the design of a stand-alone hybrid generation system, including energy storage devices, was proposed, based on an index able to take into account the probability that loss of power supply occurs.

3.2.2. Problem formulation and solving procedure

An industrial facility's electrical distribution system in which one or more transformers connect the distribution grid to the lines of the users' power system is considered. A BESS is assumed to be connected at the secondary side of the transformers with the aim of reducing the electricity bill. The following four-step procedure to solve the problem of BESS sizing under uncertainty is proposed:

1. A set of possible futures is specified, and each future is characterized by a probability assigned by the DM. Here, each future is associated with a different industrial facility's load demand and the way in which the electricity bill is calculated, depending on electricity use at each time of the day.
2. Several possible BESS design alternatives are specified. Each design alternative is based on the BESS energy ratings, with its associated installation and maintenance costs.
3. The total BESS costs are calculated for each future specified in the first step and for each sizing alternative specified in the second step. The total costs take into account the installation cost, maintenance cost, and the benefits derived from the operation of the BESS. The benefits are obtained by solving an optimization problem in which the objective function to be minimized is the electricity bill and the constraints of which include the need to maximize the BESS's lifetime.
4. Decision theory is applied to choose, among the alternatives of the second step, the best BESS sizing solution by considering the futures with their probabilities, as specified in step 1. The applied decision theory approaches used the future probabilities assigned in step 1 and the total cost of the BESS calculated in step 3; they are the minimization of the expected cost, the min-max regret, and the stability areas' criteria. These approaches have been used extensively and successfully for the solution of several important power system planning problems [28-31].

Figure 3.10 shows the flowchart of the proposed procedure. The DM, based on her or his understanding of the nature of the uncertainties relevant to the BESS sizing problem, selects possible futures and alternatives of steps 1 and 2 and assigns the future probabilities [28-31]. Three approaches usually are used to estimate the probabilities to be assigned when the future uncertainties are modeled probabilistically [28]:

- the first approach is based completely on the observed information;
- the second approach is based completely on the subjective judgment of the DM;
- the third approach is a mix of the above two approaches, and it combines the DM's judgmental information with the observed information.

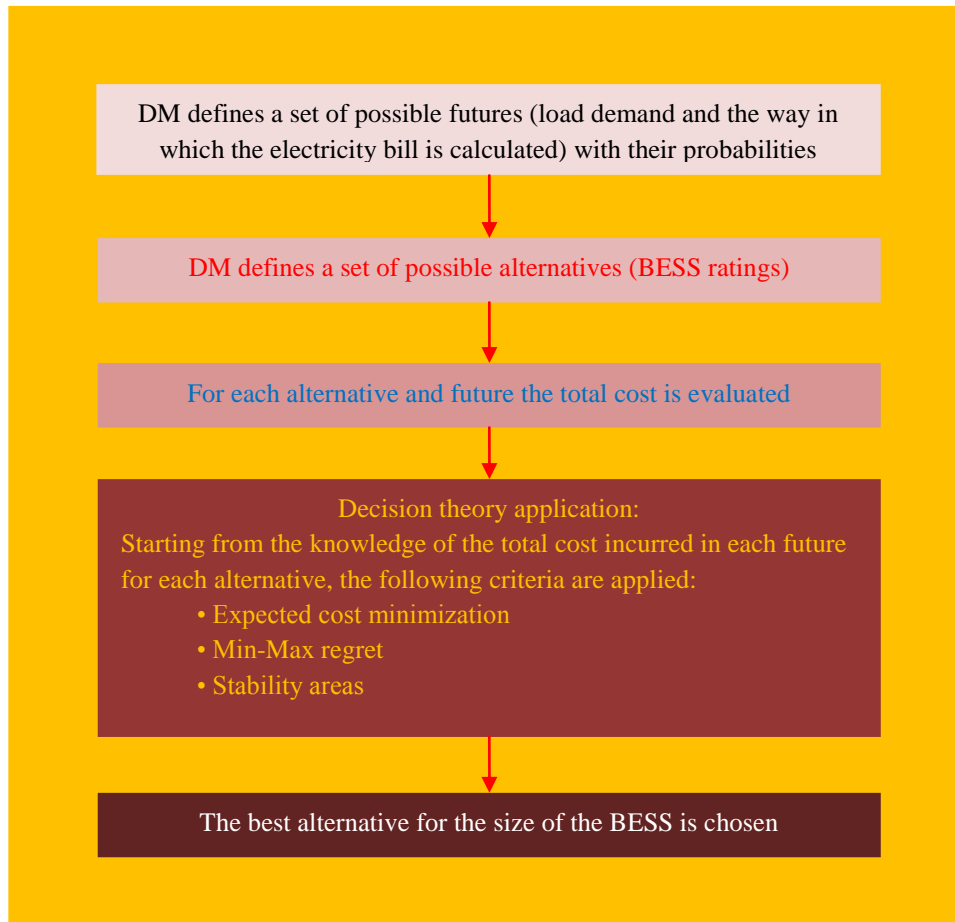


Figure 3.10: Flowchart of the proposed procedure.

In this thesis, we used the second approach (subjective judgment of the DM). In fact, even if it may seem unsound to assign values of probabilities with little or no empirical information, surprisingly positive results can be obtained when the DM has a good understanding of the nature of the uncertainties relevant to the problem and uses this understanding to assign probabilities in a subjective manner [28-32].

In the next subsections, the details of the optimization problem to be solved in step 3 and the decision theory criteria of step 4 are shown.

i. Formulation of the optimization problem for calculating the total costs for the BESS

The third step of the proposed procedure, as shown in figure 3.10, consists in calculating the total BESS costs for each future specified in the first step and for each sizing alternative specified in the second step.

As shown in the previous section the total cost can be evaluated as (3.1). In this application, however, the total energy cost C_{en} in equation (3.1) can be calculated for 24 h (one day) [33], assuming as input data a typical daily profile of the industrial facility's load power and the hourly electricity price coefficients for the day. Also, more typical days can be considered, *i.e.*, to cover weekly, monthly, and seasonal variations [34]. Once the typical daily electricity costs are known, they can be extended to cover the costs during the lifetime of the BESS to which this case refers.

However, the evaluation of the daily cost is not an easy task, since, while the BESS operation is aimed at reduction of the electricity bill, at the same time technical constraints able to

maximize the battery lifetime have to be met. In particular, constraints on the depth of discharge and the number of charging/discharging cycles per day have to be satisfied [15]. To do that, a control strategy based on a constrained optimization problem is needed. In this application, the procedure proposed in [12] is used.

This procedure obtains the daily electricity bill with the BESS by solving an optimization problem whose general mathematical formulation is expressed by equations (2.1) and (2.2) of section 2.1.

Before specifying the objective function and constraints, it is important to recall that, also in this case, the optimization model refers to a day split into n_t time intervals of length Δt and that, in order to limit one charging/discharging cycle, the day is separated into three intervals, as shown in figure 2.23, with the first interval being the charging stage, the second interval being the discharging stage, and the third interval also referring to the charging stage. In this way, the condition of one cycle per day is clearly satisfied, because the last charging stage of the day continues with the first charging stage of the following day.

The time steps in which the discharging mode starts and ends ($n_{in}^{dis}, n_{fin}^{dis}$) are optimization variables of the problem subjected to the constraint $n_{in}^{dis} \leq n_{fin}^{dis}$ (bounded by 1 and n_t). Based on the daytime steps of figure 2.23, it is possible that the battery, at the beginning of the day, is either in charging mode (if $n_{in}^{dis} > 1$) or in discharging mode (if $n_{in}^{dis} = 1$); moreover, it is possible that, at the end of the day, the battery is either in charging mode (if $n_{fin}^{dis} < n_t$) or in discharging mode (if $n_{fin}^{dis} = n_t$).

The objective function (2.1) to be minimized is obviously the daily electricity bill, given by:

$$f_{obj} = \sum_{t=1}^{n_t} Pr_{En,t} P_{grid,t} \Delta t_t \quad (3.21)$$

where $P_{grid,t}$ is the power requested by the facility from the grid, $Pr_{En,t}$ is the energy price, both at the t -th time interval and Δt_t is the duration of the t -th time step.

The first equality constraint in relationship (2.2) to be met refers to the power balance, and it requires that the total power value requested by the facility be equal to the algebraic sum of the BESS power and load demand power for all time intervals of the day. Comparing with the power balance equation in (2.15) which is considered at each time interval for the following 24 hours, here, similar power balance equation imposes that the power value requested by the facility to the grid is equal to the algebraic sum of the BESS power and facility load power, at all the time intervals of the day.

Further equality constraints require that the daily balance of charging and discharging energy is satisfied:

$$\sum_{t=1}^{n_t} k_t P_{b,t} \Delta t_t = 0 \quad , \quad k_t = \begin{cases} \frac{1}{\eta_{dis}} & t = n_{in}^{dis}, \dots, n_{fin}^{dis} \\ \eta_{ch} & otherwise \end{cases} \quad (3.22)$$

where η_{ch} and η_{dis} are the BESS efficiency in charging and discharging mode, respectively; n_t is the number of day time intervals and n_{in}^{dis} , n_{fin}^{dis} are shown in figure 2.23.

Moreover, according to inequality constraints in (2.5) and (2.6) the BESS can only charge during the charging period and only discharge otherwise.

A further inequality constraint (2.7) imposes that the state of charge during the discharging stage cannot be less than a minimum value (which depends on the maximum depth of discharge of the BESS).

Similar to the inequality constraint in (2.30), the state of charge during the charging stage cannot be greater than a maximum value (the size of the BESS).

Finally, the BESS at the beginning of the day is bounded by the BESS capacity and minimum value of the energy that can be stored in the battery based on the allowable depth of discharge. It has to be highlighted that, during the lifetime of the battery, its features (e.g., efficiency, maximum storage capacity, and minimum storage capacity) vary with time based on the battery's aging characteristics [35]. Generally speaking, it could be possible to consider the effects of aging by dividing the planning problem into different time intervals, each one characterized by a specific set of storage properties (e.g., the battery's capacity or efficiency), depending on the aging effects versus time. However, to the best of our knowledge, this approach has never been used in the relevant literature in case of the BESS sizing; rather, the pertinent literature only takes into account the problem of the charging/discharging cycles, as was the case for [15, 19, 33].

The above optimization model was solved with a hybrid approach based on a GA and a linear optimization that operated inside the GA as an inner loop, as shown in details in chapter 2. The GA was used to obtain only the time intervals in which the BESS operates in the charging and discharging modes, while the linear optimization determined the state of charge of the BESS at the beginning of the day and the optimal charging/discharging powers of the BESS inside the above intervals to minimize the electricity bill cost function in equation (3.21).

In more detail, the GA created populations in which the individuals referred to the times that the discharging mode started and ended. Once the GA has generated an individual and, hence, the charging and discharging intervals were unequivocally determined, the linear optimization algorithm solved the optimization problems in equations (2.1) and (2.2).

When the inner linear optimization problem converges, the value assumed by the objective function in equation (3.21) also represents the value of the fitness function related to each individual of the GA. The procedure terminates when the GA converges, *i.e.*, when the best value of the fitness function remains constant over an assigned number of generations or when a maximum number of iterations is reached.

ii. Decision Theory criteria for the choice of the best size for the BESS

As previously shown in steps 1 and 2 of the proposed BESS sizing procedure, several futures are specified, with each future characterized by an assigned probability, and several design alternatives for the BESS are specified in terms of the ratings of the installed BESS and, then, of the energy to be produced by the BESS. In addition, in step 3, for each future specified in the first step and for each alternative specified in the second step, the total cost of the BESS was calculated by optimizing the operation of the BESS.

Decision theory was used in step 4 to choose, among the alternatives of step 2, the best solution with respect to the size of the BESS by considering the futures with their probabilities as specified in step 1 and considering the total costs calculated in step 3.

Let the uncertainties in the sizing of the BESS be represented by a set of N_F futures, F_k ($k = 1, \dots, N_F$), with P_k being the future probability; each future is characterized by different values of the electricity cost coefficients $Pr_{En,t}$ in equation (3.24) and the profile of the load demand $P_{l,t}$.

Let N_a alternatives A_i ($i = 1, \dots, N_a$) also be available, each corresponding to a different size of the BESS. Then, the problem of choosing the best solution must be solved. To solve the above problem, we apply three different decision theory approaches based on:

- a. the minimization of the expected cost
- b. the minimization of the maximum regret felt by the DM
- c. a combination of (a) and (b).

It should be noted that the application of decision theory requires knowledge of the total cost incurred in each future for each alternative, that is the value of the objective function (3.21) calculated as the solution of the optimization problem.

Approach (a) may be applied as follows. The expected value of the cost of alternative A_i associated with all the N_F futures can be calculated as:

$$E[C(A_i)] = \sum_{k=1}^{N_F} P_k C_{ik} \quad (3.23)$$

where symbol $E[\cdot]$ means the expected value, C_{ik} is the cost incurred in the k^{th} future F_k by the i^{th} alternative A_i . For each alternative A_i , the expected value of the cost associated with all the N_F futures can be calculated.

Among all the possible alternatives, *i.e.*, A_i ($i = 1, \dots, N_a$), the alternative to be chosen is the one associated with the minimum value of the expected value of the cost:

$$\min_i \{E[C(A_i)]\} = \min_i \left\{ \sum_{k=1}^{N_F} P_k C_{ik} \right\} \quad (3.24)$$

The solution of the optimization problem in equation (3.24) is A_{opt} , that is the alternative to be chosen. Basically, applying Approach (a) means that the DM selects the alternative that satisfies the mean of the futures that can occur. However, this choice does not avoid solutions that lead to bad performance in the future if an unfavorable future were to really occur. Basically, Approach (b) tries to avoid such situations. In fact, minimizing the maximum regret means that the DM chooses the best solution among the worst solutions in order to avoid solutions that lead to a bad performance in the future [28-31].

In more detail, Approach (b) indicates the best solution as the one that minimizes the maximum regret felt by the DM after verifying that the decision he or she made was not optimal with respect to the future that actually occurred. The criterion is based on the calculation of the regret felt for having chosen a certain alternative A_i when the k^{th} future occurred; the regret is calculated as follows:

$$RG_{ik} = C_{ik} - C_k^{min} \quad (3.25)$$

where C_k^{min} is the minimum cost for the k^{th} future and RG_{ik} is the regret felt for having chosen a certain alternative A_i when the k^{th} future occurred. Once the regret given by equation (3.25) is known, it is possible to calculate the weighted regret with the probability of the associated future as:

$$WRG_{ik} = P_k RG_{i,k} \quad (3.26)$$

where P_k is the probability of the k^{th} future and WRG_{ik} is the weighted regret; when all of the weighted regrets are given by equation (3.26), for each sizing alternative, A_i , the maximum weighted regret is determined as:

$$\max_k (WRG_{ik}) \quad (3.27)$$

Finally, the sizing alternative, A_{opt} , to be chosen among the N_a possible alternatives, is the one associated with the lowest value of equation (3.27), *i.e.*, the minimum of the maximum weighted regrets:

$$\min_i \left[\max_k P_k RG_{ik} \right] \quad (3.28)$$

It should be noted that a critical aspect of both the above criteria (based on the expected cost and the regret) is the assignment of the probabilities P_k ($k = 1, \dots, N_F$) that quantify the randomness of the sizing of the BESS, provided that both the expected costs and the weighted regrets depend on the probabilities. Several approaches for estimating these probabilities have been proposed [28], but none may fully overcome the probability assignment problem, either in the case of a high randomness or when the DM does not have a good understanding of the nature of the uncertainties relevant to the problem. Also, it can be useful to introduce a criterion based on the results of both procedures based on the DM's assessment.

In order to overcome the above problems, it may be convenient to refer to the "stability areas" concept proposed in [29]. Based on this concept, each scenario probability is treated as a parameter that randomly varies in the range of [0, 1] while meeting the following constraint:

$$\sum_{k=1}^{N_F} P_k = 1 \quad (3.29)$$

When the results of (a) and (b) criteria are superimposed, the "stability area" of each sizing alternative is the area that corresponds to the probability for which both the Approaches (a) and (b) give the same recommended solution for sizing the BESS. Based on the knowledge of all of the sizing alternatives characterized by a stability area different from zero (and of the corresponding area value), the DM can determine the sizing solution he or she considers to be the best. For example, the DM's final choice (*i.e.*, the best size) could be the sizing

alternative characterized by the greatest area, *i.e.*, the one that appears most frequently as the best solution for both the criteria (a) and (b).

It should be also noted that assigning alternatives and futures is an important aspect in the proposed approach. In the decision-making context, the DM identifies alternatives and futures on the basis of her/his understanding of the nature of the planning problem to be solved. In case of BESS sizing, these choices should be effected also considering that:

- a maximum amount of investment cost can exist, imposed by the owner of the industrial facility;
- there is a range of sizes within which the DM can forecast that the optimal solution will occur more frequently;
- the use of a very small number of futures can generate final decisions that will lead to bad performance in the future.

3.2.3. Numerical application

The proposed optimal procedure was used to size a BESS to be connected to the secondary side of the transformers that connect an actual industrial facility to the medium voltage distribution grid. Among the batteries that are commercially available, either Li-ion or redox batteries can be used, both characterized by a long useful lifetime even with a significant depth of discharge [15, 36]. A total value of 1000 \$/kWh for the investment and maintenance costs is considered [10, 15, 33, 37]; these costs include the controls and power conditioning system, and they take into account the forecasted decrease in the cost of the new generation electric battery [38]. A lifetime of about 4500 cycles was assumed and it takes into account the forecasted increase in the lifetime of the new generation electric battery [10, 38]. Then, having imposed one cycle per day, the period taken into consideration for the planning study is 12 years. The BESS is connected to the secondary side of the transformers by a pulse-width modulation controlled static converter. As is well known, the efficiency of the battery system depends on both the charge/discharge rate and the state of charge [39]; in this application, the charging efficiency was assumed to be 0.90, and the discharging efficiency was assumed to be 0.93 [15]. The maximum depth of discharge is 80%.

In order to better show the proposed sizing procedure, two different case studies are presented [37]:

- **Case 1:** only three futures are considered ($N_F = 3$); in this very simple case, the stability area criteria have a very simple graphical representation and, then, the proposed sizing approach can be more easily illustrated.
- **Case 2:** nine futures are considered ($N_F = 9$).

With reference to the sizing alternative, 16 sizes for the BESS were considered ($A_1 = 0$, $A_2 = 100$, $A_3 = 200$, $A_4 = 300$, $A_5 = 400$, $A_6 = 500$, $A_7 = 600$, $A_8 = 625$, $A_9 = 650$, $A_{10} = 675$, $A_{11} = 700$, $A_{12} = 725$, $A_{13} = 750$, $A_{14} = 775$, $A_{15} = 800$, $A_{16} = 900$ kWh).

The sizing alternatives are chosen considering that:

- a maximum amount of investment cost exists, imposed by the owner of the industrial facility, constraining the maximum value of the size to 900 kWh;

- there is a range of sizes (between 600 kWh and 800 kWh) within which the DM forecasts that the optimal solution will occur more frequently, as will be shown later. Alternative A1 = 0 means that no BESS is installed.

Case 1)

The following three futures were considered:

- *Future 1*: the hourly energy price ($Pr_{En,t}$) profile reported in [33] for micro grids with storage system applications was assumed (figure 3.11). The profile of the industrial facility's load demand was obtained by multiplying the profile in figure 3.12 by 0.85.
- *Future 2*: same as future 1 except that the profile of the industrial facility's load demand was taken from figure 3.12.
- *Future 3*: same as future 1, except that the profile of the industrial facility's load demand was obtained by multiplying the profile in figure 3.12 by 1.15.

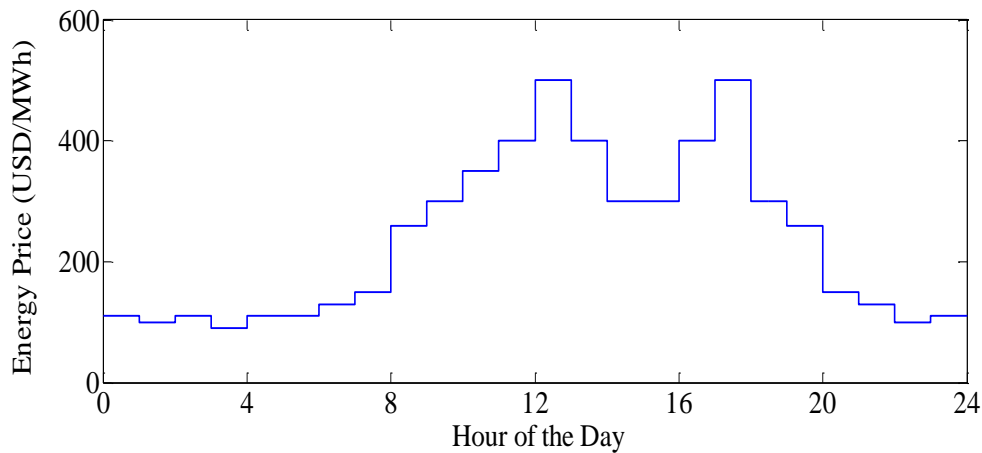


Figure 3.11: Hourly energy price.

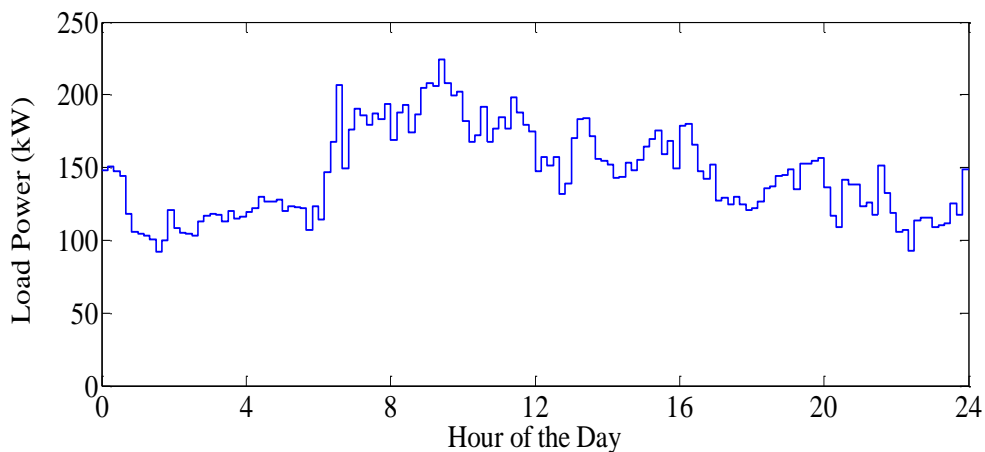


Figure 3.12: Load demand daily profile.

Three possible demand profiles are considered, as suggested in [34]. The electricity costs were assumed to have a yearly rate of increase of 5%; a discount rate of 5% was assumed for the present value calculation. Then, the three decision theory approaches were taken into account [approaches *a*, *b* and *c*]. For the application of the first two criteria, initially the following probabilities were assigned to each future, *i.e.*, $P_1 = 0.2$, $P_2 = 0.3$ and $P_3 = 0.5$.

Table 3.3 presents the values of the total cost of the BESS (*i.e.*, the sum of the energy bill and the investment/maintenance costs over the whole planning period) for each future and for each alternative as a decision matrix. For each future, the minimum total cost is clearly marked.

From the analysis of the results in table 3.3, it clearly appears that a slight variation of the load demand profile can generate a change in the size of the BESS that has the minimum cost (*i.e.*, a 15% increase in the load profile generates the change from A7 to A9 and to A13 sizing alternatives, which are the optimal solutions for each future). Moreover, it is also interesting to observe that, for an assigned future, the total costs change slightly versus the size of the BESS, because the increasing values of the investment/maintenance costs for the BESS versus its size are compensated by the significant decreases in the electricity bill (*i.e.*, by the increasing benefits derived from the installation of the BESS); as an example, in the case of the minimum cost sizing alternative when future 2 occurs, *i.e.*, A9 = 650 kWh, the benefits derived from installing the BESS (*i.e.*, the reduction of the electricity bill due to the availability of the BESS over the planning period) in the case of the load profile of figure 3.12 (Future F2) are equal to \$703,780 (18%).

Alternative	Future		
	F1	F2	F3
A1 = 0	3,247.81	3,820.96	4,394.10
A2 = 100	3,239.27	3,812.41	4,385.55
A3 = 200	3,230.72	3,803.86	4,377.01
A4 = 300	3,222.17	3,795.32	4,368.46
A5 = 400	3,213.63	3,786.77	4,359.91
A6 = 500	3,205.08	3,778.22	4,351.37
A7 = 600	3,202.88	3,769.68	4,342.82
A8 = 625	3,203.66	3,767.93	4,340.69
A9 = 650	3,204.90	3,767.17	4,338.55
A10 = 675	3,206.63	3,767.43	4,336.41
A11 = 700	3,208.87	3,767.91	4,334.38
A12 = 725	3,211.12	3,768.69	4,332.86
A13 = 750	3,213.36	3,769.67	4,332.25
A14 = 775	3,215.61	3,771.10	4,332.53
A15 = 800	3,217.85	3,773.04	4,332.95
A16 = 900	3,226.82	3,782.01	4,337.29

Table 3.3: Decision matrix: total cost (k\$) for each size (kWh) - Case 1.

Table 3.4 shows the decision matrix of the weighted regrets associated with each future scenario and for each alternative; for each alternative, the maximum weighted regret is clearly marked. From the analysis of the results in table 3.4, it clearly appears that the regret is equal to zero for the minimum total cost scenario, as expected.

Table 3.5 shows the expected value of the costs associated with the 16 alternatives and the maximum weighted regret calculated using the results in table 3.4, and it should be noted that some slight numerical inaccuracies can arise in all tables' results due to digit truncation. From the analysis of the results in table 3.5, it follows that the alternatives (BESS sizing)

recommended by Approaches (a) and (b) are slightly different, and they are given by $A_{12} = 725 \text{ kWh}$ and $A_{11} = 700 \text{ kWh}$, respectively.

Alternative	Future		
	F1	F2	F3
A1 = 0	8,986.37	16,136.42	30,925.44
A2 = 100	7,277.12	13,572.58	26,652.42
A3 = 200	5,567.90	11,008.74	22,379.36
A4 = 300	3,858.67	8,444.89	18,106.28
A5 = 400	2,149.46	5,881.05	13,833.20
A6 = 500	440.23	3,317.21	9,560.14
A7 = 600	0.00	753.37	5,287.08
A8 = 625	156.69	229.75	4,218.80
A9 = 650	404.63	0.00	3,150.52
A10 = 675	750.22	79.57	2,082.28
A11 = 700	1,198.92	222.81	1,064.98
A12 = 725	1,647.61	457.85	307.48
A13 = 750	2,096.30	751.09	0.00
A14 = 775	2,545.00	1,179.10	139.41
A15 = 800	2,993.69	1,760.41	348.65
A16 = 900	4,788.46	4,452.57	2,522.22

Table 3.4: Decision matrix of weighted regrets (\$) for each size (kWh) - Case 1.

Alternative	$E[C(A_i)]$	$\max_k P_k R_{ik}$
A1 = 0	3,992.90	30,925.44
A2 = 100	3,984.35	26,652.42
A3 = 200	3,975.81	22,379.36
A4 = 300	3,967.26	18,106.28
A5 = 400	3,958.71	13,833.20
A6 = 500	3,950.17	9,560.14
A7 = 600	3,942.89	5,287.08
A8 = 625	3,941.46	4,218.80
A9 = 650	3,940.41	3,150.52
A10 = 675	3,939.76	2,082.28
A11 = 700	3,939.34	1,198.92
A12 = 725	3,939.26	1,647.61
A13 = 750	3,939.70	2,096.30
A14 = 775	3,940.71	2,545.00
A15 = 800	3,941.95	2,993.69
A16 = 900	3,948.61	4,788.46

Table 3.5: Expected value of the costs (k\$) and maximum weighted regret (\$) of each size (kWh) - Case 1.

The stability areas for approach (c) (figure 3.13.c) were derived by superimposing those of approaches (a) and (b) (figures 3.13.a, 3.13.b). To do that, many sets of three values of probabilities were generated randomly by varying P_1 , P_2 and P_3 while meeting equation (3.29). Approaches (a) and (b) were applied separately for each set of probabilities, and the sets were evaluated to identify and choose the optimal sizing alternative.

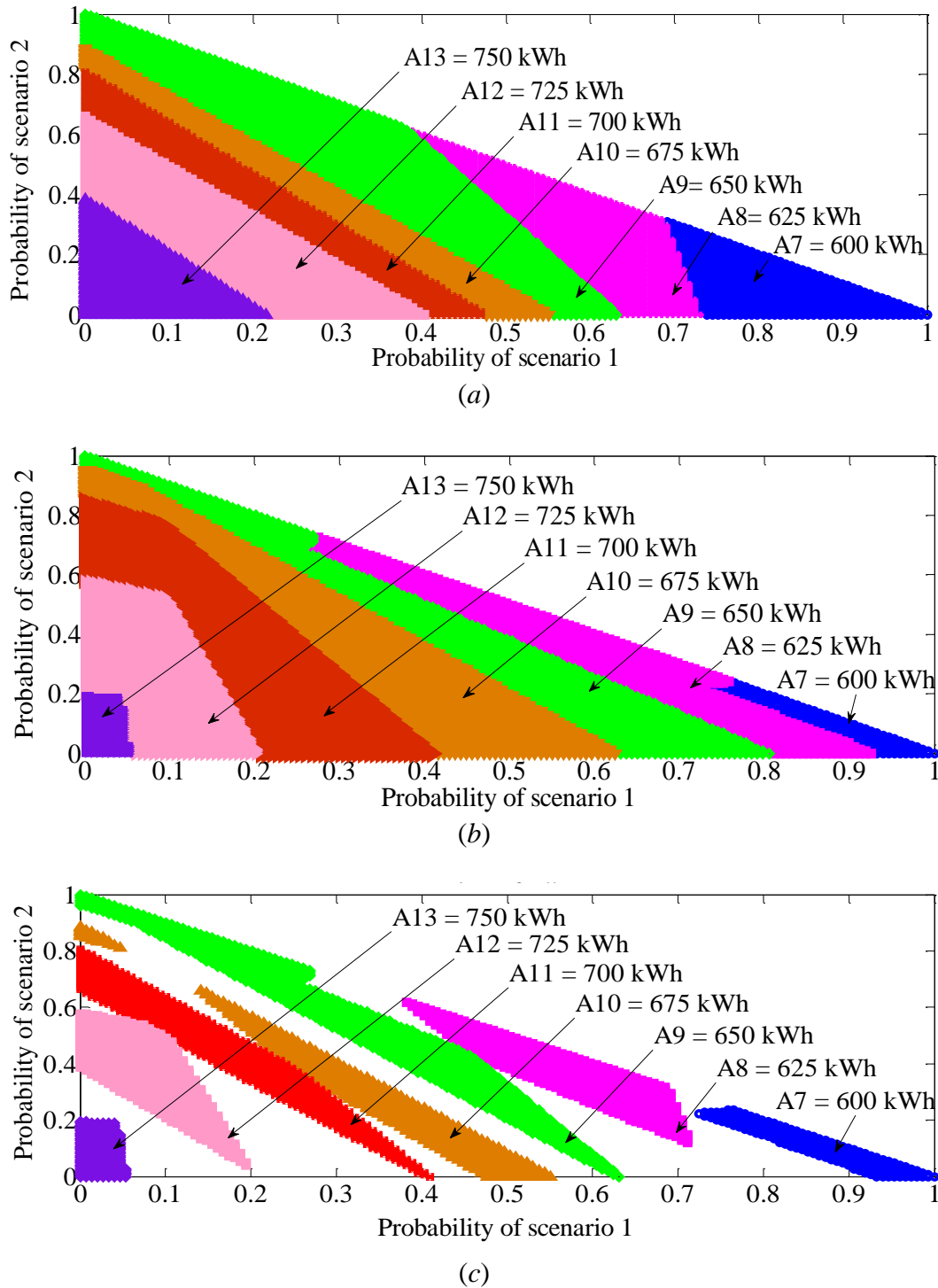


Figure 3.13: Stability areas - (a) approach (a); (b) approach (b); and (c) approach (c).

Since it is trivial that $P_3 = 1 - P_1 - P_2$ and an x - y plot is enough, a marker for each couple of probabilities P_1, P_2 , the color of which distinguishes the optimal size obtained, is reported in figure 3.13.a [for approach (a)] and figure 3.13.b [for approach (b)].

Then, overlapping the results of approaches (a) and (b), the stability areas were identified, thus obtaining figure 3.13.c, in which, for each couple of probabilities P_1, P_2 , only the optimal solutions that contemporaneously satisfy both approaches (a) and (b) are shown with a marker, the color of which distinguishes the optimal size obtained. The white area corresponds to

couples of probabilities that furnish different solutions when approaches (a) and (b) are applied.

The analysis of the stability area in figure 3.13 provides the DM with a significant amount of information about the sizing process that can help her or him in the selection of the best size for the BESS.

Figure 3.13.c shows that the alternative that occurs with the greatest frequency (area) is $A9 = 650 \text{ kWh}$ (about 12%). It is interesting to observe that both approaches (a) and (b) furnish seven sizing alternatives with varying future probabilities (figures 3.13.a, 3.13.b). While the solution alternative suggested by approach (c), *i.e.*, $A9 = 650 \text{ kWh}$, was suggested most frequently, it is evident that other solutions were characterized by a significant stability area dimension; for example, about 9% of the trials gave the preferred solution as $A11 = 700 \text{ kWh}$, and about 50% of trials presented different solutions with the same future probabilities (white area in figure 3.13). All of the optimal sizing solutions are included between solution $A7 = 600 \text{ kWh}$ and solution $A13 = 750 \text{ kWh}$, as forecasted by the DM.

It also is interesting to observe that the solutions in figure 3.13 include the sizing alternatives when a deterministic future is assumed; for example, if the DM considers the future F1 to be the one that is actual occurring (*i.e.*, the DM thinks Future 1 is a deterministic future), it follows that $P_1 = 1$ and that $P_2 = P_3 = 0$. Then, from figure 3.13.a, the sizing alternative is $A7 = 600 \text{ kWh}$, as is also evident from the analysis of table 3.3 (first column). In order to verify the effectiveness of the constraint of one cycle per day, some further simulations were performed by allowing more than one cycle. However, the results were that one cycle per day is always the optimal solution.

Case 2)

The peak price and the gap between the minimum and maximum prices can have a strong influence on the benefits derived from the use of the BESS and, therefore, on the sizing of the BESS. Motivated by the above consideration, two price profiles were considered in addition to the profile in figure 3.12: the first decreases in the peak price and in the gap between the minimum and maximum prices, while the second increases in the peak price and the gap between the minimum and maximum prices. Then, nine futures were considered that consisted of the combinations of the three profiles of the industrial facility's load requirements of case 1 with the three profiles of the hourly energy prices obtained by multiplying the values of case 1 by 0.85, 1.0 and 1.15, respectively. In other words, the load profile of the first (third) future is assumed to be 15% lesser (larger) than the load profile of the second future.

As an example, the following probabilities P_i at each scenario i are assigned: $P_1 = 0.1$, $P_2 = 0.1$, $P_3 = 0.1$, $P_4 = 0.1$, $P_5 = 0.1$, $P_6 = 0.1$, $P_7 = 0.2$, $P_8 = 0.1$ and $P_9 = 0.1$ for the application of the first two criteria.

Table 3.6 reports the decision matrix, where, for each scenario, the corresponding values of the total cost of the BESS are shown. From the analysis of the results in table 3.6, it is interesting to observe that, when the energy cost coefficients are low (futures 1, 3 and 7), the minimum cost solution is always $A1 = 0 \text{ kWh}$ (no BESS installation). In this case, the benefits due to the reduction of the electricity bill are not enough to justify the installation of the BESS; obviously, the same conclusion would arise if a reduction greater than 15% (*i.e.*, 25% or 50%) was considered. On the contrary, when the energy cost coefficients are high

(Futures 3, 6 and 9), the minimum cost solution is always $A_{16} = 900 \text{ kWh}$ (the maximum size of the BESS as constrained by the owner of the industrial facility).

Alternative	Future								
	F1	F2	F3	F4	F5	F6	F7	F8	F9
A1 = 0	2,760.64	3,247.81	3,767.98	3,247.81	3,820.96	4,394.10	3,734.98	4,394.10	5,053.21
A2 = 100	2,768.37	3,239.27	3,710.16	3,255.55	3,812.41	4,369.27	3,742.72	4,385.55	5,028.39
A3 = 200	2,776.11	3,230.72	3,685.33	3,263.28	3,803.86	4,344.44	3,750.46	4,377.01	5,003.56
A4 = 300	2,783.84	3,222.17	3,660.50	3,271.02	3,795.32	4,319.62	3,758.19	4,368.46	4,978.73
A5 = 400	2,791.58	3,213.63	3,635.67	3,278.76	3,786.77	4,294.79	3,765.93	4,359.91	4,953.90
A6 = 500	2,799.31	3,205.08	3,610.84	3,286.49	3,778.23	4,269.96	3,773.66	4,351.37	4,929.07
A7 = 600	2,812.44	3,202.88	3,593.31	3,294.23	3,769.68	4,245.13	3,781.40	4,342.82	4,904.25
A8 = 625	2,816.86	3,203.66	3,590.46	3,296.49	3,767.93	4,239.37	3,783.33	4,340.69	4,898.04
A9 = 650	2,821.66	3,204.90	3,588.14	3,299.59	3,767.17	4,234.74	3,785.27	4,338.55	4,891.83
A10 = 675	2,826.88	3,206.63	3,586.14	3,303.57	3,767.43	4,231.30	3,787.20	4,336.41	4,885.62
A11 = 700	2,832.54	3,208.88	3,585.21	3,307.72	3,767.91	4,228.10	3,789.22	4,334.38	4,879.54
A12 = 725	2,838.20	3,211.12	3,584.04	3,312.14	3,768.69	4,225.25	3,791.68	4,332.86	4,874.04
A13 = 750	2,843.86	3,213.36	3,582.87	3,316.72	3,769.67	4,222.62	3,794.91	4,332.25	4,869.59
A14 = 775	2,849.52	3,215.61	3,581.70	3,321.68	3,771.10	4,220.51	3,798.90	4,332.53	4,866.16
A15 = 800	2,855.17	3,217.85	3,580.53	3,327.08	3,773.04	4,218.99	3,803.00	4,332.95	4,862.89
A16 = 900	2,877.80	3,226.82	3,575.85	3,349.71	3,782.01	4,214.31	3,821.70	4,337.29	4,852.89

Table 3.6: Decision matrix: total cost ($k\$$) for each size (kWh) - Case 2.

Table 3.7 shows the decision matrix of the weighted regrets, and table 3.8 shows the expected value of the costs associated with the 16 alternatives and the maximum weighted regret. The effect of unequal probabilities is evident in table 3.7, since Future F7 most heavily influences the weighted regrets, since $P_7 = 0.2$ but all other probabilities are 0.1.

Alternative	Future								
	F1	F2	F3	F4	F5	F6	F7	F8	F9
A1 = 0	0.00	4,493.19	19,213.80	0.00	5,378.81	17,978.80	0.00	6,185.09	20,032.75
A2 = 100	773.58	3,638.56	13,431.00	773.58	4,524.19	15,495.92	1,547.14	5,330.48	17,549.94
A3 = 200	1,547.16	2,783.95	10,948.19	1,547.17	3,669.58	13,013.20	3,094.31	4,475.87	15,067.13
A4 = 300	2,320.73	1,929.34	8,465.32	2,320.74	2,814.97	10,530.39	4,641.48	3,621.26	12,584.34
A5 = 400	3,094.31	1,074.73	5,982.58	3,094.32	1,960.35	8,047.52	6,188.63	2,766.64	10,101.42
A6 = 500	3,867.89	220.12	3,499.77	3,867.90	1,105.74	5,564.78	7,735.77	1,912.03	7,618.72
A7 = 600	5,180.79	0.00	1,746.64	4,641.48	251.13	3,081.98	9,282.94	1,057.42	5,135.92
A8 = 625	5,622.38	78.35	1,461.74	4,868.12	76.58	2,506.24	9,669.74	843.76	4,515.22
A9 = 650	6,102.76	202.32	1,229.30	5,178.03	0.00	2,043.18	10,056.53	630.10	3,894.52
A10 = 675	6,624.64	375.11	1,053.02	5,575.57	26.53	1,698.69	10,443.31	416.46	3,273.81
A11 = 700	7,190.33	599.46	935.96	5,991.15	74.27	1,378.59	10,847.43	213.00	2,664.84
A12 = 725	7,756.02	823.81	819.01	6,432.75	152.62	1,093.69	11,339.90	61.50	2,115.62
A13 = 750	8,321.72	1,048.15	702.02	6,890.75	250.36	831.10	11,985.35	0.00	1,669.90
A14 = 775	8,887.42	1,272.50	585.01	7,387.11	393.03	620.18	12,782.72	27.88	1,326.96
A15 = 800	9,453.11	1,496.85	468.01	7,926.81	586.80	468.00	13,603.88	69.73	1,000.08
A16 = 900	11,715.9	2,394.23	0.00	10,189.6	1,484.19	0.00	17,342.89	504.44	0.00

Table 3.7: Decision matrix of weighted regrets ($\$$) for each size (kWh) - Case 2.

From the results in table 3.8, it follows that, once again, the alternatives recommended by approaches (a) and (b) are different, and they are given by $A_9 = 650 \text{ kWh}$ and $A_6 = 500 \text{ kWh}$, respectively.

The stability areas for approach (c) were derived by superimposing those of approaches (a) and (b). In this case, the stability area criterion cannot be represented with simple graphs as was done in figure 3.13. The alternatives that resulted with a stability area different from zero were $A_6 = 500 \text{ kWh}$, $A_8 = 635 \text{ kWh}$, $A_9 = 650 \text{ kWh}$, $A_{10} = 675 \text{ kWh}$, $A_{12} = 725 \text{ kWh}$, $A_{13} = 750 \text{ kWh}$, $A_{14} = 775 \text{ kWh}$, $A_{15} = 800 \text{ kWh}$ and $A_{16} = 900 \text{ kWh}$. The sizing alternative with the greatest area was $A_{13} = 750 \text{ kWh}$, followed by alternative $A_9 = 650 \text{ kWh}$. As a final consideration on the sizing procedure, it should be noted that, even if the DM chooses a very high number of futures (much greater than nine) and if each optimization problem shown in the previous section is solved using GA and linear optimization, this does not result in excessive computational effort because the computations occur in the planning stage and new computers and configurations (parallel distributed processing and environment) can easily handle massive computational requirements.

Alternative	$E[C(A_i)]$	$\max_k P_k R G_{ik}$
A1 = 0	3,815.65	20,032.75
A2 = 100	3,805.44	17,549.94
A3 = 200	3,798.52	15,067.13
A4 = 300	3,791.60	12,584.34
A5 = 400	3,784.68	10,101.42
A6 = 500	3,777.76	7,735.77
A7 = 600	3,772.75	9,282.94
A8 = 625	3,772.01	9,669.74
A9 = 650	3,771.71	10,056.53
A10 = 675	3,771.86	10,443.31
A11 = 700	3,772.27	10,847.43
A12 = 725	3,772.97	11,339.90
A13 = 750	3,774.07	11,985.35
A14 = 775	3,775.65	12,782.72
A15 = 800	3,777.44	13,603.88
A16 = 900	3,786.00	17,342.89

Table 3.8: Expected value of the costs ($k\$$) and maximum weighted regret ($\$$) of each size (kWh) - Case 2.

3.3. References

- [1] S. Bahramirad and H. Daneshi, "Optimal sizing of smart grid storage management system in a microgrid," in *Proc. Innovative Smart Grid Technologies, ISGT 2012*, Washington, DC, USA, 16-20 January. 2012.
- [2] H. Xiao, W. Pei, Y. Yang, and L. Kong, "Sizing of battery energy storage for micro-grid considering optimal operation management," in *Proc. 2014 International Conference on Power System Technology, POWERCON 2014*, Chengdu, China, 20-22 October, 2014.
- [3] EUROBATT, (2013). Battery energy storage for smart grid applications. [Online]. Available: http://www.eurobat.org/sites/default/files/eurobat_smartgrid_publication_may_2013_0.pdf

- [4] S. Borenstein, M. Jaske, and A. Rosenfeld, (2002). Dynamic pricing, advanced metering and demand response in electricity markets. Center for the Study of Energy Markets. Berkeley, CA. [Online].Available: <http://www.escholarship.org/uc/item/11w8d6m4>
- [5] G. Carpinelli, S. Khormali, F. Mottola, and D. Proto, "Battery energy storage sizing when time of use pricing is applied," *The Scientific World Journal*, vol. 2014, pp. 1-8, September 2014.
- [6] T.Y Lee, and N. Chen, "Determination of optimal contract capacities and optimal sizes of battery energy storage systems for time-of-use rates industrial customers," *IEEE Trans. on Energy Conversion*, vol. 15(3), pp. 562-568, September 1995.
- [7] A. K. Barnes, J. C. Balda, S. O. Geurin, and A. Escobar-Mejia, "Optimal battery chemistry, capacity selection, charge/discharge schedule, and lifetime of energy storage under time-of-use pricing," in Proc. 2nd IEEE PES International Conference and exhibition on innovative smart grid Technologies, ISGT Europe 2011, Manchester, UK, 5-7 December, 2011.
- [8] B. Aksanli, and T. Rosing, "Optimal battery configuration in a residential home with time-of-use pricing," in Proc. IEEE international conference on Smart Grid Communications, SmartGridComm 2013, Vancouver, BC, Canada, 21-24 October, 2013.
- [9] Norsok Standard, (1996). Life cycle cost for production facility. [Online].Available: <http://www.standard.no/pagefiles/1137/o-cr-002r1.pdf>
- [10] A. A. Akhil, G. Huff, A. B. Currier, B. C. Kaun, D. M. Rastler, S. B. Chen, A. L. Cotter, D. T. Bradshaw, and W. D. Gauntlett, (2013). Electricity storage handbook. Sandia National Laboratories. [Online].Available: <http://www.sandia.gov/ess/publications/SAND2013-5131.pdf>
- [11] Y. Zheng, Z. Y. Dong, Y. Xu, K. Meng, J. H. Zhao, and J. Qiu, "Electric vehicle battery charging/swap stations in distribution systems: comparison study and optimal planning," *IEEE Trans. on Power Systems*, vol.29(1), pp. 221-229, January 2014.
- [12] G. Carpinelli, S. Khormali, F. Mottola, and D. Proto, "Optimal operation of electrical energy storage systems for industrial applications," in Proc. *IEEE Power and Energy Society General Meeting*, Vancouver, BC, Canada, 21-25 July, 2013.
- [13] G. Carpinelli, G. Celli, S. Mocci, F. Mottola, F. Pilo, and D. Proto, "Optimal integration of distributed energy storage devices in smart grids," *IEEE Trans. on Smart Grid*, vol.4(2), pp. 985-995, June 2013.
- [14] G. Carpinelli, F. Mottola, D. Proto, and A. Russo, "Optimal allocation of dispersed generators, capacitors and distributed energy storage systems in distribution networks," in Proc. *International Symposium on Modern Electric Power Systems, MEPS 2010*, Wroclaw, Poland, 20-22 September, 2010.
- [15] K. C. Divya, and J. Østergaard, "Battery energy storage technology for power systems: an overview," *Electric Power Systems Research*, vol. 79(4), pp. 511-520, April 2009.
- [16] <http://www.pge.com/tariffs/>
- [17] A. Oudalov, D. Chartouni, C. Ohler, and G. Linhofer, "Value analysis of battery energy storage applications in power systems," in Proc. *IEEE Power Systems Conference and Exposition*, Atlanta, GA, USA, 29 October-1 November, 2006.

- [18] R. C. Leou, "An economic analysis model for the energy storage system applied to a distribution substation," *International Journal of Electric Power & Energy Systems*, vol. 34(1), pp. 132-137, January 2012.
- [19] M. P. Johnson, A. Bar-Noy, O. Liu, and Y. Feng, "Energy peak shaving with local storage," *Sustainable Computing: Informatics and Systems*, vol. 1(3), pp. 177-188, September 2011.
- [20] J. P. Barton, and D. G. Infield, "A probabilistic method for calculating the usefulness of a store with finite energy capacity for smoothing electricity generation from wind and solar power," *Journal of Power Sources*, vol. 162(2), pp. 943-948, November 2006.
- [21] P. Pinson, G. Papaefthymiou, B. Klöckl, and J. Verboomen, "Dynamic sizing of energy storage for hedging wind power forecast uncertainty," in *Proc. IEEE Power & Energy Society General Meeting*, Calgary, AB, Canada, 26-30 July, 2009.
- [22] J. V. Paatero, and P. D. Lund, "Effect of energy storage on variations in wind power," *Wind Energy*, vol. 8(4), pp. 421-441, October/December 2005.
- [23] G. Koepfel, and M. Korpås, "Improving the network infeed accuracy of non-dispatchable generators with energy storage devices," *Electric Power Systems Research*, vol. 78(12), pp. 2024-2036, December 2008.
- [24] Y. Zhang, Z. Songzhe, and A. A. Chowdhury, "Reliability modeling and control schemes of composite energy storage and wind generation system with adequate transmission upgrades," *IEEE Trans. on Sustainable Energy*, vol. 2(4), pp. 520-526, June 2011.
- [25] H. Bludszweit, and J. A. Domínguez-Navarro, "A probabilistic method for energy storage sizing based on wind power forecast uncertainty," *IEEE Trans. on Power Systems*, vol. 26(3), pp. 1651-1658, August 2011.
- [26] G. Capizzi, F. Bonanno, and G. M. Tina, "Experiences on the design of stand-alone photovoltaic system by deterministic and probabilistic methods," in *Proc. International Conference on Clean Electrical Power, ICCEP 2011*, Ischia, Italy, 14-16 June, 2011.
- [27] A. Testa, S. De-Caro, R. La-Torre, and T. Scimone, "Optimal design of energy storage systems for stand-alone hybrid wind/pv generators," in *Proc. International Symposium on Power Electronics Electrical Drives Automation and Motion, SPEEDAM 2010*, Pisa, Italy, 14-16 June, 2010.
- [28] G. J. Anders, "*Probability concepts in electric power systems*," New York, NY, USA, John Wiley & Sons, 1990.
- [29] V. Miranda, and L. M. Proenca, "Why risk analysis outperforms probabilistic choice as the effective decision support paradigm for power system planning," *IEEE Trans. on Power Systems*, vol. 13(2), pp. 643-648, May 1988.
- [30] E. Carpaneto, G. Chicco, P. Mancarella, and A. Russo, "Cogeneration planning under uncertainty. part II: decision theory-based assessment of planning alternatives," *Applied Energy*, vol. 88(4), pp. 1075-1083, April 2011.
- [31] G. Carpinelli, G. Celli, F. Pilo, and A. Russo, "Embedded generation planning under uncertainty including power quality issues," *European Trans. on Electrical. Power*, vol. 13(6), pp. 381-389, November/December 2003.
- [32] G. Carpinelli, G. Ferruzzi, and A. Russo, "Trade-off analysis to solve a probabilistic multi-objective problem for passive filtering system planning," *International Journal of Emerging Electric Power Systems*, vol. 14(3), pp. 275-284, June 2013.

- [33] S. X. Chen, H. B. Gooi, and M. Q. Wang, "Sizing of energy storage for microgrids," *IEEE Trans. on Smart Grid*," vol. 3(1), pp. 142-151, March 2012.
- [34] F. Yahyaie, and T. Soong, "Optimal operation strategy and sizing of battery energy storage systems," in *Proc. 25th IEEE Canadian Conference on Electrical and Computer Engineering, CCECE 2012*, Montreal, QC, Canada, 29 April-2 May, 2012.
- [35] S. S. Choi, and H. S. Lim, "Factors that affect cycle-life and possible degradation mechanisms of a Li-ion cell based on LiCoO₂," *Journal of Power Sources*, vol. 111(1), pp. 130-136, September 2002.
- [36] K. Zaghbi, M. Dontigny, A. Guerfi, P. Charest, I. Rodrigues, A. Mauger, and C. M. Julien, "Safe and fast-charging Li-ion battery with long shelf life for power applications," *Journal of Power Sources*, vol. 196(8), pp. 3949-3954, April 2011.
- [37] G. Carpinelli, A. R. di Fazio, S. Khormali, and F. Mottola, "Optimal sizing of battery storage systems for industrial applications when uncertainties exist," *Energies*, vol. 7(1), pp. 130-149, January 2014.
- [38] U.S. Department of Energy, (2010). The recovery act: transforming america's transportation sector-batteries and electrical vehicles. [Online].Available: <http://bit.ly/fGaZPB>
- [39] V. H. Johnson, "Battery performance models in ADVISOR," *Journal of Power Sources*, vol. 110(2), pp.321-329, August 2002.

Conclusions

In this thesis, the optimal integration of BESSs in the frame of different services at distribution system and end-use customer levels has been proposed. The grid gained major technical improvements and economic benefits based on the optimal integration of storage devices which is strictly depending on optimal operation strategy and optimal sizing of BESS. With reference to optimal operation, advanced optimal BESS operating strategies were proposed with the aim of leveling the load active powers requested by the loads connected to a distribution system, reducing the electricity costs sustained by an end-use customer that provides DR and scheduling a μ G with DR resources PEVs and DCs.

In case of load leveling service, the problem of leveling the power of a distribution substation with an electrical energy storage system was analyzed. A two-step strategy was proposed that involved day-ahead scheduling and real-time control to obtain an optimal leveling of the substation power. Two optimization models were formulated and solved. The day-ahead model was a linear constrained optimization model, while the real-time control involved non-linearity.

The main outcomes were the following:

- the two step-procedure involving both day-ahead scheduling and real-time control is a powerful tool for performing an optimal leveling of the distribution substation power;
- the proposed strategy showed good performance allowing a reduction of about 15% of the peak power and an improvement of about 20% of the load factor in the examined cases;
- the improvement of the forecasting of feeder power would give further benefits.

The results of the simulations demonstrated the robustness of the proposed method and also satisfied technical constraints of the BESS.

The second application considered in the thesis was focused on the use of BESS to enhance DR solutions for the industrial sector under the RTP electricity bill scheme which gives customers time varying rates that reflect the value and cost of electricity in different time periods. This application proposed a strategy for the optimal operation of a multi-battery system of an industrial facility for the minimization of the costs sustained by the industry owner related to energy consumption. The numerical applications on an actual industrial facility showed that an optimal operation of battery systems can significantly reduce the costs and that the solution based on more than a single battery bank seems the most adequate choice under particular tariff schemes.

The third application of the thesis performed the DR service under the EDC tariff which involves a structure directly linked to both the consumed energy and the peak load. DR for this sector is then achievable by means of storage based solutions which allow reducing loads without altering electricity consumption but, at the same time, prevent the full potential of demand side response solutions. In this thesis, aimed at exploiting the benefits obtainable by the use of such devices in industrial facilities, a proposal for the optimal operation of a BESS was presented. The proposed strategy, once again based on a two-step procedure, is aimed at:

- reducing the electricity costs related to the time of use energy charge;
- reducing the electricity costs related to the peak power demand charge;

- managing the forecasting errors deriving from uncertainties of load requirements;
- operating the battery by guaranteeing its maximum efficiency and lifecycle.

In particular, the numerical applications showed the efficacy of the two step procedure in terms of minimization of energy costs and satisfaction of technical constraints so demonstrating the potential advantages of adopting such devices in manufacturing facilities.

Regarding the scheduling of μ Gs, different optimal strategies were presented in the thesis. The strategies, which are based on single-objective approaches, allow the scheduling of μ Gs for pursuing specific services (e.g., energy savings or load leveling), as well as for satisfying the operating constraints of network and those of other components (DCs, PEVS, loads and DG units). Several numerical applications were performed, whose results showed the effectiveness of each strategy.

With reference to the optimal sizing, the case of a BESS to be installed in an industrial facility was considered, and the sizing was performed in order to reduce the facility's electricity bill based on both deterministic and probabilistic approaches.

Relating to deterministic approach, a simplified procedure was proposed. At this aim, a closed form procedure was presented under TOU tariff pricing schemes. A sensitivity analysis was performed on the basis of the variation of some parameters that affect the profitability of BESSs. By the analyses performed it emerged that the parameters that mainly determine the profitability of BESSs are the "on peak - off peak" price variations, the installation costs and financial parameters (i.e. effective rates of change and discount rates). BESS efficiency and annual load variation, slightly contribute to the increase or decrease of the benefit.

The main outcome of the performed analysis is that the significance of the benefit achievable by using storage systems is mainly related to two aspects:

- the need to reduce installation costs which are still quite high;
- the energy tariff which should be characterized by a larger spread between on-peak and off peak prices.

Finally, in case of optimal sizing based on probabilistic approach, the sizing problem was conducted by using a decision theory that took into account the unavoidable uncertainties involved with the electricity bill cost coefficients and the profile of the industrial facility's load demand. The choice of the optimal size for the BESS was made by using a stepwise procedure based on different decision theory-based approaches, and the results were compared.

The main observations and outcomes of analyses were:

- the probabilities of the futures can significantly influence the optimal BESS sizing;
- the BESS optimal sizes obtained using the decision theory approaches involved various optimal sizing solutions with different stability areas, thus furnishing extensive and useful information for the DM's use in identifying the best solution;
- decision theory appears to be a powerful tool in that it was able to solve the BESS sizing problem for industrial applications even when there were significant uncertainties, just as it has been for several other important problems associated with planning power systems.